Soft handover issues in radio resource management for 3G WCDMA networks

Chen, Yue

Soft Handover Issues in Radio Resource Management for 3G WCDMA Networks

Yue Chen

Submitted for the degree of Doctor of Philosophy

Department of Electronic Engineering
Queen Mary, University of London

September 2003

To my family

Abstract

Mobile terminals allow users to access services while on the move. This unique feature has driven the rapid growth in the mobile network industry, changing it from a new technology into a massive industry within less than two decades.

Handover is the essential functionality for dealing with the mobility of the mobile users. Compared with the conventional hard handover employed in the GSM mobile networks, the soft handover used in IS-95 and being proposed for 3G has better performance on both link and system level.

Previous work on soft handover has led to several algorithms being proposed and extensive research has been conducted on the performance analysis and parameters optimisation of these algorithms. Most of the previous analysis focused on the uplink direction. However, in future mobile networks, the downlink is more likely to be the bottleneck of the system capacity because of the asymmetric nature of new services, such as Internet traffic.

In this thesis, an in-depth study of the soft handover effects on the downlink direction of WCDMA networks is carried out, leading to a new method of optimising soft handover for maximising the downlink capacity and a new power control approach.

Acknowledgement

I would like to thank Prof. Laurie Cuthbert for his supervision, knowledge, support and persistent encouragement during my PhD at Queen Mary, University of London. Many other staff including John Bigham, John Schormans and Mark Rayner, have given me help and valuable advice during this period, they have my thanks.

My studies would not have been complete without the help and the friendship of others, Felicia, Enjie, Eliane, Laurissa, Rob and Veselin gave me so much help and support when I first came to UK. They will always have a place in my fond memories at QMUL. Also, I want to thank many other friends, Jib, Yong, Ning, Xiaoyan, Huai, Shaowen and Bo for the good times and the friendship.

I would also like to extend my thanks to the numerous members of support staff who have made the technical and financial part of my work possible.

Finally, with my love and gratitude, I want to dedicate this thesis to my family who have supported me throughout, especially to my mother and my late father.

Table of Contents

List of Figures

List of Tables

Glossary

2G	2nd Generation
3G	3rd Generation
3GPP	3rd Generation Partnership Project (produces WCDMA standard)
3GPP2	3rd Generation Partnership Project 2 (produces cdma2000 standard)
4G	4th Generation
AC	Admission Control
AGC	Automatic Gain Control
AMPS	Advanced Mobile Phone Service
AMR	Adaptive Multirate (speech codec)
B(T)S	Base (Transceiver) Station
B3G systems	systems Beyond 3G
BER	Bit Error Rate
BoD	Bandwidth on Demand
BPSK	Binary Phase Shift Keying
CDF	Cumulative Distribution Function
CDMA	Code Division Multiple Access
CN	Core Network
CPICH	Common Pilot Channel
DAB	Digital Audio Broadcasting
DECT	Digital Enhanced Cordless Telecommunication
DL	Downlink
DPCCH	Dedicated Physical Control Channel
DPDCH	Dedicated Physical Data Channel
DQPSK	Differential Quadrature Phase Shift Keying
DS-CDMA	Direct-Sequence Code Division Multiple Access

DVB	Digital Video Broadcasting
EDGE	Enhanced Data Rates for GSM Evolution
ETSI	European Telecommunication Standard Institute
FCC	Federal Communication Commission (US)
FDD	Frequency Division Duplex
FDMA	Frequency Division Multiple Access
FPLMTS	Future Public Land Mobile Telecommunications System
GMSK	Gaussian Minimum Shift Keying
GPRS	General Packet Radio Service
GPS	Global Positioning System
GSM	Global System for Mobile Communications
HHO	Hard Handover
HO	Handover
HSCSD	High Speed Circuit Switched Data
IMT-2000	International Mobile Telecommunications - 2000
IS-136	D-AMPS, US-TDMA system
IS-95	cdmaOne, US-CDMA system
ISDN	Integrated Services Digital Network
ITU	International Telecommunications Union
JDC	Japanese Digital Cellular
LOS	Line-of-sight
MBWA	Mobile Broadband Wireless Access (IEEE 802.20)
MS	Mobile Station
MUD	Multiuser Detection
NMT	Nordic Mobile Telephones
NTT	Nippon Telephone and Telegraph
O&M	Operation and Maintenance
O-QPSK	Offset Quadrature Phase Shift Keying
OVSF	Orthogonal Variable Spreading Factor

PC	Power Control
PDC	Personal Digital Cellular
PSK	Phase Shift Keying
QoS	Quality of Service
RAM	Radio Access Mode
RAT	Radio Access Technology
RF	Radio Frequency
RNC	Radio Network Controller
RRC	Radio Resource Control
RRM	Radio Resource Management
SCH	Synchronization Channel
SHO	Soft Handover
SIR	Signal to Interference Ratio
SSMA	Spread-Spectrum Multiple Access
TACS	Total Access Communication Systems
TDD	Time Division Duplex
TDMA	Time Division Multiple Access
TPC	Transmit Power Control
UE	User Equipment
UL	Uplink
UMTS	Universal Mobile Telecommunication Services
UTRA	UMTS Terrestrial Radio Access
UTRAN	UMTS Terrestrial Radio Access Network
UWC	Universal Wireless Communications
WARC	World Administrative Radio Conference
WCDMA	Wideband Code Division Multiple Access
WLAN	Wireless Local Access Network
WWRF	Wireless World Research Forum

Chapter 1 Introduction

1.1 Introduction

Handover deals with the mobility of the end users in a mobile network: it guarantees the continuity of the wireless services when the mobile user moves across the cellular boundaries.

In first and second generation mobile networks, hard handover is employed; in third generation networks, which are predominantly based on CDMA technology, the soft handover concept is introduced. Compared with the conventional hard handover, soft handover has the advantages of smoother transmission and less ping-pong effects. As well as leading to continuity of the wireless services, it also brings macrodiversity gain to the system. However, soft handover has the disadvantages of complexity and extra resource consumption. Therefore, optimisation is crucial for guaranteeing the performance of soft handover. Until now, several algorithms have been proposed aiming at maximising the macrodiversity gain and minimising the handover failure rate and extensive research has been conducted on the optimisation of the parameters for these soft handover algorithms.

It has been proved that the individual link quality can be improved by soft handover and in the uplink soft handover can increase the capacity and expand the coverage. However, in the downlink, there are no qualified results about the trade-off between the macrodiversity gain and the extra resource consumption caused by soft handover. Because the downlink is more likely to be the bottleneck of the system capacity in the future mobile networks, the system level performance of soft handover in the downlink needs to be further investigated.

In this thesis, an in-depth study of the soft handover effects on the downlink direction of WCDMA networks is carried out, leading to a new method for optimising soft handover and a new power control approach.

Fast downlink power control and initial cell selection schemes that had been ignored by most of the previous literature are both included in the analysis. This work quantifies the trade-off between the macrodiversity gain and the extra resource

consumption, proposes a new method for optimising soft handover in order to maximise the downlink capacity and a new power control approach for increasing the soft handover gain by mitigating the interference. The optimisation of soft handover is valuable for radio network dimensioning and the new power control scheme is shown to have better performance when compared with the balanced power control scheme adopted by 3GPP.

1.2 Contribution

The major contributions of the work in this thesis are:

- An in-depth study of soft handover effects on the downlink direction of the WCDMA networks, which quantifies the trade-off between the macrodiversity gain and the extra resource consumption.

- Sensitivity analysis of the soft handover gain to different cell selection schemes, different power control conditions and different radio parameters gives a better understanding of soft handover effects on the downlink capacity.

- A new method for optimising soft handover is proposed in order to maximise the downlink capacity. The optimum soft handover overhead and threshold ranges are obtained. The results are valuable for the radio resource management in future mobile networks where the downlink is more likely to be the bottleneck of the whole system.

- A new power division approach is proposed for controlling the power division between the Base Stations (BSs) in the active set during the soft handover. The new approach has a better performance than the balanced power division scheme adopted by 3GPP, minimising the interference and maintaining the benefits from the macrodiversity at the same time.

The author's papers are list in Appendix A.

1.3 Organisation of the Thesis

Chapter 2 gives a brief overview of the evolution of mobile networks. The key technologies and landmark features of different generation mobile networks are

described. This chapter also introduces the basic concepts of CDMA technology and functionalities of radio resource management that are used throughout this thesis.

Chapter 3 mainly introduces **handover**. The difference between hard and soft handover, principles, algorithms, previous work and existing problems about soft handover are presented. This chapter reveals the motivation of the work in this thesis.

Chapter 4 begins with the downlink interference analysis, followed by the link level performance analysis of soft handover in terms of total power consumption. The work is new and it sets the foundation for the system level performance analysis in later chapters and provides a theoretical basis for the soft handover optimisation and the new power control approach.

In Chapter 5, the system level performance of soft handover is analysed. The trade-off between the macrodiversity gain and the extra resource consumption is quantified. The effects of different cell selection schemes and different power control conditions on the soft handover gain are evaluated and the sensitivity of the soft handover gain to radio parameters and multi-service environments is also estimated.

Chapter 6 proposes a new method for optimising the soft handover in order to maximising the downlink capacity. The optimum soft handover overhead and threshold ranges are obtained. The results are valuable for radio resource management in future mobile networks where the downlink is more likely to be the bottleneck of the whole system.

Chapter 7 presents the new approach for optimising power division during the soft handover. The performance is verified by comparing to the balanced power division strategy adopted by 3GPP.

Chapter 8 summarises the work in this thesis, draws the conclusions and also discusses the future work.

Verification and validation are very important in any research work: details of that used for this work is given in Appendix B.

Chapter 2 Mobile Communication Networks

2.1 Evolving Mobile Networks

2.1.1 First-generation analogue mobile systems

In 1980 the mobile cellular era had started, and since then mobile communications have undergone significant changes and experienced enormous growth. Figure 2.1 shows the evolution of the mobile networks.

First-generation mobile systems used analogue transmission for speech services. In 1979, the first cellular system in the world became operational by Nippon Telephone and Telegraph (NTT) in Tokyo, Japan. The system utilised 600 duplex channels over a spectrum of 30 MHz in the 800 MHz band, with a channel separation of 25 kHz. Two years later, the cellular epoch reached Europe. The two most popular analogue systems were Nordic Mobile Telephones (NMT) and Total Access Communication Systems (TACS). In 1981, the NMT-450 system was commercialised by NMT in Scandinavia. The system operated in the 450 MHz and 900 MHz band with a total bandwidth of 10 MHz. TACS, launched in the United Kingdom in 1982, operated at 900 MHz with a band of 25 MHz for each path and a channel bandwidth of 25 kHz. Extended TACS was deployed in 1985. Other than NMT and TACS, some other analogue systems were also introduced in 1980s across the Europe. For example, in Germany, the C-450 cellular system, operating at 450 MHz and 900 MHz (later), was deployed in September in 1985. All of these systems offered handover and roaming capabilities but the cellular networks were unable to interoperate between countries. This was one of the inevitable disadvantages of first-generation mobile networks. In the United States, the Advanced Mobile Phone System (AMPS) was launched in 1982. The system was allocated a 40-MHz bandwidth within the 800 to 900 MHz frequency range. In 1988, an additional 10 MHz bandwidth, called Expanded Spectrum (ES) was allocated to AMPS.

2.1.2 Second-generation & phase 2+ mobile systems

Second-generation (2G) mobile systems were introduced in the end of 1980s. Low bit rate data services were supported as well as the traditional speech service. Digital

transmission rather than analogue transmission was used by these systems. Consequently, compared with first-generation systems, higher spectrum efficiency, better data services, and more advanced roaming were offered by 2G systems. In Europe, the Global System for Mobile Communications (GSM) was deployed to provide a single unified standard. This enabled seamless services through out Europe by means of international roaming. The earliest GSM system operated in the 900 MHz frequency band with a total bandwidth of 50 MHz. During development over more than 20 years, GSM technology has been continuously improved to offer better services in the market. New technologies have been developed based on the original GSM system, leading to some more advanced systems known as 2.5 Generation (2.5G) systems. So far, as the largest mobile system worldwide, GSM is the technology of choice in over 190 countries with about 787 million subscribers [GSMweb].

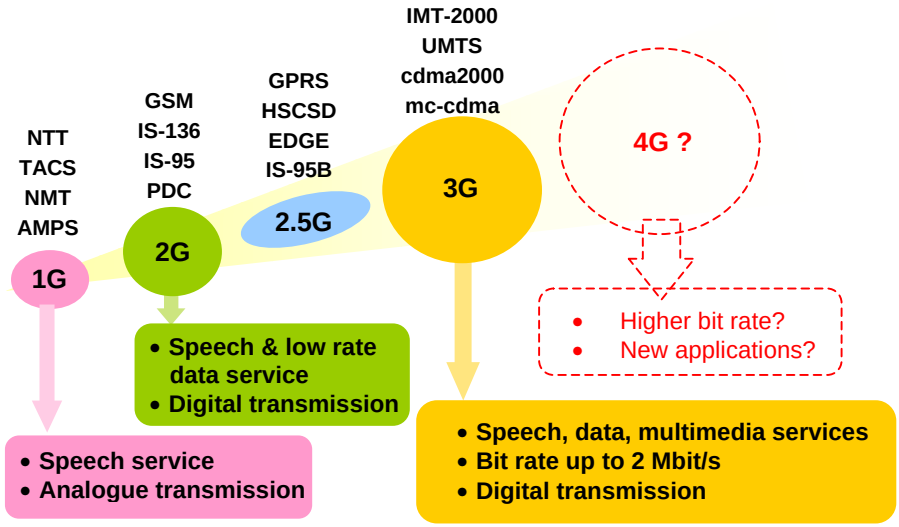

Figure 2.1 Evolution of mobile networks

In the United States, there were three lines of development in second-generation digital cellular systems. The first digital system, introduced in 1991, was the IS-54 (North America TDMA Digital Cellular), of which a new version supporting additional services (IS-136) was introduced in 1996. Meanwhile, IS-95 (cdmaOne) was deployed in 1993. The US Federal Communications Commission (FCC) also auctioned a new block of spectrum in the 1900 MHz band (PCS), allowing GSM1900 to enter the US market. In Japan, the Personal Digital Cellular (PDC) system, originally known as JDC (Japanese Digital Cellular) was initially defined in 1990.

Commercial service was started by NTT in 1993 in the 800 MHz band and in 1994 in the 1.5 GHz band. Table 2.1 shows the technical parameters of four typical second-generation digital mobile systems.

	GSM	**IS-136**	**IS-95**	**PDC**
Multiple access	TDMA	TDMA	CDMA	TDMA
Modulation	GMSK	π/4-DQPSK Coherent π/4-DQPSK Coherent 8-PSK	QPSK/O-QPSK	π/4-DQPSK
Carrier spacing	200 kHz	30 kHz	1.25 kHz	25 kHz
Carrier bit rate	270.833 kbit/s	48.6 kbit/s (π/4-DQPSK) 72.9 kbit/s (8-PSK)	1.2288 Mchip/s	42 kbit/s
Frame Length	4.615 ms	40 ms	20 ms	20 ms
Slots per frame	8/16	6	1	3/6
Frequency band (uplink/downlink) (MHz)	880-915/935-960 1720-1785/1805-1880 1930-1990/1850-1910	824-849/869-894 1930-1990/1850-1910	824-849/869-894 1930-1990/1850-1910	810-826/940-956 1429-1453/ 1477-1501
Maximum possible data rate (kbit/s)	HSCSD: 57.6 GPRS: 115.2-182.4	IS-136+: 43.2	IS-95A: 14.4 IS-95B: 115.2	28.8
Handover	Hard	Hard	Soft	Hard

Table 2.1 Technical parameters of second-generation digital systems

Nowadays, second-generation digital cellular systems still dominate the mobile industry throughout the whole world. However, they are evolving towards third-generation (3G) systems because of the demands imposed by increasing mobile traffic and the emergence of new type of services. The new systems, such as HSCSD (High Speed Circuit Switched Data), GPRS (General Packet Radio Service), and IS-95B, are commonly referred as generation 2.5 (2.5G).

HSCSD, GPRS and EDGE are all based on the original GSM system. HSCSD is the first enhancement of the GSM air interface: it bundles GSM timeslots to give a theoretical maximum data rate of 57.6 kbit/s (bundling 4×14.4 kbit/s full rate timeslots). HSCSD provides both symmetric and asymmetric services and it is relatively easy to deploy. However, HSCSD is not easy to price competitively since each timeslot is effectively a GSM channel.

Following HSCSD, GPRS is the next step of the evolution of the GSM air interface. Other than bundling timeslots, 4 new channel coding schemes are proposed. GPRS

provides “always on” packet switched services with bandwidth only being used when needed. Therefore, GPRS enables GSM with Internet access at high spectrum efficiency by sharing time slots between different users. Theoretically, GPRS can support data rate up to 160 kbit/s (current commercial GPRS provides 40 kbit/s). Deploying GPRS is not as simple as HSCSD because the core network needs to be upgraded as well.

EDGE uses the GSM radio structure and TDMA framing but with a new modulation scheme, 8QPSK, instead of GMSK, thereby increasing by three times the GSM throughput using the same bandwidth. EDGE in combination with GPRS will deliver single user data rates of up to 384 kbit/s. For more details on GSM phase 2+ and on GSM’s evolution towards 3G systems, refer to [ZJK98].

2.1.3 Third-generation mobile systems and beyond

The massive success of 2G technologies is pushing mobile networks to grow extremely fast as ever-growing mobile traffic puts a lot of pressure on network capacity. In addition, the current strong drive towards new applications, such as wireless Internet access and video telephony, has generated a need for a universal standard at higher user bitrates: 3G. Figure 2.2 shows the bit rate requirements for some of the applications that are predicated for 3G networks. Most of the new services require bitrates up 2 Mbit/s.

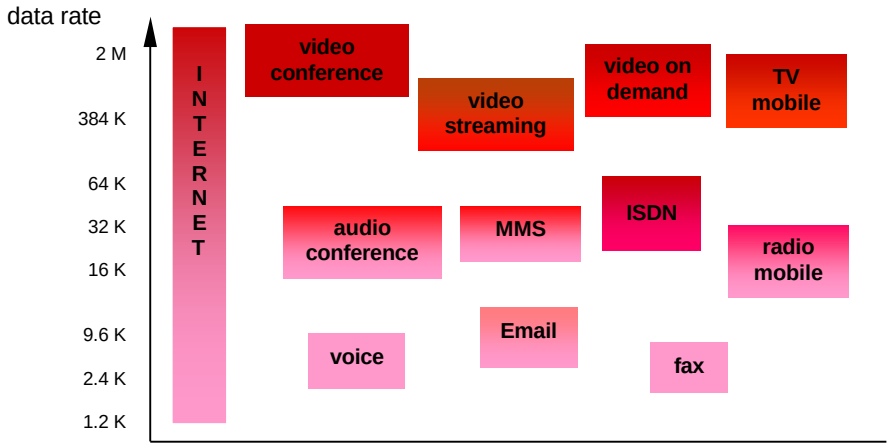

Figure 2.2 Bit rate requirements for some 3G applications [Sau02]

Because of these drivers, the International Telecommunications Union (ITU) has been developing 3G since 1985. 3G networks are referred as IMT-2000 (International Mobile Telephony) within ITU and UMTS (Universal Mobile Telecommunications Services) in Europe. In ETSI (European Telecommunications Standards Institute), UMTS standardisation started in 1990.

2.1.3.1 Objectives and requirement

Third generation systems are designed for multimedia communications: person-to-person communication can be enhanced with high quality images and video. Also, access to information and services on public and private networks will be enhanced by the higher data rates and new flexible communication capabilities of these systems. Third generation systems can offer simultaneous multiple services for one user and services with different Quality of Service (QoS) classes.

The main objectives for the IMT-2000 systems can be summarised as:

- Full coverage and mobility for 144 kbit/s, preferably 384 kbit/s;
- Limited coverage and mobility for 2 Mbit/s;
- Provides both symmetric and asymmetric data transmission;
- Provides both circuit switched and packet switched connections;
- Capable of carrying Internet Protocol (IP) traffic;
- Global roaming capabilities;
- High spectrum efficiency compared to existing systems;
- High flexibility to introduce new services;

The bit-rate targets have been specified according to the integrated services digital network (ISDN). The 144 kbit/s data rate provides the ISDN 2B+D channel configuration, 384 kbit/s provides the ISDN H0 channel, and 1.92 Mbit/s provides the ISDN H12 channel. Figure 2.3 shows the relation between bit rates and mobility for the different systems.

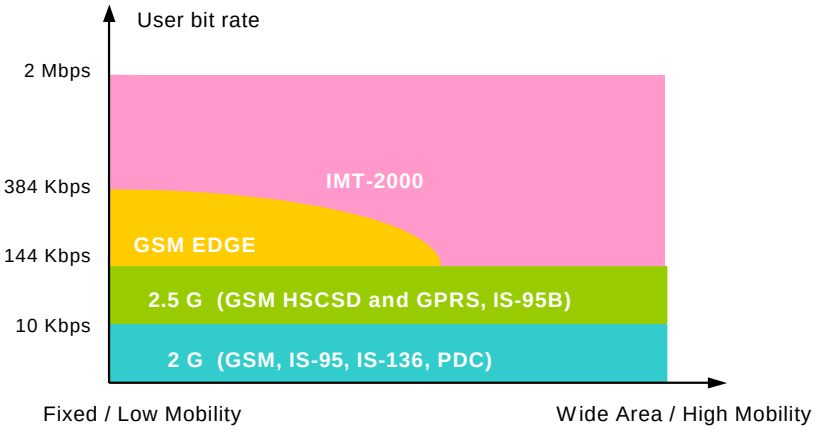

Figure 2.3 User bit rate versus coverage and mobility

2.1.3.2 Air Interface and spectrum allocation

Within the IMT-2000 framework, several different air interfaces are defined for 3G systems, based on either CDMA or TDMA technology. Currently, there are five interfaces agreed by ITU and being under standardisation as shown in Figure 2.4.

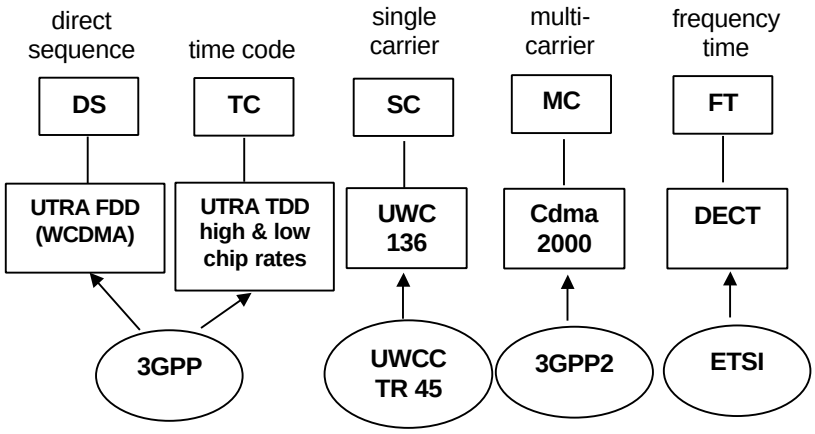

Figure 2.4 IMT-2000 air interfaces [Scr02]

Among these interfaces, WCDMA has been adopted as the radio access technology of UMTS; it is also to be used in Asia, including Japan and Korea. More details about WCDMA technology will be presented in section 2.2. Multicarrier CDMA (cdma2000) can be used as an upgrade solution for the existing IS-95.

In 1992, the World Administrative Radio Conference (WARC) allocated spectrum bands 1885 – 2025 MHz and 2100 – 2200 MHz for IMT-2000 systems, and in WRC2000, two further spectrum bands 1710 – 1885 MHz and 2500 – 2690 MHz were added. However, different countries have their own usage because of the different choices of 3G air interface and the different existing 2G systems. Figure 2.5 shows the spectrum allocations for 3G systems in different countries and Table 2.2 shows the expected frequency bands and geographical areas where different air interfaces are likely to be applied [HT00].

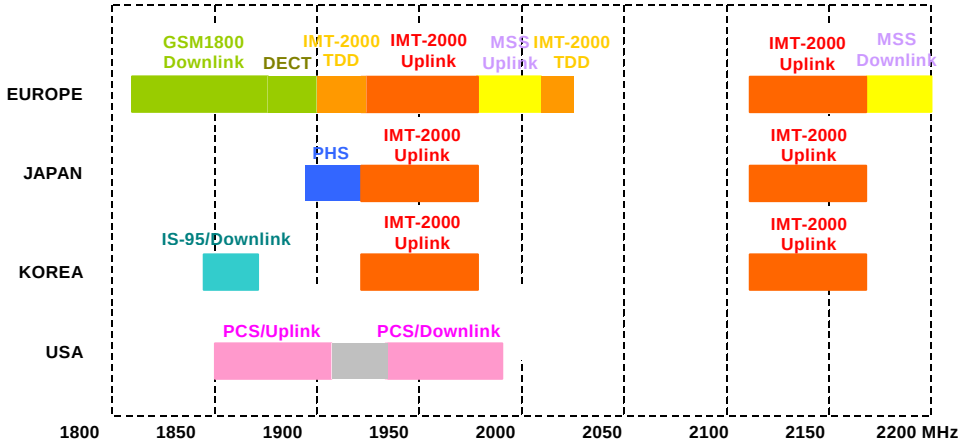

Figure 2.5 Spectrum allocation in different countries

Area	*Frequency band*	*Air Interface*
Europe	IMT-2000 band	WCDMA
	GSM 1800 band	EDGE
Americas	In the existing bands that are already used by second generation systems.	EDGE, WCDMA, and multicarrier CDMA (cdma2000)
Asia	IMT-2000 band	WCDMA
	GSM 1800 band	EDGE
Japan	IMT-2000 band	WCDMA
Korea	IMT-2000 band	WCDMA

Table 2.2 Expected spectrums and air interfaces for providing 3G services.

2.1.3.3 3G systems and beyond

Currently 3G technologies are starting to be launched commercially; for example, Hutchison launched 3G in the UK in 2002.

Recently, systems beyond 3G (B3G systems) are attracting more and more attention. Many international Forums such as ITU-R WP8F Vision Group and the EU initiated Wireless World Research Forum (WWRF) are undertaking research on B3G systems. In 2002, ITU-R WP8F held the 9th meeting, subtitled “System Capabilities for system beyond 3G”. Figure 2.6 shows the expected capabilities for B3G systems from that. Higher bit rate with higher mobility is expected to be required for future new applications.

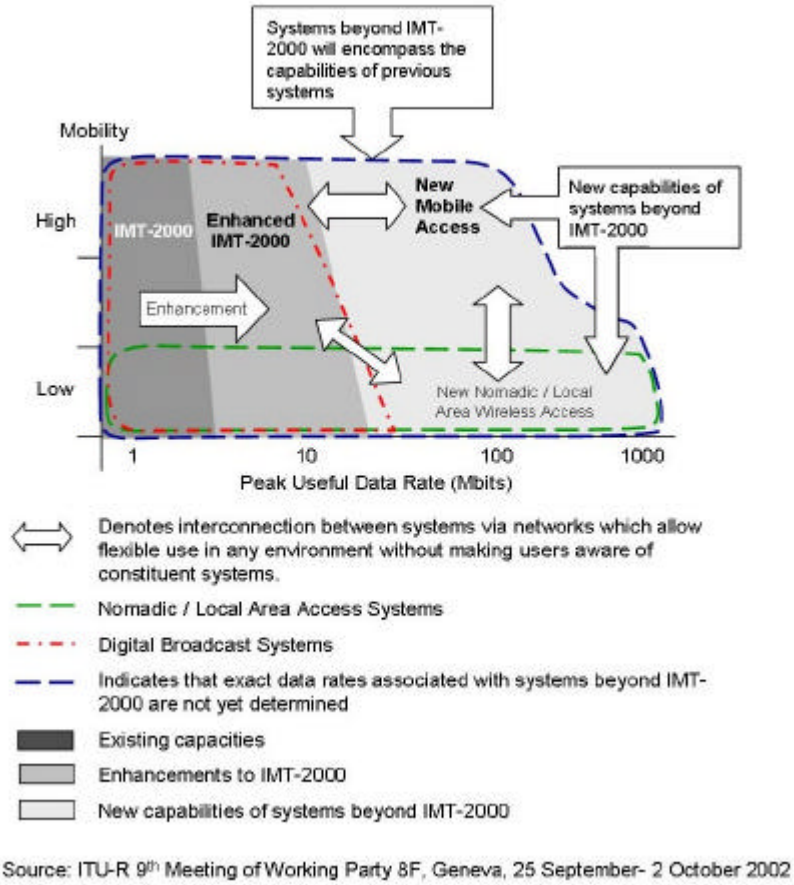

Source: ITU-R 9th Meeting of Working Party 8F, Geneva, 25 September- 2 October 2002

Figure 2.6 Systems beyond 3G (*Source:* ITU-R M. [FPLMTS.REVAL])

Meanwhile, fourth-generation mobile networks branded 4G have already been proposed. Although there is no uniform definition about what 4G is and what exactly marks the generation, the vision for the 4G mobile networks is developing, with different views being taken in different areas around the world. In Asia, 4G is being foreseen as an air interface that could support up to 100 Mbit/s for high mobility and up to 1 Gbit/s for low mobility.

In the US, 4G is expected to be the combination of Wireless Local Access Network (WLAN) and IEEE 802.20[1]. In Europe, the understanding of 4G is a network of networks, which includes multiple interworking networks and devices. In this kind of network, the following different technologies might coexist with seamless interworking being supported between them.

- Cellular Mobile (2/2.5/3G)
- Wireless LAN (IEEE802.11x)
- Personal Area Networking (Bluetooth)
- Digital Broadcasting (video, audio, DVB, DAB)
- Home Entertainment Wireless Networking
- Multi-Modal Services

Figure 2.7 shows the concept of the heterogeneous network.

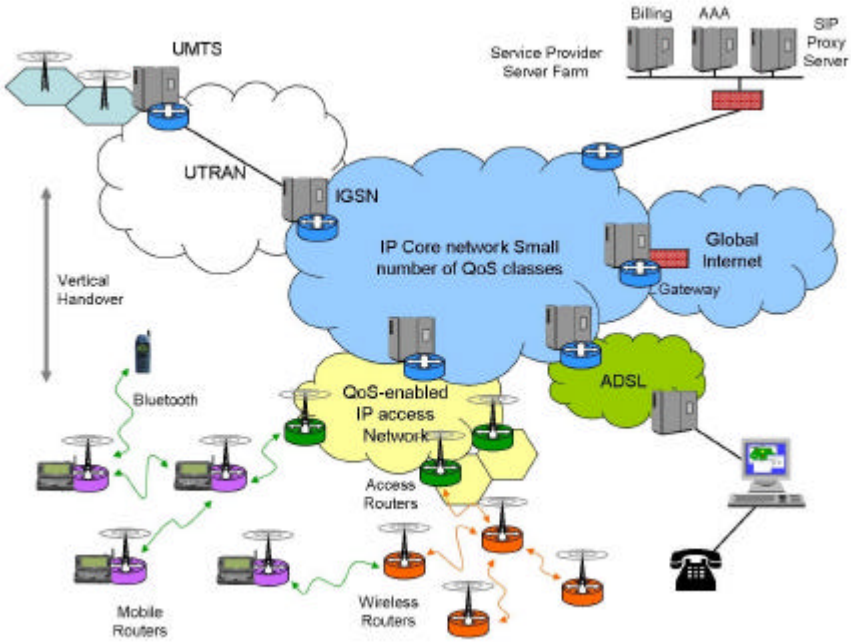

Figure 2.7 Heterogeneous network with interworking access systems for next generation [W02]

[1] On 11 December 2002, the IEEE Standards Board approved the establishment of IEEE 802.20, the Mobile Broadband Wireless Access (MBWA) Working Group. IEEE 802.20 specifies an efficient packet based air interface that is optimized for the transport of IP based services. The goal is to enable worldwide deployment of affordable, ubiquitous, always-on and interoperable multi-vendor mobile broadband wireless access networks that meet the needs of business and residential end user markets.

In the future, wireless communication is going to move towards universal communication that uses a very flexible networking infrastructure and dynamically adapts to the changing requirements.

2.2 Overview of CDMA Technology

2.2.1 Principles of spectrum spreading (CDMA)

Digital communications systems are designed to maximise capacity utilisation. From Shannon's channel capacity principle expressed as (2.1), it is obvious that the channel capacity can be increased by increasing the channel bandwidth.

$$C = B \cdot \log_2\left(1 + S/N\right) \tag{2.1}$$

Where B is the bandwidth (Hz), C is the channel capacity (bit/s), S is the signal power and N is the noise power. Thus, for a particular S/N ratio (Signal to Noise Ratio: SNR), the capacity is increased if the bandwidth used to transfer information is increased. CDMA is a technology that spreads the original signal to a wideband signal before transmission. CDMA is often called as Spread-Spectrum Multiple Access (SSMA).

The ratio of transmitted bandwidth to information bandwidth is called the processing gain G_p (also called spreading factor).

$$G_p = \frac{B_t}{B_i} \quad or \quad G_p = \frac{B}{R} \tag{2.2}$$

Where B_t is the transmission bandwidth, B_i is the bandwidth of the information bearing signal, B is the RF bandwidth and R is the information rate. Relating the S/N ratio to the E_b/I_0 ratio, where E_b is the energy per bit, and I_0 is the noise power spectral density, leading to:

$$\frac{S}{N} = \frac{E_b \times R}{I_0 \times B} = \frac{E_b}{I_0} \times \frac{1}{G_p} \tag{2.3}$$

Therefore, for certain E_b/I_0 requirement, the higher the processing gain, the lower the S/N ratio required. In the first CDMA system, IS-95, the transmission bandwidth is 1.25 MHz. In WCDMA system, the transmission bandwidth is about 5 MHz.

In CDMA, each user is assigned a unique code sequence (spreading code) that is used to spread the information signal to a wideband signal before being transmitted. The receiver knows the code sequence for that user, and can hence decode it and recover the original data.

2.2.2 Spreading and de-spreading

Spreading and de-spreading are the most basic operations in DS-CDMA systems, shown as Figure 2.8. User data here is assumed to be a BPSK-modulated bit sequence of rate *R*. The spread operation is the multiplication of each user data bit with a sequence of *n* code bits, called chips. Here, *n*=8, and hence the spreading factor is 8. This is also assumed for the BPSK spreading modulation. The resulting spread data is at a rate of 8×R and has the same random (pseudo-noise-like) appearance as the spreading code. The increase of data rate by a factor 8 corresponds to a widening (by a factor 8) of the occupied spectrum of the spread user data signal. This wideband signal would then be transmitted across a radio channel to the receiving end.

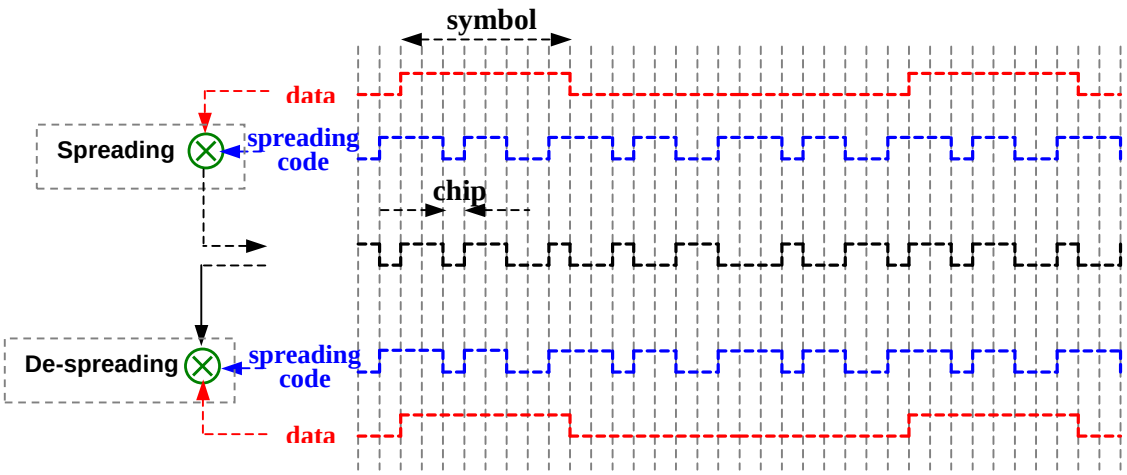

Figure 2.8 Spreading and de-spreading

During de-spreading, the spread user data/chip sequence is multiplied bit by bit with the same 8 code chips as used during the spreading process. As shown, the original users data is recovered perfectly.

2.2.3 Multiple access

A mobile communication network is a multi-user system, in which a large number of users share a common physical resource to transmit and receive information. Multiple access capability is one of the fundamental components. The spectral spreading of the transmitted signal gives the feasibility of multiple access to CDMA systems. Figure 2.9 shows three different multiple access technologies: TDMA, FDMA and CDMA.

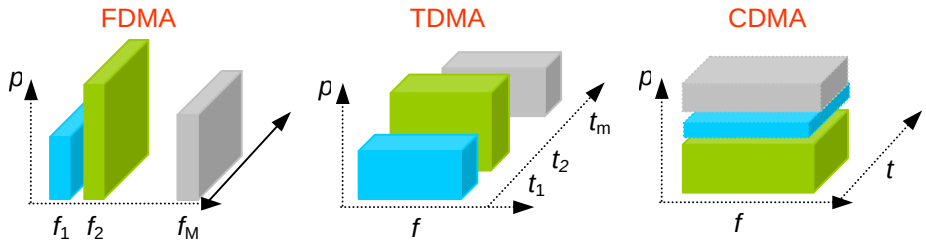

Figure 2.9 Multiple access technologies

In FDMA, (Frequency Division Multiple Access), signals for different users are transmitted in different channels each with a different modulating frequency; in TDMA, (Time Division Multiple Access), signals for different users are transmitted in different time slots. With these two technologies, the maximum number of users who can share the physical channels simultaneously is fixed. However, in CDMA, signals for different users are transmitted in the same frequency band at the same time. Each user's signal acts as interference to other user's signals and hence the capacity of the CDMA system is related closely to the interference level: there is no fixed maximum number, so the term *soft capacity* is used. Figure 2.10 shows an example of how 3 users can have simultaneous access in a CDMA system.

At the receiver, user 2 de-spreads its information signal back to the narrow band signal, but nobody else's. This is because that the cross-correlations between the code of the desired user and the codes of other users are small: coherent detection will only put the power of the desired signal and a small part of the signal from other users into the information bandwidth.

The processing gain, together with the wideband nature of the process, gives benefits to CDMA systems, such as high spectral efficiency and soft capacity.

However, all these benefits require the use of tight power control and soft handover to avoid one user's signal cloaking the communication of others. Power control and soft handover will be explained in more detailed level in section 2.3.2.1 and Chapter 3 respectively.

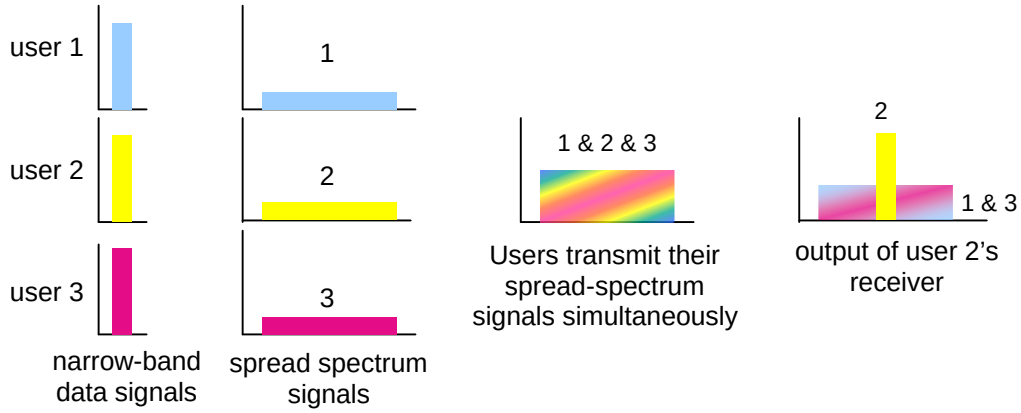

Figure 2.10 Principle of spread-spectrum multiple access

2.2.4 Features of WCDMA

Wideband-CDMA (WCDMA) has been adopted by UMTS as the multiple access technology and it is also referred to as UMTS terrestrial radio access (UTRA). This section introduces the principles of the WCDMA air interface. Special attention is drawn to those features by which WCDMA differs from GSM and IS-95.

Table 2.3 summarises the main parameters related to the WCDMA air interface. Some of the items that characterise WCDMA are:

- **WCDMA is a wideband CDMA system**. User information bits are spread over a wide bandwidth (5 MHz) by multiplying with spreading codes before transmission and are recovered by decoding in the receiver [OP98].

- The **chip rate of 3.84 Mchip/s** used leads to **a carrier bandwidth of approximately 5 MHz**. In GSM, carrier bandwidth is only 200 kHz. Even in narrowband CDMA systems, such as IS-95, the carrier bandwidth is only 1.25 MHz. The inherently wide carrier bandwidth of WCDMA supports high user data

rates and also has certain performance benefits, such as increased multipath diversity [TR00].

- **WCDMA supports highly variable user data rates**; in other words the concept of obtaining Bandwidth on Demand (BoD) is well supported. Each user is allocated frames of 10 ms duration, during which the user data rate is kept constant. However, the data capacity among the users can change from frame to frame.

- **WCDMA supports two basic modes of operation**: Frequency Division Duplex (FDD) and Time Division Duplex (TDD). In FDD mode, separate 5MHz carriers are used for the uplink and downlink respectively, whereas in TDD only one 5 MHz is time-shared between uplink and downlink.

- **WCDMA supports the operation of asynchronous base stations**. Unlike the synchronous IS-95 system, there is no need for a global time reference, such as a GPS, so making deployment of indoor and micro base stations easier.

- **WCDMA employs coherent detection on uplink and downlink** based on the use of pilot symbols or common pilot. In IS-95 coherent detection is only used on the downlink. The use of coherent detection on uplink will result in an overall increase of coverage and capacity on the uplink. This makes the downlink more likely to be the bottleneck of the whole system.

- The WCDMA air interface has been crafted in such a way that advanced CDMA receiver concepts, such as **multiuser detection** (MUD) [Ver86][OPH98][JL00] and **smart adaptive antennas** [VMB00] [LA01], can be deployed by the network operator as a system option to increase capacity and/or coverage. In most second generation systems no provision has been made for such concepts.

- WCDMA is designed to be deployed in conjunction with GSM. Therefore, **handovers between GSM and WCDMA are supported**.

Multiple access method	DS-CDMA
Duplexing method	FDD/TDD
Base station synchronisation	Asynchronous operation
Chip rate	3.84 Mcps
Frame length	10 ms
Service multiplexing	Multiple services with different quality of service requirements multiplexed on one connection
Multirate concept	Variable spreading factor and multicode
Detection	Coherent using pilot symbols or common pilot
Multiuser detection, Smart antennas	Supported by the standard, optional in the implementation

Table 2.3 Main WCDMA parameters

2.3 Radio Resource Management

2.3.1 RRM in mobile networks

Radio Resource Management (RRM) in 3G networks is responsible for improving the utilisation of the air interface resources. The objectives of using RRM can be summarised as follows:

- Guarantee the QoS for different applications
- Maintain the planned coverage
- Optimise the system capacity

In 3G networks, pre-allocating resource and over-dimensioning the network are not feasible any more because of the unpredictable need and the variable requirements of different services. Therefore, radio resource management is composed of two parts: radio resource configuration and re-configuration. Radio resource configuration is responsible for allocating the resource properly to new requests coming into the system so that the network is not overloaded and remains stable. But, as congestion might occur in 3G networks because of the mobility of users, radio resource re-configuration is responsible for re-allocating the resource within the network when load is building up or congestion starts to appear. It is responsible for returning the overloaded system quickly and controllably back to the targeted load.

2.3.2 Functionalities of RRM

Radio resource management can be divided into power control, handover, admission control and load control functionalities. Figure 2.11 shows the typical locations of RRM functionalities within a WCDMA network.

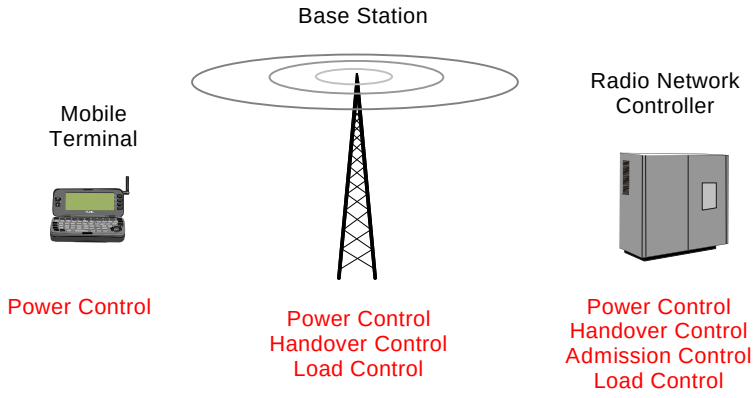

Figure 2.11 Typical locations of RRM functionalities within a WCDMA network

2.3.2.1 Power control

Power control is a necessary element in all mobile systems because of the battery life problem and safety reasons, but in CDMA systems, power control is essential because of the interference-limited nature of CDMA.

In GSM slow (frequency approximately 2 Hz) power control is employed. In IS-95 fast power control with 800 Hz is supported in the uplink, but in the downlink, a relatively slow (approximately 50 Hz) power control loop controls the transmission power. In WCDMA fast power control with 1.5kHz frequency is supported in both uplink and downlink [OP98]. Tight and fast power control is one of the most important aspects of WCDMA systems.

The reasons for using power control are different in the uplink and downlink. The overall objectives of power control can be summarised as follows:

- Overcoming the near-far effect in the uplink
- Optimising system capacity by controlling interference
- Maximising the battery life of mobile terminals (not considered further)

Figure 2.12 shows near-far problem [SL-SWJ99] in the **uplink**. Signals from different MSs are transmitted in the same frequency band simultaneously in WCDMA systems. Without power control, the signal coming from the MS that is nearest to the BS may block signals from other MSs that are much farer away from the BS. In the worst situation one over-powered MS could block a whole cell. The solution is to apply power control to guarantee that signals coming from different terminals have the same power or the same SIR (Signal-to-interference Ratio) when they arrive at the BS.

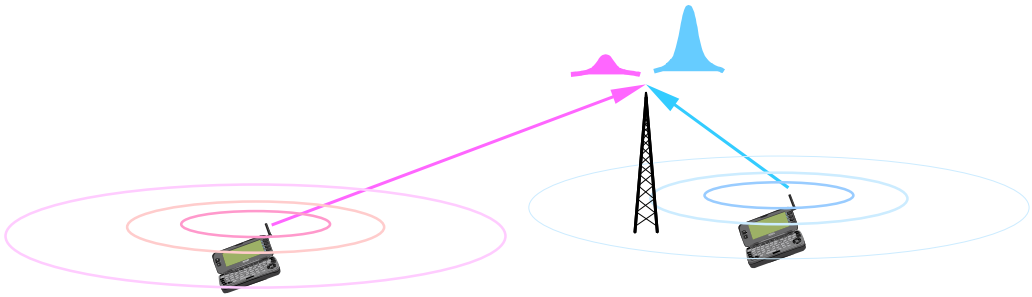

Figure 2.12 Near-Far effects (power control in UL)

In the **downlink** direction, there is no near-far problem due to the one-to-many scenario. Power control is responsible for compensating the inter-cell interference suffered by the mobiles, especially those near cell boundaries as shown in Figure 2.13. Moreover, power control in the downlink is responsible for minimising the total interference by keeping the QoS at its target value.

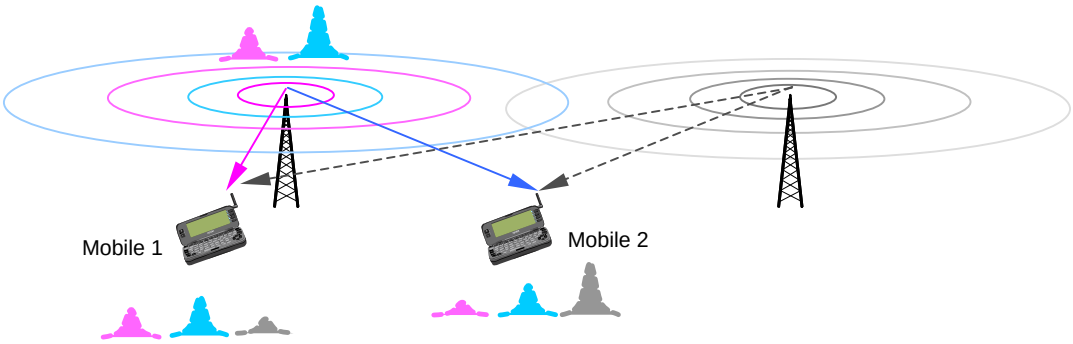

Figure 2.13 Compensating the inter-cell interference (power control in DL)

In Figure 2.13, mobile 2 suffers more inter-cell interference than mobile 1. Therefore, to meet the same quality target, more power needs to be allocated to the downlink channel between the BS and mobile 2.

There are three types of power control in WCDMA systems: open-loop power control, closed-loop power control, and outer-loop power control.

1. Open-loop power control

Open-loop power control is used in the UMTS FDD mode for the mobile initial power setting. The mobile estimates the path loss between the base station and the mobile by measuring the received signal strength using an automatic gain control (AGC) circuit. According to this estimate of path loss, the mobile can decide its uplink transmit power. Open-loop power control is effective in a TDD system because the uplink and downlink are reciprocal, but it is not very effective with FDD system because the uplink and downlink channels operate on different frequency bands and the Rayleigh fading in the uplink and downlink is independent. So open-loop power control can only roughly compensate distance attenuation. That is why it is only used as an initial power setting in FDD systems.

2. Closed-loop power control

Closed-loop power control, also called fast power control in WCDMA systems, is responsible for controlling the transmitted power of the MS (uplink) or of the base station (downlink) in order to counteract the fading of the radio channel and meet the SIR (signal-to-interference ratio) target set by the outer-loop. For example, in the uplink, the base station compares the received SIR from the MS with the target SIR once every time slot (0.666ms). If the received SIR is greater than the target, the BS transmits a TPC command “0” to the MS via the downlink dedicated control channel. If the received SIR is lower than the target, the BS transmits a TPC command “1” to the MS. Because the frequency of closed-loop power control is very fast it can compensate fast fading as well as slow fading.

3. Outer-loop power control

Outer-loop power control is needed to keep the quality of communication at the required level by setting the target for the fast closed-loop power control. It aims at providing the required quality: no worse, no better. The frequency of outer-loop power control is typically 10-100Hz. Figure 2.14 shows the general algorithm of outer-loop power control.

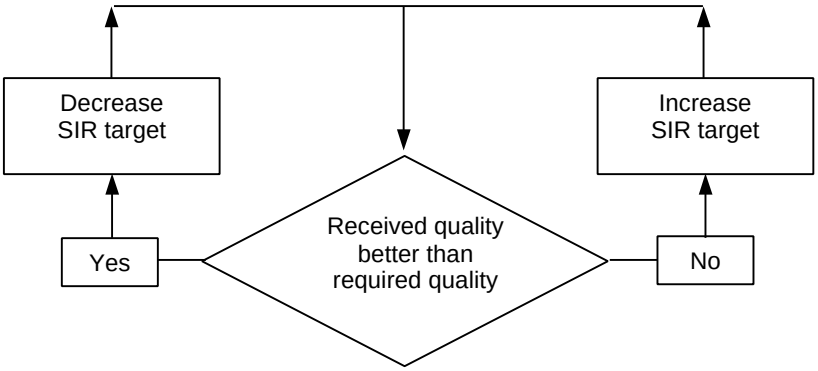

Figure 2.14 General outer-loop power control algorithm

The outer-loop power control compares the received quality to the required quality. Usually the quality is defined as a certain target Bit Error Rate (BER) or Frame Error Rate (FER). The relationship between the SIR target and the quality target depends on the mobile speed and the multipath profile. If the received quality is better, it means the current SIR target is high enough for guaranteeing the required QoS. In order to minimise the headroom, the SIR target will be reduced. However, if the received quality is worse than the required quality, the SIR target needs to be increased for guaranteeing the required QoS.

2.3.2.2 Handover control

Handover is an essential component of mobile cellular communication systems. Mobility causes dynamic variations in link quality and interference levels in cellular systems, sometimes requiring that a particular user change its serving base station. This change is known as handover. More detailed information is presented in the next chapter (Chapter 3).

2.3.2.3 Admission control

If the air interface loading is allowed to increase excessively, the coverage area of the cell is reduced below the planned values (so called “cell breathing”), and the QoS of the existing connections cannot be guaranteed. The reason for the “cell breathing” phenomenon is because of the interference-limited feature of CDMA systems. Therefore, before admitting a new connection, admission control needs to check that

admitting the new connection will not sacrifice the planned coverage area or the QoS of existing connections. Admission control accepts or rejects a request to establish a radio access bearer in the radio access network. The admission control functionality is located in RNC where the load information of several cells can be obtained.

The admission control algorithm estimates the load increase that the establishment of the bearer would cause in the radio access network. The load estimation is applied for both uplink and downlink. The requesting bearer can be admitted only if the admission controls in both directions admit it, otherwise it is rejected because of the excessive interference that it adds to the network.

Several admission control schemes have been suggested. In [DKOPR94] [HY96] and [KBPY97], the use of the total power received by the base station is supported as the primary uplink admission control decision criterion. In [DKOPR94] and [KBPY98] a downlink admission control algorithm based on the total downlink transmission power is presented.

Generally, the admission control strategies can be divided into two types: wideband power-based admission control strategy and throughput-based admission control strategy.

Figure 2.15 shows the wideband power-based admission control.

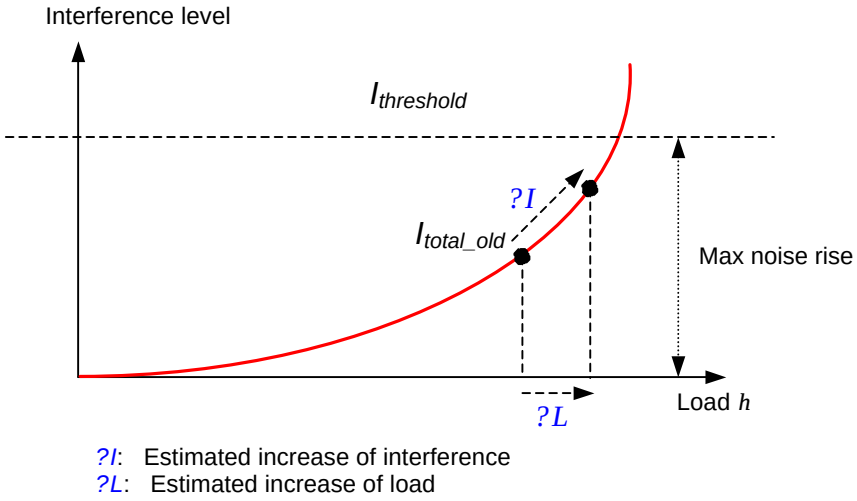

Figure 2.15 Load curve

The new user is not admitted if the new resulting total interference level is higher than the threshold value:

$$\begin{cases} reject: & I_{total\_old} + \Delta I > I_{threshold} \\ admit: & I_{total\_old} + \Delta I < I_{threshold} \end{cases} \quad (2.4)$$

The threshold value is the same as the maximum uplink noise increase and can be set by radio network planning.

In throughput-based admission control strategy the new requesting user is not admitted into the radio access network if the new resulting total load is higher than the threshold value:

$$\begin{cases} reject: & h_{total\_old} + \Delta L > h_{threshold} \\ admit: & h_{total\_old} + \Delta L < h_{threshold} \end{cases} \quad (2.5)$$

It should be noted that as the admission control is applied separately for uplink and downlink, different admission control strategies can be used in each direction.

2.3.2.4 Load control (congestion control)

One important task of the radio resource management functionality is to ensure that the system is not overloaded and remains stable. If the system is properly planned, and the admission control works well, overload situations should be exceptional. However, in mobile networks, overload somewhere is inevitable because the radio resource cannot be pre-allocated within the network. When overload is encountered, the load control, also called congestion control, returns the system quickly and controllably back to targeted load, which is defined by the radio network planning. The possible load control actions in order to reduce or balance load are listed below:

- Deny downlink power-up commands received from the MS.
- Reduce the uplink E_b/I_0 target used by uplink fast power control.
- Change the size of soft handover zone to accommodate more users.
- Handover to another WCDMA carrier (inter-frequency handover).
- Handover to overlapping network (another UMTS network or GSM network).
- Decrease bit rates of real-time users, e.g. AMR speech codec.
- Reduce the throughput of packet data traffic (non-real-time service).

- Drop calls in a controlled way.

The first two in the list are fast actions that are carried out within the BS. These actions can take place within one timeslot, i.e. with 1.5kHz frequency, and provide prioritisation of the different services. The third method, changing the size of soft handover zone is especially useful to a downlink-limited network and this is discussed in more detail in the next chapter.

The other load control actions are typically slower. Inter-frequency handover and inter-system handover can overcome overload by balancing the load. The final action is to drop real-time users (i.e. speech or circuit switched data users) in order to reduce the load. This action is taken only if the load of the whole network remains very high even after other load control actions have been effected in order to reduce the overload. The WCDMA air interface and the expected increase of non-real-time traffic in third generation networks give a large selection of possible actions to handle overload situations, and therefore the need to drop real-time users to reduce overload should be very rare.

2.4 Summary

This chapter gives a brief overview of the evolution of mobile networks and introduces the basic concepts of CDMA technology and functionalities of radio resource management. As one of the crucial components of radio resource management, handover (the focus of this thesis) is described in the next chapter. The basic principle, previous research and existing problems of soft handover are presented, which bring out the motivation of the work.

Chapter 3 Handover

3.1 Overview of Handover in Mobile Networks

Mobile networks allow users to access services while on the move so giving end users “freedom” in terms of mobility. However, this freedom does bring uncertainties to mobile systems. The mobility of the end users causes dynamic variations both in the link quality and the interference level, sometimes requiring that a particular user change its serving base station. This process is known as handover (HO).

Handover is the essential component for dealing with the mobility of end users. It guarantees the continuity of the wireless services when the mobile user moves across cellular boundaries.

In first-generation cellular systems like AMPS, handovers were relatively simple. Second-generation systems like GSM and PACS are superior to 1G systems in many ways, including the handover algorithms used. More sophisticated signal processing and handover decision procedures have been incorporated in these systems and the handover decision delay has been substantially reduced. Since the introduction of CDMA technology, another idea that has been proposed for improving the handover process is **soft handover** and this is the focus of the work in this thesis.

3.1.1 Types of handover in 3G WCDMA systems

There are four different types of handovers in WCDMA mobile networks. They are:

- **Intra-system HO**

  Intra-system HO occurs within one system. It can be further divided into **Intra-frequency HO** and **Inter-frequency HO**. Intra-frequency occurs between cells belonging to the same WCDMA carrier, while Inter-frequency occurs between cells operate on different WCDMA carriers.

- **Inter-system HO**

  Inter-system HO takes places between cells belonging to two different Radio Access Technologies (RAT) or different Radio Access Modes (RAM). The most frequent case for the first type is expected between WCDMA and GSM/EDGE

systems. Handover between two different CDMA systems also belongs to this type. An example of inter-RAM HO is between UTRA FDD and UTRA TDD modes.

- **Hard Handover (HHO)**

  HHO is a category of HO procedures in which all the old radio links of a mobile are released before the new radio links are established. For real-time bearers it means a short disconnection of the bearer; for non-real-time bearers HHO is lossless. Hard handover can take place as intra or inter-frequency handover.

- **Soft Handover (SHO) and Softer HO**

  During soft handover, a mobile simultaneously communicates with two (2-way SHO) or more cells belonging to different BSs of the same RNC (intra-RNC) or different RNCs (inter-RNC). In the downlink (DL), the mobile receives both signals for maximal ratio combining: in the uplink (UL), the mobile code channel is detected by both BSs (2-way SHO), and is routed to the RNC for selection combining. Two active power control loops participate in soft handover: one for each BS. In the softer handover situation, a mobile is controlled by at least two sectors under one BS, the RNC is not involved and there is only one active power control loop. SHO and softer HO are only possible within one carrier frequency and therefore, they are intra-frequency handover processes.

Figure 3.1 shows some scenarios of different types of HO.

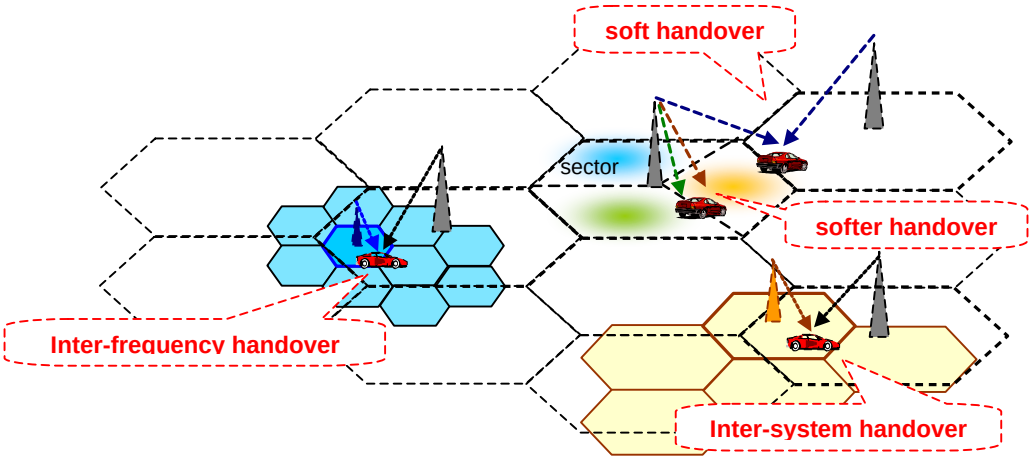

Figure 3.1 Scenarios of different types of handover.

3.1.2 Objectives of handover

Handover can be initiated in three different ways: mobile initiated, network initiated and mobile assisted.

- **Mobile Initiated**: the Mobile makes quality measurements, picks the best BS, and switches, with the network's cooperation. This type of handover is generally triggered by the poor link quality measured by the mobile.

- **Network Initiated**: the BS makes the measurements and reports to the RNC, which makes the decision whether to handover or not. Network initiated handover is executed for reasons other than radio link control, e.g. to control traffic distribution between cells. An example of this is the BS-controlled Traffic Reason Handover (TRHO). TRHO is a load-based algorithm that changes the handover threshold for one or more outgoing adjacencies for a given source cell depending on its load. If the load of the source cell exceeds a given level, and the load in a neighbouring cell is below another given level, then the source cell will shrink its coverage, handing over some traffic to the neighbouring cell. Therefore, the overall blocking rate can be reduced, leading to a greater utilisation of the cell resource.

- **Mobile Assisted**: here the network and the mobile both make measurements. The mobile reports the measurement results from nearby BSs and the network makes the decision of handing over or not.

The objectives of handover can be summarised as follows:

- Guaranteeing the continuity of wireless services when the mobile user moves across the cellular boundaries
- Keep required QoS
- Minimising interference level of the whole system by keeping the mobile linked to the strongest BS or BSs.
- Roaming between different networks
- Distributing load from hot spot areas (load balancing)

The triggers that can be used for the initiation of a handover process could be the link quality (UL or DL), the changing of service, the changing of speed, traffic reasons or O&M (Operation & Maintenance) intervention.

3.1.3 Handover measurements and procedures

The handover procedure can be divided into three phases: measurement, decision and execution phases as illustrated in Figure 3.2.

In the handover measurement phase, the necessary information needed to make the handover decision is measured. Typical downlink measurements performed by the mobile are the E_c/I_0[2] of the Common Pilot Channel (CPICH) of its serving cell and neighbouring cells. For certain types of handover, other measurements are needed as well. For example, in an asynchronous network like UTRA FDD (WCDMA), the relative timing information between the cells needs to be measured in order to adjust the transmission timing in soft handover to allow coherent combining in the Rake receiver. Otherwise, the transmissions from the different BSs would be difficult to combine and especially the power control operation in soft handover would suffer additional delay.

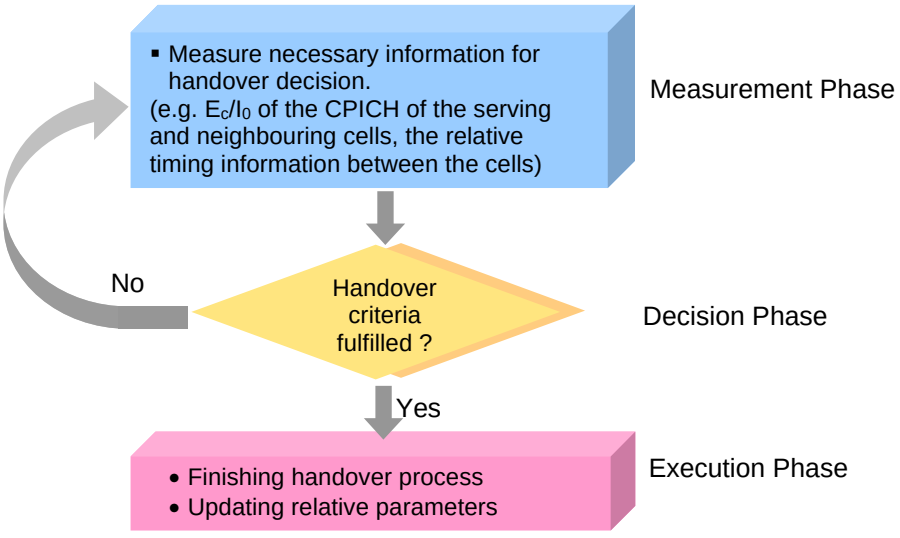

Figure 3.2 Handover procedures

[2] E_c is the pilot energy per chip and I_0 is the total interference power spectral density.

In the handover decision phase, the measurement results are compared against the predefined thresholds and then it is decided whether to initiate the handover or not. Different handover algorithms have different trigger conditions.

In the execution phase, the handover process is completed and the relative parameters are changed according to the different types of handover. For example, in the execution phase of the soft handover, the mobile enters or leaves the soft handover state, a new BS is added or released, the active set is updated and the power of each channel involved in soft handover is adjusted.

3.2 Soft Handover (SHO)

Soft handover was introduced by CDMA technology. Compared to the conventional hard handover, soft handover has quite a few inherent advantages. However, it also has the disadvantages of complexity and extra resource consumption. Planning of soft handover overhead is one of the fundamental components of the radio network planning and optimisation [HT00]. In this section, the basic principles of soft handover are presented.

3.2.1 Principles of soft handover

Soft handover is different from the traditional hard handover process. With hard handover, a definite decision is made on whether to handover or not and the mobile only communicates with one BS at a time. With soft handover, a conditional decision is made on whether to handover or not. Depending on the changes in pilot signal strength from the two or more BSs involved, a hard decision will eventually be made to communicate with only one. This normally happens after it is clear that the signal coming from one BS is considerably stronger than those come from the others. In the interim period of soft handover, the mobile communicates simultaneously with all the BSs in the active set[3]. The difference between hard and soft handover is like the difference between a swimming relay and track-and-field relay events. Hard handover happens on a time point; while, soft handover lasts for a period of time.

[3] Active set: The active set is the list of cells that are presently having connections with the mobile.

Figure 3.3 shows the basic process of hard and soft handover (2-way case). Assuming there is a mobile terminal inside the car moving from cell 1 to cell 2, BS_1 is the mobile's original serving BS. While moving, the mobile continuously measures the pilot signal strength received from the nearby BSs. With hard handover shown as (a) in Figure 3.3, the trigger of the handover can be simply described as:

```
If (pilot_Ec/I0)2 - (pilot_Ec/I0)1 > D and BS1 is the serving BS
        Handover to BS2 ;
else
        do not handover ;
end
```

Where $(pilot\_\ E_c/I_0)_1$ and $(pilot\_\ E_c/I_0)_2$ are the received pilot E_c/I_0 from BS_1 and BS_2 respectively; D is the hysteresis margin.

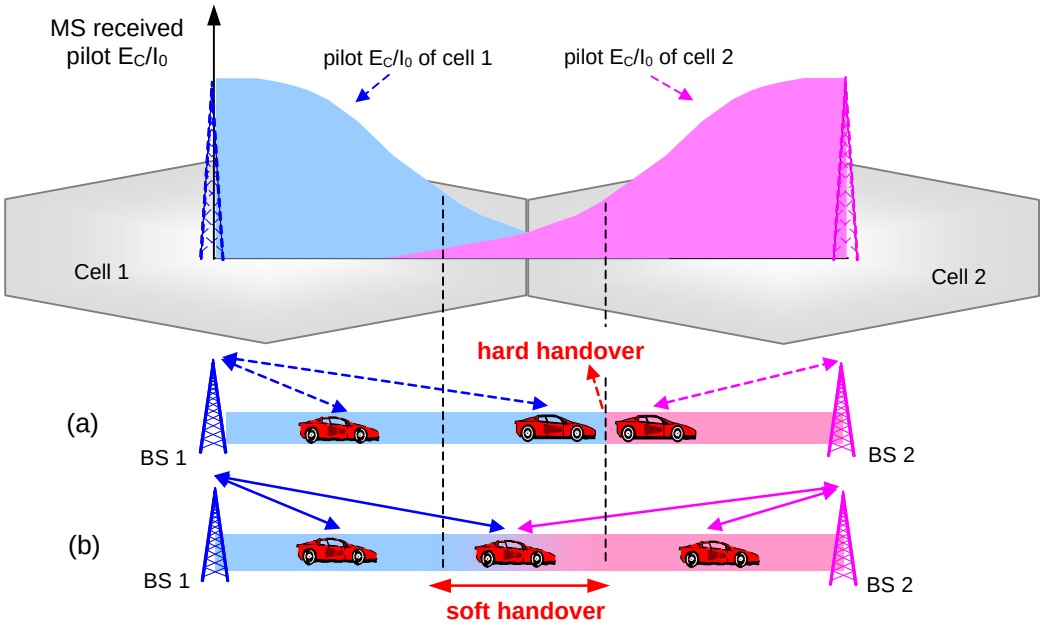

Figure 3.3 Comparison between hard and soft handover

The reason for introducing the hysteresis margin in the hard handover algorithm is to avoid a "ping-pong effect", the phenomenon that when a mobile moves in and out of cell's boundary, frequent hard handover occurs. Apart from the mobility of the mobile, fading effects of the radio channel can also make the "ping-pong" effect more serious. By introducing the hysteresis margin, the "ping-pong" effect is mitigated because the mobile does not handover immediately to the better BS. The bigger the margin, the less the "ping-pong" effect. However, a big margin, means more delay. Moreover, the

mobile causes extra interference to neighbouring cells due to the poor quality link during the delay. Therefore, to hard handover, the value of the hysteresis margin is fairly important. When hard handover occurs, the original traffic link with BS_1 is dropped before the setting up of the new link with BS_2 so hard handover is a process of "break before make".

In the case of soft handover, shown as (b) in Figure 3.3, before $(pilot\_\ E_c/I_0)_2$ goes beyond $(pilot\_\ E_c/I_0)_1$, as long as the soft handover trigger condition is fulfilled, the mobile enters the soft handover state and a new link is set up. Before BS_1 is dropped (handover dropping condition is fulfilled), the mobile communicates with both BS_1 and BS_2 simultaneously. Therefore, unlike hard handover, soft handover is a process of "make before break". So far, several algorithms have been proposed to support soft handover and different criteria are used in different algorithms.

The soft handover process is not the same in the different transmission directions. Figure 3.4 illustrates this. In the uplink, the mobile transmits the signals to the air through its omnidirectional antenna. The two BSs in the active set can receive the signals simultaneously because of the frequency reuse factor of one in CDMA systems. Then, the signals are passed forward to the RNC for selection combining. The better frame is selected and the other is discarded. Therefore, in the uplink, there is no extra channel needed to support soft handover.

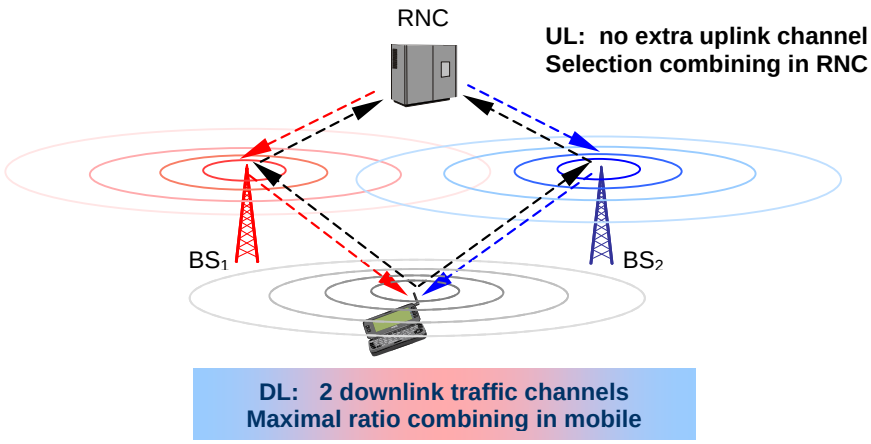

Figure 3.4 Principles of soft handover (2-way case)

In the downlink, the same signals are transmitted through both BSs and the mobile can coherently combine the signals from different BSs since it sees them as just

additional multipath components. Normally maximum ratio combining strategy is used, which provides an additional benefit called macrodiversity. However, to support soft handover in the downlink, at least one extra downlink channel (2-way SHO) is needed. This extra downlink channel acts to other users acts like additional interference in the air interface. Thus, to support soft handover in the downlink, more resource is required. As a result, in the downlink direction, the performance of the soft handover depends on the trade-off between the macrodiversity gain and the extra resource consumption.

3.2.2 Algorithm of soft handover

The performance of soft handover is related closely to the algorithm. Figure 3.5 shows the IS-95A soft handover algorithm (also called basic cdmaOne algorithm) [EIA/TIA/IS-95A] [Qualcomm97] [L-SJSWK99].

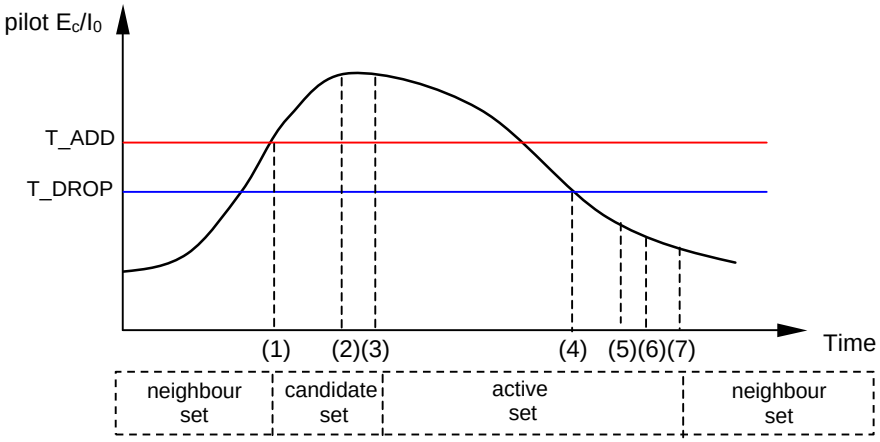

(1) Pilot E_c/I_0 exceeds *T_ADD*, Mobile sends a Pilot Strength Measurement Message (PSMM) and transfers pilot to the candidate set.
(2) BS sends a Handover Direction Message (HDM)
(3) Mobile transfers pilot to the active set and sends a Handover Completion Message (HCM).
(4) Pilot E_c/I_0 drops below *T_DROP*, mobile starts the handover drop timer.
(5) Handover drop timer expires. Mobile sends a PSMM.
(6) BS sends a HDM
(7) Mobile transfers pilot from the active set to the neighbour set and sends a HCM

Figure 3.5 IS-95A soft handover algorithm

The active set is the list of cells that currently have connections to the mobile; the candidate set is the list of cells that are not presently used in the soft handover connection, but whose pilot E_c/I_0 values are strong enough to be added to the active

set; the neighbouring set (monitored set) is the list of cells that the mobile continuously measures, but whose pilot E_c/I_0 values are not strong enough to be added to the active set.

In IS-95A, the handover threshold is a fixed value of received pilot E_c/I_0. It is easy to implement, but has difficulty in dealing with dynamic load changes. Based on the IS-95A algorithm, several modified cdmaOne algorithms were proposed for IS-95B and cdma2000 systems with dynamic rather than fixed thresholds.

In WCDMA, more complicated algorithm is used, as illustrated in Figure 3.6 [ETSI TR 125 922].

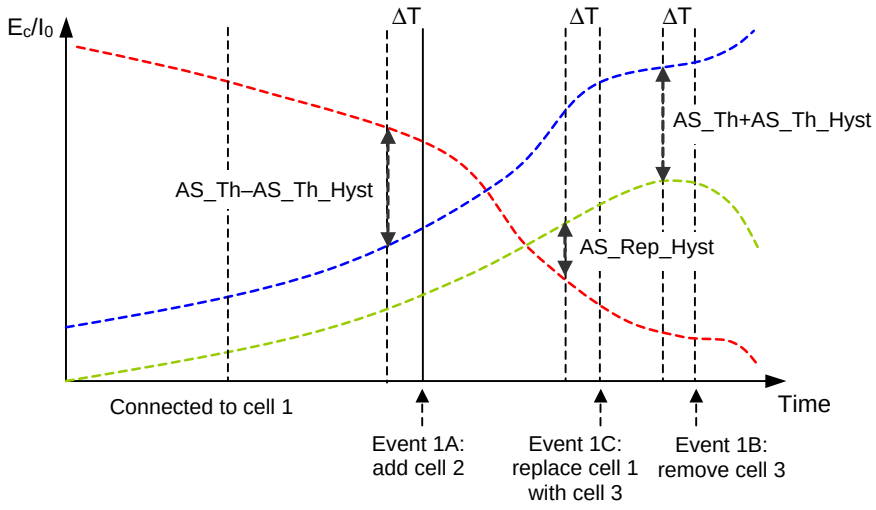

- AS_Th — Threshold for macro diversity (reporting range);
- AS_Th_Hyst — Hysteresis for the above threshold;
- AS_Rep_Hyst — Replacement Hysteresis;
- ΔT — Time to Trigger;
- AS_Max_Size — Maximum size of Active Set;

Figure 3.6 WCDMA soft handover algorithm

The WCDMA soft handover algorithm can be described as follows:

- If *pilot_E_c/I_0 > Best_ pilot_E_c/I_0 – (AS_Th – AS_Th_Hyst)* for a period of *DT* and the active set is not full, the cell is added to the active set. This is called **Event 1A** or **Radio Link Addition**.

- If *pilot_E_c/I_0 < Best_ pilot_E_c/I_0 – (AS_Th + AS_Th_Hyst)* for a period of *DT*, then the cell is removed from the active set. This is called **Event 1B** or **Radio Link Removal**.

- If the active set is full and *Best_ candidate_pilot_E_c/I_0 >Worst_Old_pilot_E_c/I_0 + AS_Rep_Hyst* for a period of *DT*, then the weakest cell in the active set is replaced by the strongest candidate cell. This is called **Event 1C** or **Combined Radio Link Addition and Removal**. The maximum size of the active set in Figure 3.6 is assumed to be two.

Where *pilot_E_c/I_0* is the measured and filtered quantity of E_c/I_0 of CPICH; *Best_ pilot_E_c/I_0* is the strongest measured cell in the active set; *Best_ candidate_pilot_E_c/I_0* is the strongest measured cell in the monitored set; *Worst_Old_pilot_E_c/I_0* is the weakest measured cell in the active set.

In the WCDMA algorithm, relative thresholds rather than absolute threshold are used. Compare to IS-95A, the greatest benefit of this algorithm is its easy parameterisation with no parameter tuning being required for high and low interference areas due to the relative thresholds.

Most of the work in this thesis is based on the WCDMA soft handover algorithm.

3.2.3 Features of soft handover

Compared to the traditional hard handover, soft handover shows some obvious advantages, such as eliminating the “ping-pong” effect (as mentioned in section 3.2.1), and smoothing the transmission (there is no break point in soft handover). No “ping-pong” effect means lower load on the network signalling and with soft handover, there is no data loss due to the momentary transmission break that happens in hard handover.

Apart from handling mobility, there is another reason for implementing soft handover in CDMA; together with power control, soft handover is also used as an interference-reduction mechanism. Figure 3.7 shows two scenarios. In the top one, shown as (a), only power control is applied; in the lower one, shown as (b), power control and soft handover are both supported. Assume that the mobile is moving from

BS₁ towards *BS₂*. At the current position, the pilot signal received from *BS₂* is already stronger than that from *BS₁*. This means *BS₂* is "better" than *BS₁*.

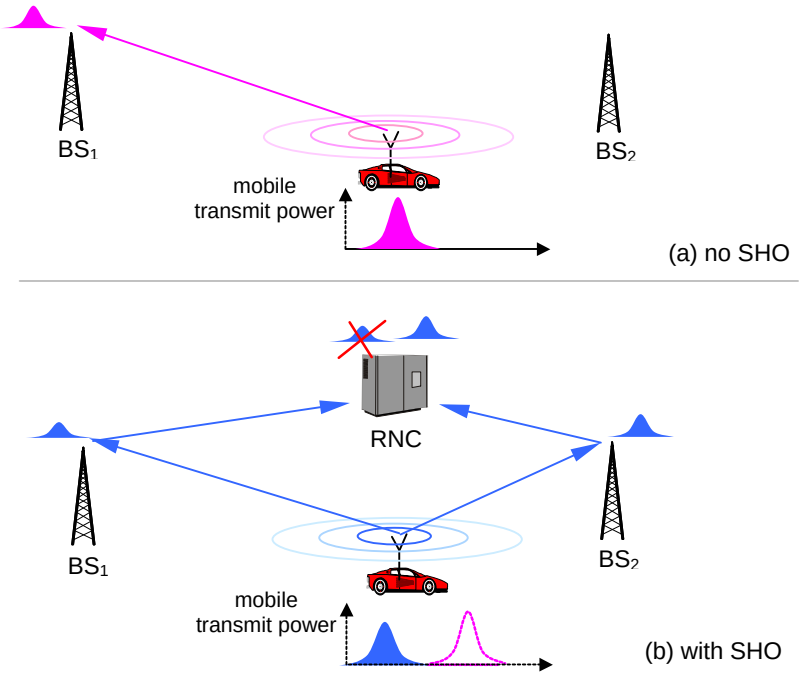

Figure 3.7 Interference-reduction by SHO in UL

In (a), the power control loop increases the mobile transmit power to guarantee the QoS in the uplink when the mobile moves away from its serving BS, *BS₁*. In (b), the mobile is in soft handover status: *BS₁* and *BS₂* both listen to the mobile simultaneously. The received signals, then, are passed forward to the RNC for combining. In the uplink direction, selection combining is used in soft handover. The stronger frame is selected and the weaker one is discarded. Because *BS₂* is "better" than *BS₁*, to meet the same QoS target, the required transmit power (shown in blue) from the mobile is lower compared to the power (shown in pink) needed in scenario (a). Therefore, the interference contributed by this mobile in the uplink is lower under soft handover because soft handover always keeps the mobile linked to the best BS. In the downlink direction, the situation is more complicated. Although the maximum ratio combining gives macrodiversity gain, extra downlink channels are needed to support soft handover.

Summarising the features of soft handover:

A. Advantages

- Less the “ping-pong” effect, leading to reduced load on the network signalling and overhead.
- Smoother transmission with no momentary stop during handover.
- No hysteresis margin, leading to lower delay being equivalent to “instantaneous” macroscopic selection diversity.
- Reduced overall uplink interference, leading to:
  - Better communication quality for a given number of users
  - More users (greater capacity) for the same required QoS
- Fewer time constraints on the network. There is a longer mean queuing time to get a new channel from the target BS, this helps to reduce the blocking probability and dropping probability of calls.

B. Disadvantages

- More complexity in implementation than hard handover
- Additional network resources are consumed in the downlink direction (code resource and power resource)

3.3 Motivation for the Work in this Thesis

3.3.1 Previous work on soft handover

Soft handover concept was firstly introduced for IS-95 systems. Since then, quite a lot of research has been conduced on soft handover. Most published research can be divided into three broad categories:

- Evaluation of soft handover performance by checking the **link level indicators**, such as the average E_b/I_0 and fade margin improvement for individual radio links.

  For example, the fade margin analysis in [VVGZ94] shows how individual uplink performance can benefit from selective diversity offered by soft handover; in [MLG99], a comparison in terms of signal-to-interference ratio (SIR) between soft handover and hard handover is carried out. That paper verified that, compared with hard handover, soft handover has better performance in terms of SIR for individual

links; In [KMJA99], the uplink soft handover gain offered by the selection combining is estimated from a link level simulation;

- The second category uses **system level indicators** estimating the performance of soft handover. The possible indicators could be related to the quality of service, such as outage probability, call blocking probability and handover failure rate for a given load; or related to the system optimisation, such as capacity and coverage gain for a given quality of service requirement.

  For example, [SCH96] analyses soft handover based on a CDMA model with a birth-death Markov process and shows the effect of soft handover in terms of improving blocking and handoff refused probabilities; in [LUK96], the initiation condition is modified based on IS-95 algorithm for adapting the Manhattan street microcell environment. The reduction of call dropping rate proves that the modified approach can bring benefit to the system; [Che95] researches the use of soft handover as a means of alleviating hot spot loading in order to reduce the blocking rate. in [HKB00], IS-95B has been verified as having better performance than IS-95A in terms of lower call/handover blocking probability; in [NT01] system performance of soft handover is analysed in terms of call blocking rate; [CS01] proposed an adaptive channel reservation scheme for soft handover that can control the size of reservation capacity according to varying the number of soft handover attempts. Results show this new approach yields a considerable enhancement in terms of new call blocking and soft handover failure probabilities when compared with the conventional fixed channel reservation scheme; [WW93] and [LLWBFX00] prove that soft handover increases the uplink capacity; and the soft handover effects on the downlink capacity is analysed in [LS98] [CK01] and [FT02].

- A third category area of research is the investigation of soft handover based on the **resource efficiency indicators**, such as the mean active set number, active set update rate and handover delay time.

  For example, in [YG-NT00], four soft handover algorithms with either fixed or dynamic thresholds are analysed in terms of mean active set number, active set update rate and outage probability; and in [YG-NT01], the power-triggered and E_c/I_0–triggered UTRA soft handover algorithms are evaluated by simulation and

results show that the latter achieves a much lower active-set update rate and outage probability but higher active-set number and call blocking probability than the former. In [WSG02], an adaptive soft handover algorithm is proposed based on the IS-95A algorithm: this adaptive algorithm calculates the threshold based on the mobile location, signal strength and RF propagation statistics. Results show that it reduces the unnecessary handover probability and the mean number of BSs in active set.

3.3.2 Existing problems (motivation of the work in this thesis)

Because different combining schemes are employed in the uplink and downlink (as mentioned in section 3.2.1) and the *features of interference* are very different for the uplink and downlink, the performance of soft handover needs to be analysed separately in each direction. Previous research for analysing soft handover performance in the uplink is more comprehensive than that in the downlink. It is well believed that (i) in the uplink, soft handover can increase the capacity and enlarge the coverage [VVGZ94] [LLW00] [KMJA99] [LLWBFX00] and (ii) in the downlink direction, soft handover improves the individual link quality by providing the macro diversity. For example, in [[MLG99]], a comparison in terms of signal-to-interference ratio (SIR) between soft handover and hard handover is investigated and the paper verified that, compared with hard handover, soft handover has better performance in terms of SIR. However, from a system level point of view, different opinions exist on whether soft handover can benefit the system in the downlink direction or not: although the individual link quality can be improved by the macrodiversity provided by soft handover, extra downlink channels are needed for supporting the soft handover process. Therefore, there is a trade-off between the macrodiversity and the extra resource consumption. In [LS98], the downlink performance of soft handover is analysed on a system level for IS-95 CDMA systems. The results show that there is a small percentage loss of capacity in the downlink direction when soft handover is employed in unsectorised cells. However, this small percentage of capacity loss does not affect the system capacity, as the downlink capacity is higher than that of the uplink due to coherent demodulation. However, the paper ignored the downlink power control and simplified the soft handover as a distance-based process. More over, it is

important to note the difference between the narrow-band CDMA systems and the WCDMA systems.

It is well accepted that the capacity of the narrow-band CDMA systems is uplink limited [Vit95] because of the limited mobile transmit power and the lack of coherent detection. However, in WCDMA systems coherent detection is employed in the uplink (as well as in the downlink) using pilot symbols; this results in an overall increase of coverage and capacity on the uplink [ETSI TS 125 211]. As a result, the downlink capacity can be the limiting factor for the system capacity in certain situations especially with those systems that support asymmetric services. Most of the new applications of 3G systems are asymmetric shown as Figure 3.8.

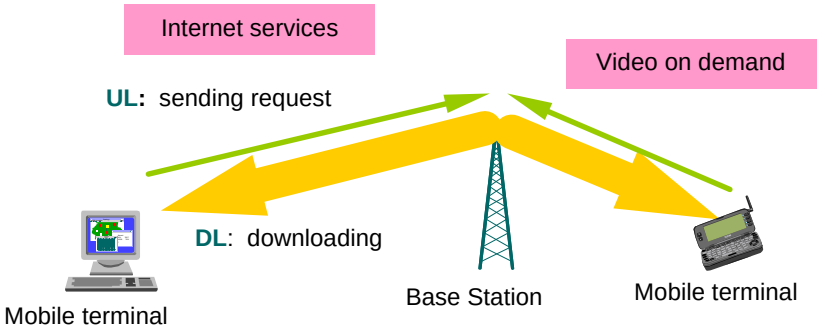

Figure 3.8 Asymmetric applications for 3G systems

The bitrate of the wireless traffic in the downlink is much heavier than that in the uplink. Therefore, in 3G WCDMA systems, the downlink is more likely to be the bottleneck of the system. Hence, the effects of soft handover on the downlink capacity need to be further investigated.

3.3.3 The work in this thesis

In this thesis, an in-depth study of the soft handover effects on the downlink direction of WCDMA networks is carried out, leading to a new method for optimising soft handover aiming at maximising the downlink capacity and a new power control approach.

The analysis starts from investigating soft handover effects on the downlink interference and the link level performance in terms of total power consumption in Chapter 4. This work is new. It provides a foundation for the system level performance

analysis in Chapter 5 and offer a theoretical basis for the new method for optimising soft handover in Chapter 6 and the new power control approach presented in Chapter 7.

In the system level performance analysis, fast downlink power control and initial cell selection schemes that had been ignored or simplified by most of the previous literature are included. The soft handover gain under three different power control conditions and three different cell selection schemes are estimated and compared. The work quantifies the trade-off between the macrodiversity gain and the extra resource consumption.

In most of the previous theoretical analysis for downlink capacity of CDMA systems, soft handover is simplified. For example, in [LS98], soft handover is simplified to a distance-based situation. The handover decision is made based on the distance between the mobile and its serving BS; in [CK01], where the downlink capacity of cdma2000 system is evaluated, the interference contributed by the user under soft handover status is approximately calculated as double that of a user that is not in soft handover. However, in the downlink, the interference contribution due to the soft handover relates closely to the mobile's location and is much more complicated than just double the power. In this thesis, the downlink capacity of WCDMA systems is analysed with the standard soft handover algorithm adopted by 3GPP. The soft handover gains of different algorithms are evaluated and compared. Moreover, the sensitivity of the soft handover gain to different radio parameters is analysed.

Based on the system level performance analysis, a new method for optimising soft handover in order to maximise the downlink capacity is proposed. The optimum soft handover overhead and threshold ranges are obtained. The results are valuable for radio resource management in future mobile networks where the downlink is more likely to be the bottleneck of the whole system.

Furthermore, a new power control scheme is proposed for optimizing the power division between the BSs in the active set during soft handover. The feasibility of the new approach is evaluated and the performance of the new scheme is investigated by comparing with the balanced power control scheme adopted by 3GPP. Results prove

that the new power control scheme has better performance in terms of downlink capacity gain.

Chapter 4 Link Level Performance Analysis

4.1 Introduction

This chapter starts with the description of the system models used in most of the analysis in this thesis. The radio channel model, the system scenario and the assumptions used in analysis are presented in section 4.2. In section 4.3, downlink interference is analysed and soft handover effects on the downlink interference are evaluated. Then, in section 4.4, the link level performance of soft handover is estimated by checking the effects of soft handover on the power allocation for the downlink dedicated channels. Finally, in section 4.5, conclusions are drawn based on the results.

The work in this chapter sets the foundation for the system level performance analysed in Chapter 5 and provides a theoretical basis for the new method for optimising soft handover and the new power division approach proposed in Chapter 6 and 7 respectively.

4.2 System Models

4.2.1 Radio environment of mobile networks

Knowledge of radio propagation characteristics is a prerequisite for the design of radio communications systems. Unlike fixed communications, the environment of mobile communications is rather difficult to predict. Traditionally, radio channels are modelled in statistical way using real propagation measurement data. Many measurements and studies have been done to obtain the characteristics of radio environment. References [ARY95] [FL96] [Mol91] and [Has93] provide a good review of these measurements. In general, the signal fading in a radio environment can be decomposed into three parts: a large-scale path loss component, a medium-scale slow varying component having a log-normal distribution, and a small-scale fast varying component with a Rician or Rayleigh distribution. The distribution of the latter part depends on the presence or absence of the line-of-sight (LOS) situation between the transmitter and the receiver [Pra98][Stu96][Hes93]. Accordingly, the three propagation components being used to describe a wireless cellular environment are

path loss, *shadowing* (also called slow fading), and *multipath fading* (also called fast fading). Figure 4.1 illustrates these three propagation phenomena.

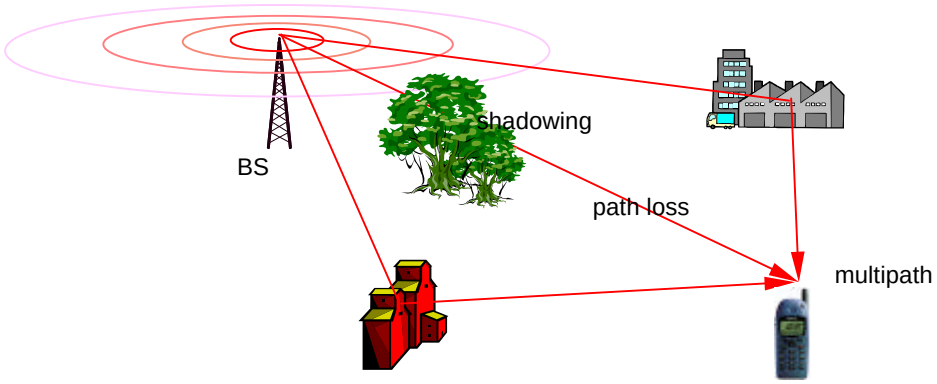

Figure 4.1 Radio channel attenuation

Path loss is the phenomenon of decreasing received power with distance due to reflection, diffraction around structures, and refraction with them. Shadowing is caused by obstruction of buildings, hills, trees and foliage. Multipath fading is due to multipath reflection of a transmitted wave by objects such as houses, buildings, other man-made structures, or natural objects such as forests surrounding a mobile unit. The different propagation path lengths of the multipath signal give rise to different propagation time delays. The sum of multipath signal results in fading dips. The short-term fluctuations caused by multipath propagation can be filtered out by means of appropriate techniques (e.g. RAKE receiver, diversity, coding with interleaving, etc.).

Depending on the radio environment, the parameters for the radio channel model are different. There are a large number of radio environments where 3G mobile systems are expected to operate; these include large and small cities, with variations in building construction, as well as tropical, rural, desert, and mountainous areas. According to [IUT-R] and [ETSI TR 101 112], these possible radio environments have been divided into three generic radio environments:

- Vehicular
- Outdoor to indoor and pedestrian
- Indoor office

These radio environments correspond to the following cell types: macrocell, microcell, and picocell respectively. In this thesis, the main concern is handover, which happens on the macro cell layer of WCDMA systems.

4.2.2 Radio channel model

The radio channel model used in this thesis was proposed in [Vit95] and most of the previous literature has used this model for theoretical analysis, work such as [VVGZ94], [LKCKW96] and [CH02].

Assuming fast fading can be effectively combated by the receiver [SH93], the radio channel is modelled as the product of the -αth power of distance, indicating the path loss, and a log-normal component representing shadowing losses. For a mobile at a distance r from its serving BS, the propagation attenuation is proportional to

$$L(r, z) = r^{-a} \cdot 10^{z/10} \tag{4.1}$$

Where α is the path loss exponent with a typical value of 4; z (in dB) follows a *Gaussian* distribution, representing the attenuation due to shadowing, with zero mean and a standard deviation of σ, which is independent of the distance; it ranges from 5 to 12 with a typical value of 8-10 dB for macro cell.

The shadowing loss is correlated between BSs. It is possible to express the random component of the dB loss for the *ith* BS as

$$z_i = ax + bx_i$$

Where ax is a component in the near field of the mobile, which is common for all the BSs; and bx_i is a component that pertains solely to a certain BS (here is BS_i), which is independent from one BS to another. The constants a and b have the relationship $a^2 + b^2 = 1$.

$E(z_i) = E(x) = E(x_i) = 0$ for all i;

$\mathrm{var}(z_i) = \mathrm{var}(x) = \mathrm{var}(x_i) = s^2$ for all i;

$E(xx_i) = 0$ for all i ;

$E(x_i x_j) = 0$ for all i and j , $i \neq j$;

Thus, the normalized covariance (correlation coefficient) of the losses to two BSs, BS_i and BS_j, is

$$\frac{E(z_i, z_j)}{s^2} = a^2 = 1 - b^2$$

Normally, the correlation between BSs is applied as $a^2 = b^2 = 1/2$.

4.2.3 System scenario

Figure 4.2 shows a WCDMA system scenario with 19 co-channel macro cells. BSs are distributed as a hexagonal grid.

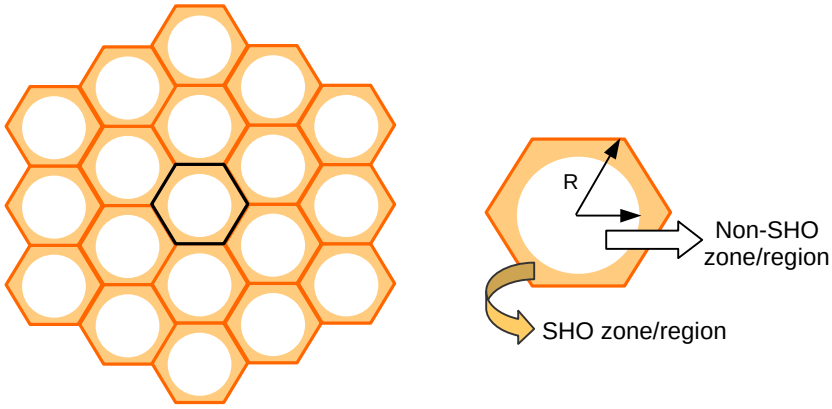

Figure 4.2 System scenario

Near the cell boundaries, the shaded areas represent the soft handover zone (also called soft handover region). All the mobiles in these areas are in soft handover status, communicating with two or more BSs simultaneously. In Figure 4.2, the shape of the non-SHO zone is a perfect circle. However, in the real situation, the actual shape of the SHO zone depends closely on the soft handover algorithm and the soft handover overhead: see more details in section 5.6. The **soft handover overhead** is defined as the total number of connections divided by the total number of users minus one [HT00]. When only two-way soft handover is considered, the soft handover overhead

equals the fraction of users in soft handover status out of the number of all the active users.

4.3 Downlink Interference Analysis

4.3.1 Overview

As mentioned in Chapter 2, CDMA systems are interference-limited and so interference evaluation is one of the fundamental procedures for analysing the CDMA systems. The total interference experienced by a mobile is composed of two parts: **intra-cell interference** and **inter-cell interference**.

In the uplink, to a certain mobile, the intra-cell interference comes from all the other mobiles served by the same BS; the inter-cell interference is composed of all the signals received from all the mobiles in other cells other than the mobile's serving cell, as shown in Figure 4.3. Therefore, in the uplink, the interference experienced by a certain mobile is related to the load distribution within the network, but not related to the mobile's own location.

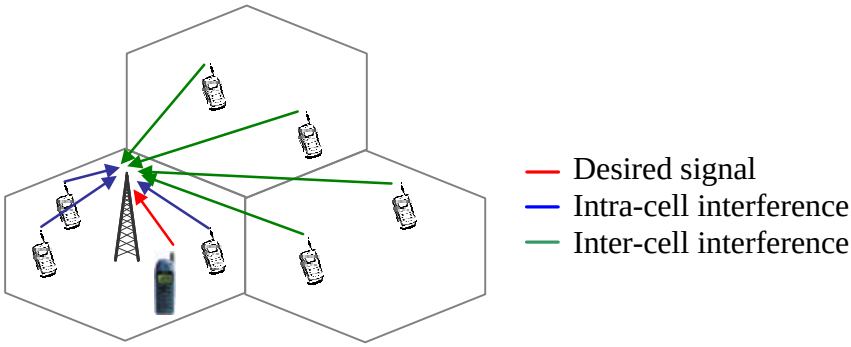

Figure 4.3 Uplink interference

In the downlink, as shown in Figure 4.4, the intra-cell interference to a certain mobile comes from its serving BS: this interference is caused by the partial loss of the orthogonality among the users due to the multipath effect. WCDMA employs the orthogonal codes in the downlink to separate users and without any multipath propagation the orthogonality remains and there is no intra-cell interference. Typically, the orthogonality is between 0.4 and 0.9 [Cas01] (1 corresponds to perfect orthogonality). The intra-cell interference actual includes part of the power for

common control channels and the power for the downlink traffic channels for other users in the same cell. The inter-cell interference is the power received by the mobile from all the other BSs except for its own serving BS. Because in WCDMA FDD mode, BSs are not synchronised, the inter-cell interference does not get benefits from the orthogonality as happens with the intra-cell interference.

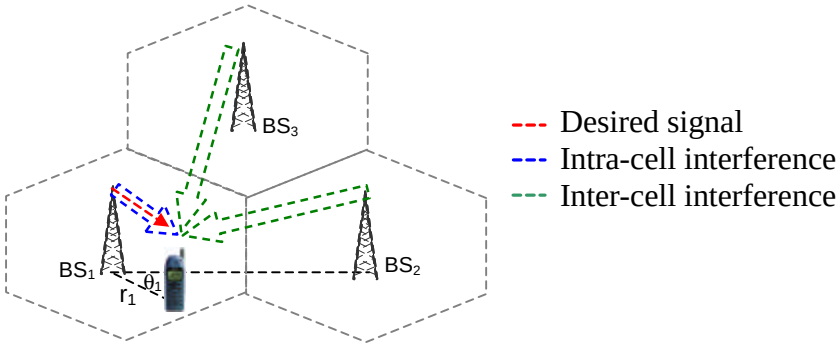

Figure 4.4 Downlink interference

Because the interference sources are fixed BSs in the downlink direction, to a certain mobile, the downlink interference is inevitably linked to the mobile's location. The following analysis shows this feature (section 4.3.2) and reveals the soft handover effects on the downlink interference (section 4.3.3).

4.3.2 Intra-cell & inter-cell interference

To the mobile located at (r_1,q_1) in Figure 4.4, assuming BS_1 is its serving BS and using the radio channel model presented in section 4.2.2, the downlink intra-cell interference, $I_{intra\text{-}cell}$, which is received from BS_1, can be expressed as:

$$I_{\text{int}ra-cell} = P_{T1}(1-a)r_1^{-a}\,10^{z_1/10} \tag{4.2}$$

Where P_{T1} is the total transmit power of BS_1; a is the downlink orthogonal factor with 1 for perfect orthogonality and 0 for non-orthogonality. Because the intra-cell interference and the desired signal are both transmitted from the same source, they experience the same attenuation. Thus, there is no need to use power control in a single cell system.

The inter-cell interference, $I_{inter\text{-}cell}$, can be expressed as

$$I_{inter-cell} = \sum_{i=2}^{M} P_{Ti} r_i^{-a} 10^{z_i/10} \tag{4.3}$$

Where P_{Ti} is the total transmit power of BS_i; r_i is the distance from the mobile to BS_i; M is the index of the BSs, which are taken into account for the inter-cell interference. Theoretically, the inter-cell interference comes from all the BSs around other than the serving BS. Here, the BSs in the first and second tiers around BS_1 are considered because the power received from the BSs outside the second tier is negligible (see Appendix C).

From (4.2), it can be seen that the intra-cell interference relies on the distance from the mobile to its serving BS, r_1, but it is independent of q_1. However, the inter-cell interference depends not only on r_1 but also on q_1 because the distance from the mobile to other BS, e.g. BS_i, r_i, is a function of r_1 and q_1.

$$r_i = \begin{cases} \sqrt{r_1^2 + \left(\sqrt{3}R\right)^2 - 2 \cdot r_1 \cdot \sqrt{3}R\cos\left[q_1 + (i-2)p/3\right]} & 2 \le i \le 7 \\ \sqrt{r_1^2 + \left(2\sqrt{3}R\right)^2 - 2 \cdot r_1 \cdot 2\sqrt{3}R\cos\left[q_1 + (i-8)p/6\right]} & i = 8,10,....18 \\ \sqrt{r_1^2 + (3R)^2 - 2 \cdot r_1 \cdot 3R\cos\left[q_1 + (i-8)p/6\right]} & i = 9,11,....19 \end{cases} \tag{4.4}$$

It is clear that to a certain mobile, the downlink interference is related closely to the mobile's location. This is because the interference sources are fixed BSs in the downlink direction. Assuming that the load is uniformly distributed within the system and the total transmit power of each BS is the same, denoted by P_T, (4.3) can be rewritten as:

$$I_{inter-cell} = P_T \sum_{i=2}^{M} r_i^{-a} 10^{z_i/10} = P_T \cdot c \qquad c = \frac{I_{inter-cell}}{P_T} \tag{4.5}$$

Where the factor c provides a measure of the inter-cell interference to the BS total transmit power. c is related to the mobile's location. Here, the cell radius R is normalised to 1. Figure 4.5 shows the mean c for mobiles at different location within one hexagonal cell. The x-y plane shows the location of the mobile and the value of c

is shown along the Z-axis. Because the cell radius R is normalised to 1, c is not the actual value of the ratio of the inter-cell interference to P_T but the relative inter-cell interference level experienced by mobiles at different locations.

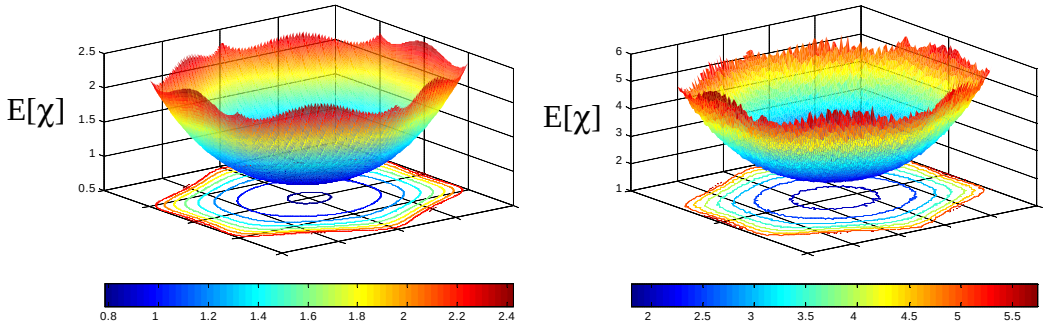

(a) a = 4, s = 0 (b) a = 4, s = 8

Figure 4.5 c, relative downlink inter-cell interference

It is obvious that the inter-cell interference is related closely to the mobile's location, not only to the distance r, but also to the angle q. The mobiles near the cell boundary (both corner and edge) receive the highest inter-cell interference. Denote the area near (r=R, q=30^0) as the cell corner and the area near (r=$\sqrt{3}/2 \cdot R$, q=0^0) as the cell edge. In (a), σ = 0 dB, only path loss is considered; in (b), σ = 8 dB, shadowing effects are included and the mean c is calculated. It can be seen that shadowing actually increases the average interference.

Ignoring the thermal noise, the ratio of the inter-cell interference to the intra-cell interference, denoted by h can be expressed as

$$h = \frac{I_{\text{int}\,er-cell}}{I_{\text{int}\,ra-cell}} = \frac{P_T \sum_{i=2}^{M} r_i^{-a}\, 10^{z_i/10}}{P_T (1-a) r_1^{-a}\, 10^{z_1/10}} = \frac{\sum_{i=2}^{M} \left(\frac{r_i}{r_1}\right)^{-a} 10^{(z_i - z_1)/10}}{1-a} \tag{4.6}$$

Figure 4.6 shows the mean of the inter-cell to intra-cell interference ratio for mobiles at different location within one hexagonal cell. Without shadowing, on the average, the inter-cell interference is about 5.5 times of the intra-cell interference to the

corner users[4]. Shadowing increases the average value of h to 32. As mentioned in Chapter 2 (section 2.3.2), inter-cell interference is the main reason for applying power control in the downlink and it is especially important to the corner users of multi-cell systems.

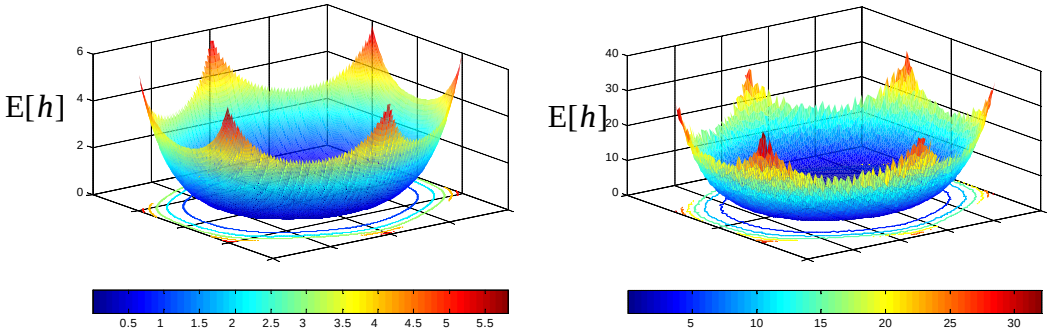

(a) a = 4, a = 0.6, s = 0 (b) a = 4, a = 0.6, s = 8

Figure 4.6 h, inter-cell to intra-cell interference ratio

Figure 4.7 shows the sensitivity of the factors c and h to different radio parameters: the x axis shows the relative distance from the mobile to its serving BS. a is the path loss exponent; s is the standard deviation of shadowing and a is the downlink orthogonal factor.

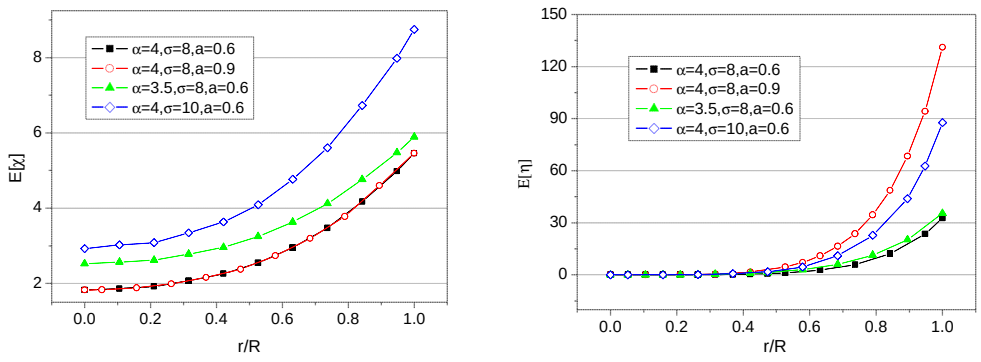

Figure 4.7 Sensitivity of relative downlink interference to radio parameters

Because in WCDMA FDD mode, the BSs are not synchronised, the inter-cell interference does not get benefit from orthogonality so the orthogonal factor, a, only

[4] Corner users are defined as the users near the corner of the hexagonal cell.

affects h. When the orthogonality between the downlink channels from the same BS is well preserved, the intra-cell interference can be alleviated. Other points to note are that a larger path loss exponent corresponds to a lower inter-cell interference and that shadowing increases the average inter-cell interference and the relative interference ratio.

4.3.3 Soft handover effects on downlink interference

To guarantee the QoS, the BS needs to allocate the proper amount of power to each mobile to compensate for the interference. If the mobile is not in soft handover status, as mobile 1 shown in Figure 4.8 (a), only one downlink channel is set up between the mobile and its serving BS, BS_1; according to the service requirement and the total downlink interference received by *mobile 1* (which is denoted by I_0) power P is allocated to the downlink channel between the mobile and BS_1. This channel acts as intra-cell interference and inter-cell interference to *mobile 2* and *mobile 3* respectively.

If *mobile 1* is in soft handover status, it communicates with BS_1 and BS_2 simultaneously. Two downlink dedicated channels are set up to support the soft handover, as shown in Figure 4.8 (b). Let P_1 and P_2 represent the power allocated to channels from BS_1 and BS_2 separately. P_1 acts as intra-cell interference to *mobile 2* and inter-cell interference to *mobile 3* and P_2 acts as inter-cell interference to *mobile 2* and intra-cell interference to *mobile 3*.

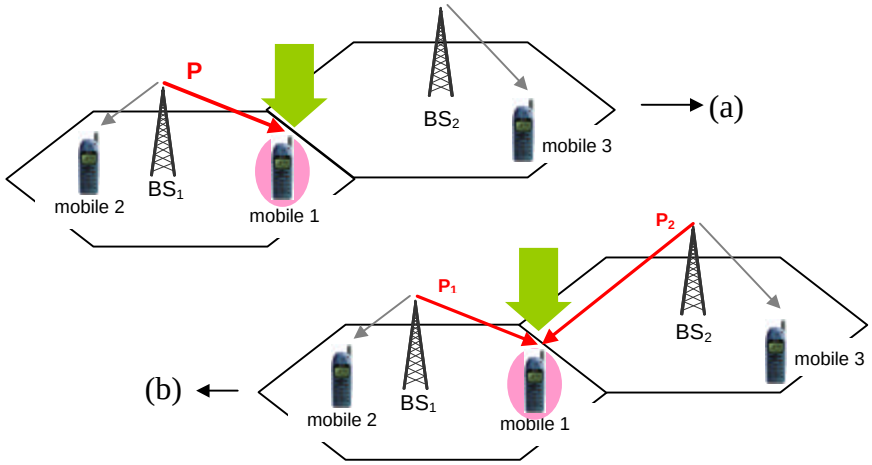

Figure 4.8 Soft handover effects on the downlink interference

Comparing the two cases, soft handover effects on the downlink interference are quite complicated. Without soft handover, mobile 1 contributes power P to the total downlink interference. With soft handover, the total contribution is the sum of P_1 and P_2. The increment of the interference due to *mobile 1* has influence on all the other active mobiles within the system: all these mobiles need to adjust their channel power to meet the change in the interference. This, in return, changes the total interference received by *mobile 1*, resulting the alteration of P or P_1 and P_2 (SHO case). This circulation repeats until the system reaches a new balance. In CDMA systems, power control is the functionality responsible for this adjustment. Because of the interference-limited feature, experiencing less interference is always the main principle of the radio resource allocation in CDMA systems. Therefore, whether soft handover leads to lower interference than the conventional hard handover or not, depends intimately on the value of P, P_1 and P_2. These powers are related to certain facts, such as the location of the mobile, the radio attenuation and the power division strategy employed during the soft handover.

4.4 Downlink Power Allocation

Power allocation is a very important procedure for CDMA systems. The total transmit power of the BS is composed of two parts: one part is for the downlink common control channels, such as the common pilot channel (CPICH) and the synchronization channel (SCH) and the other part of power is allocated for users as dedicated downlink channels. Normally, the power for common control channels represents about 20-30% of the total BS transmit power [OP98]. In order to minimise the interference and the radio resource consumption, the system tries to allocate as little power as possible to each dedicated channel for individual users, but this does depend on the QoS requirement. Under perfect downlink power control, the received bit energy-to-interference power spectral density ratio E_b/I_0 of all mobiles is kept at the target value. When the mobile is only linked to one BS, only one downlink dedicated channel is active to this mobile, but when the mobile is in soft handover status, at least two BSs are involved in the power allocation. These two situations are analysed separately.

4.4.1 Power allocation without SHO

Still consider the mobile located at (r_1,q_1) shown in Figure 4.4. Without soft handover, the mobile only communicates with one BS at a time. Assuming BS_1 is its serving BS, the mobile received E_b/I_0 can be expressed as

$$\frac{E_b}{I_0} = \frac{W}{nR} \frac{P_s r_1^{-a} 10^{z_1/10}}{P_{T1}(1-a) r_1^{-a} 10^{z_1/10} + \sum_{i=2}^{19} P_{Ti} r_i^{-a} 10^{z_i/10}} \tag{4.7}$$

Where W is the chip rate; R is the service bit rate; v is the activity factor; Here, the thermal noise is ignored. Thus, in order to keep the QoS meeting the target, the required transmit power of the downlink channel P_s can be derived from (4.7) as:

$$P_s = \frac{nR}{W} \left(\frac{E_b}{I_0} \right)_t \left[P_{T1}(1-a) + \sum_{i=2}^{19} P_{Ti} \left(\frac{r_i}{r_1} \right)^{-a} 10^{(z_i - z_1)/10} \right] \tag{4.8}$$

Where $(E_b/I_0)_t$ is the target value of E_b/I_0. The value of $(E_b/I_0)_t$ is decided by RNC. According to the BER, RNC might change the target value to maintain the QoS.

Using the same assumptions of the last section that the load is distributed evenly across the system, all BSs transmit the same amount of power. P_s can then be rewritten as:

$$P_s = \frac{nR}{W} \left(\frac{E_b}{I_0} \right)_t \left[1 - a + \sum_{i=2}^{19} \left(\frac{r_i}{r_1} \right)^{-a} 10^{(z_i - z_1)/10} \right] \cdot P_T = b_1 \cdot P_T \tag{4.9}$$

Factor b_1 shows the relative strength of the required power for the mobile located at (r_1,q_1) without soft handover.

4.4.2 Power allocation with SHO

When a mobile is in the soft handover status, all the BSs in the active set needs to allocate proper power for the downlink channels linked to this mobile. Here, 2-way and 3-way soft handover are considered separately.

A. 2-way SHO

With 2-way SHO, assuming BS_1 and BS_2 are the mobile's serving BSs, the desired signals from the two BSs are combined together. Different combining schemes can be used, but as with most of the previous work in the literature, maximal ratio combining is considered here. The received E_b/I_0 of the mobile can be expressed as:

$$\frac{E_b}{I_0} = \left[\frac{E_b}{I_0}\right]_1 + \left[\frac{E_b}{I_0}\right]_2$$
$$= \frac{W}{nR}\left[\frac{P_{s1} r_1^{-a} 10^{V_1/10}}{P_{T1}(1-a) r_1^{-a} 10^{V_1/10} + \sum_{i=2}^{19} P_{Ti} r_i^{-a} 10^{V_i/10}} + \frac{P_{s2} r_2^{-a} 10^{V_2/10}}{P_{T2}(1-a) r_2^{-a} 10^{V_2/10} + \sum_{\substack{j=1 \\ (j\neq 2)}}^{19} P_{Tj} r_j^{-a} 10^{V_j/10}}\right] \quad (4.10)$$

Where r_1 and r_2 represent the distance from the mobile to BS_1 and BS_2 respectively; P_{s1} and P_{s2} are the transmit power from BS_1 and BS_2 respectively. During the soft handover process, two power control loops are active. To prevent power drifting, several strategies are proposed, and the balanced power control, which is adopted by 3GPP [ETSI TR 125 922] is used. As well as the inner closed loop power control, an adjustment loop is employed for balancing the downlink power among active set cells during macrodiversity. This power control strategy avoids power drifting that leads to increased transmission power and stability problems. In the perfect situation, $P_{s1}=P_{s2}$. Using the same assumption, the transmit power for each downlink channel can be expressed as

$$P_{s1} = P_{s2} = \frac{\frac{nR}{W}\left(\frac{E_b}{I_0}\right)_t P_T}{\frac{1}{1-a+\sum_{i=2}^{19}\left(\frac{r_i}{r_1}\right)^{-a} 10^{(z_i - z_1)/10}} + \frac{1}{1-a+\sum_{\substack{j=1 \\ (j\neq 2)}}^{19}\left(\frac{r_j}{r_2}\right)^{-a} 10^{(z_j - z_2)/10}}} \quad (4.11)$$

Therefore, the total power needed for supporting this mobile is

$$P_{s1}+P_{s2}=\frac{2\dfrac{nR}{W}\left(\dfrac{E_b}{I_0}\right)_t}{\dfrac{1}{1-a+\sum_{i=2}^{19}\left(\dfrac{r_i}{r_1}\right)^{-a}10^{(z_i-z_1)/10}}+\dfrac{1}{1-a+\sum_{\substack{j=1\\(j\neq 2)}}^{19}\left(\dfrac{r_j}{r_2}\right)^{-a}10^{(z_j-z_2)/10}}}\cdot P_T=b_2\cdot P_T \qquad (4.12)$$

Factor b_2 shows the relative strength of the total required power for the mobile under 2-way soft handover.

B. 3-way SHO

Similar to the analysis for 2-way SHO, for a mobile under 3-way SHO, the received E_b/I_0 is

$\frac{E_b}{I_0}=\left[\frac{E_b}{I_0}\right]_1+\left[\frac{E_b}{I_0}\right]_2+\left[\frac{E_b}{I_0}\right]_3$ which gives

$$P_{s1}=P_{s2}=P_{s3}=\frac{\dfrac{nR}{W}\left(\dfrac{E_b}{I_0}\right)_t P_T}{\dfrac{1}{1-a+\sum_{i=2}^{19}\left(\dfrac{r_i}{r_1}\right)^{-a}10^{(z_i-z_1)/10}}+\dfrac{1}{1-a+\sum_{\substack{j=1\\(j\neq 2)}}^{19}\left(\dfrac{r_j}{r_2}\right)^{-a}10^{(z_j-z_2)/10}}+\dfrac{1}{1-a+\sum_{\substack{k=1\\(k\neq 3)}}^{19}\left(\dfrac{r_k}{r_3}\right)^{-a}10^{(z_k-z_3)/10}}} \qquad (4.13)$$

The total power needed for supporting this mobile is:

$$P_{s1}+P_{s2}+P_{s3}=\frac{3\dfrac{nR}{W}\left(\dfrac{E_b}{I_0}\right)_t}{\dfrac{1}{1-a+\sum_{i=2}^{19}\left(\dfrac{r_i}{r_1}\right)^{-a}10^{(z_i-z_1)/10}}+\dfrac{1}{1-a+\sum_{\substack{j=1\\(j\neq 2)}}^{19}\left(\dfrac{r_j}{r_2}\right)^{-a}10^{(z_j-z_2)/10}}+\dfrac{1}{1-a+\sum_{\substack{k=1\\(k\neq 3)}}^{19}\left(\dfrac{r_k}{r_2}\right)^{-a}10^{(z_k-z_3)/10}}}\cdot P_T=b_3\cdot P_T \qquad (4.14)$$

Factor b_3 shows the relative strength of the total required power for the mobile under 3-way soft handover.

The power allocated to a certain user acts as interference for other users. Therefore, b_1, b_2, b_3 also indicate how much interference is being brought by the mobiles in different situations. Figure 4.9 shows the mean value of b_1, b_2, b_3 for mobiles at

different locations. r_1/R is the normalised distance from the mobile to BS_1. (a), (b), (c), (d) correspond to different s and q_1. Other parameters use typical values as W=3840kchip/s, R=12.2kbit/s, n=0.5, a=4, a=0.6, $(E_b/I_0)_t$=5dB.

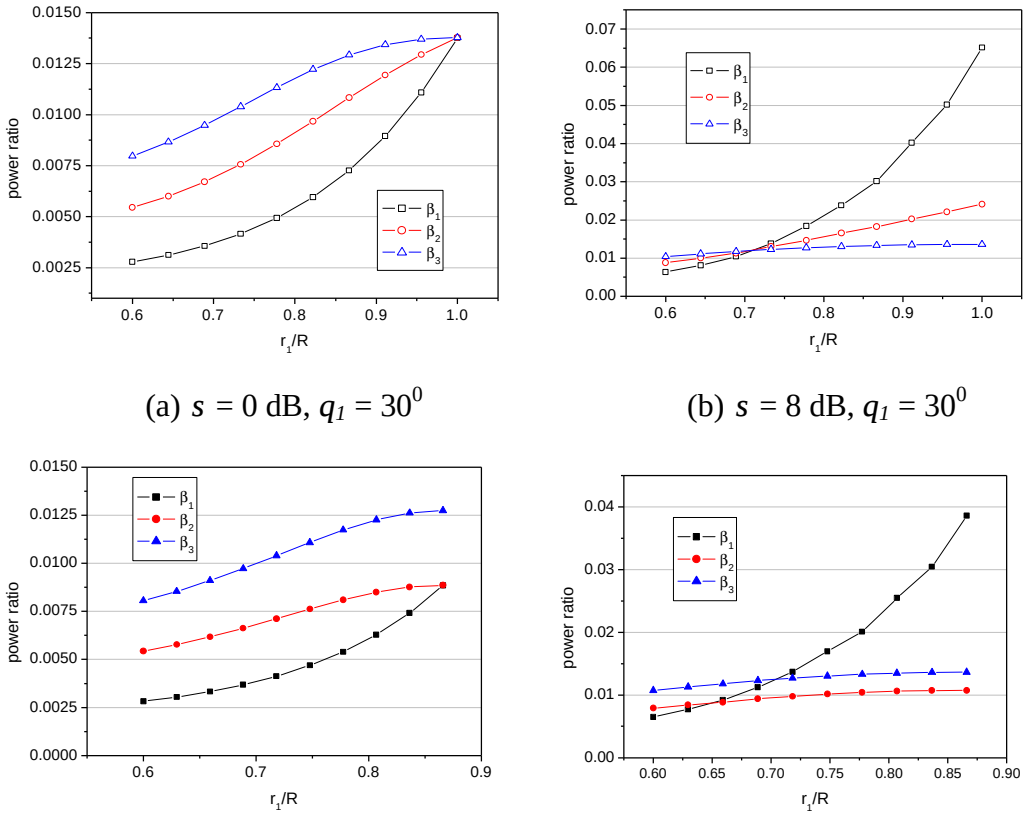

(a) s = 0 dB, q_1 = 30^0 (b) s = 8 dB, q_1 = 30^0

(c) s = 0 dB, q_1 = 0^0 (d) s = 8 dB, q_1 = 0^0

no SHO	mobile only links to BS_1	$P_{t1} = P_s = b_1 P_T$
2-way SHO	mobile link to BS_1 & BS_2	$P_{t2} = P_{s1} + P_{s2} = b_2 P_T$
3-way SHO	mobile link to BS_1, BS_2 & BS_3	$P_{t3} = P_{s1} + P_{s2} + P_{s3} = b_3 P_T$

Figure 4.9 Mean b_1, b_2, b_3 vs. mobile location

The results in the cases (with and without shadowing) can be explained as follows. When shadowing is not considered, shown as (a) and (c), the relationship between b_1, b_2 and b_3 is: $b_1 \le b_2 \le b_3$. This means more power is needed to support soft handover in order to keep the same E_b/I_0 target: the more BSs there are in the active set, the more power that is required. When shadowing is considered, the attenuation of the radio channel is dynamically changing. To meet the same E_b/I_0 target, the power that needs to be allocated should be changing as well. In (b) and (d), the mean values of b_1, b_2, b_3 are shown with σ=8dB. It is clear that for the mobiles near the cell boundary, with soft

handover, less average power is needed to meet the same E_b/I_0 target. For corner users, 3-way SHO leads to even lower total power than 2-way SHO. In (b) when $r/R > 0.8$, $b_3 < b_2$. However, for the mobiles on the line with $q=0^0$, 2-way SHO always has better performance than 3-way SHO.

Figure 4.10 shows the Cumulative Distribution Function (CDF) of b_1, b_2, b_3 for the corner user located at (r_1=R, $\theta_1=30^0$). b_3 has the smallest mean and standard deviation. Smaller standard deviation of the total transmit power corresponds to a lower fade margin. Therefore, similar to the effects in the uplink [VVGZ94], soft handover can benefit the downlink by decreasing the fade margin needed for satisfying a certain QoS at cell edge too. 3-way soft handover has even better performance than 2-way soft handover in terms of reduction of the fade margin.

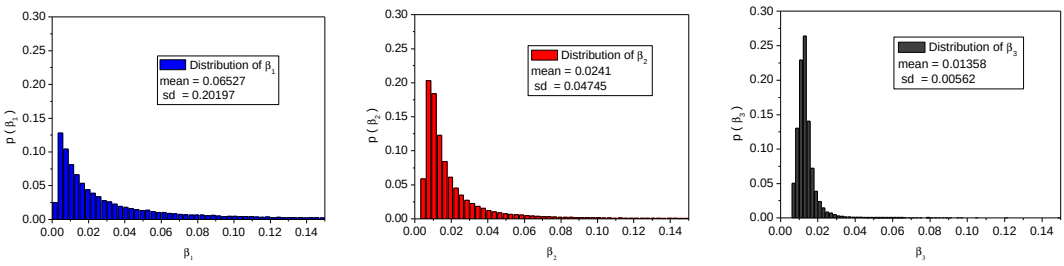

Figure 4.10 Cumulative distribution function of b_1, b_2, b_3

Figure 4.11 shows the relationship between the mean value of b_1, b_2 and b_3 in a two dimensional cell plane. Different colours correspond to different situations as shown in the caption. It is clear that soft handover can decrease the power required for the downlink channel by the mobiles at the cell boundaries. This means the average downlink interference brought by these mobiles to other users is alleviated with soft handover.

It should be noted that all the results shown so far are based on the ideal situation: guaranteed QoS, perfect power control and no power limits. However, in a real network, there are predefined limits on the power. The purpose is to avoid extensive interference caused by fast power control against a bad radio channel. In most cases, fast and accurate power control can bring benefits to the system by compensating for

the transmission loss in the radio channel. However, for a bad radio channel, the BS may allocate high power, causing extensive interference to other active channels.

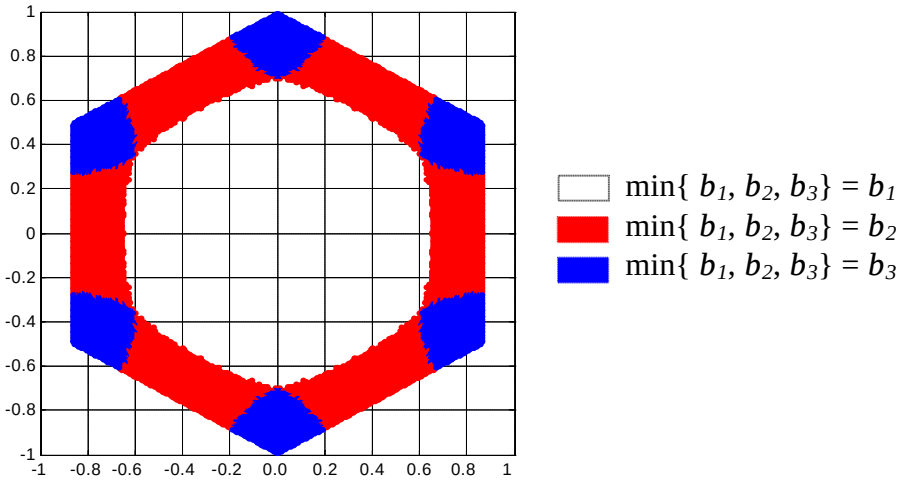

Figure 4.11 Mean total power vs. mobile location

The typical values of power limits for a macro cell environment are 43dBm (20w) and 30dBm (1w) for the maximum total BS transmit power and maximum downlink traffic channel power respectively [Cas01]. Assuming all the BSs are transmitting power at the maximum value, P_T = 43dBm, Figure 4.11 shows the average downlink traffic channel power for mobiles at different locations ($\theta=30^0$). The X-axis shows the relative distance from the mobile to the cell radius. Assume that when r/R > 0.82, the mobile is in soft handover status.

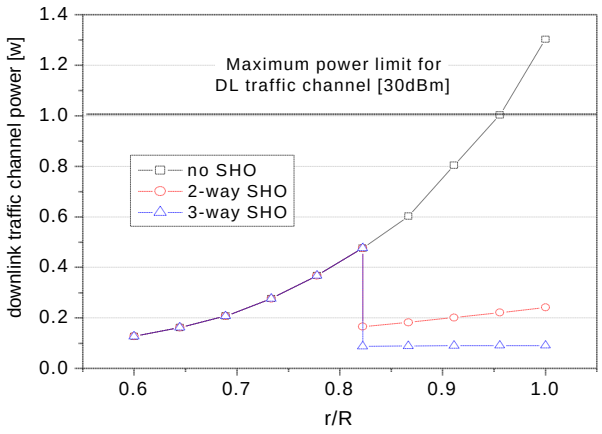

Figure 4.12 Downlink traffic channel power

It is clear that without implementing soft handover, in order to keep the E_b/I_0 at the target value, the average downlink traffic channel power needed for the mobile at the cell boundary is higher than the maximum power limit when all the BSs are transmitting power at the maximum level. The user could be either rejected or served with QoS under the target value. Soft handover can solve the problem by splitting power between the two BSs. For the mobile at the cell boundary, the E_b/I_0 can be guaranteed to meet the target value without allocating high power to each downlink channel. Of course, if the system is not fully loaded, the power for the corner user might not be over the maximum level even if soft handover is not supported. The point here is that soft handover reduces the probability of QoS deterioration. Another advantage of implementing soft handover is that the power floating due to shadowing loss is not as much as the case with a single BS because the two signals being combined are transmitted through different radio channels.

4.5 Conclusions

Based on the analysis of the downlink interference and soft handover effects on the individual link, conclusions can be drawn as follows:

- In the downlink, the inter-cell interference is related closely to the location of the mobile users.
- To the users at the cell boundaries, the inter-cell interference is the main part of the total interference, especially with higher orthogonality.
- Shadowing increases the average interference level.
- Soft handover effects on the downlink interference are quite complicated, depending on such factors as the location of the mobile, the radio attenuation and the power division strategy employed.
- SHO decreases the fade margin of the individual connections in the downlink as well as in the uplink.
- SHO decreases the total average power needed by the mobiles at the cell boundaries.

- For corner users, the average interference introduced by 3-way SHO is less than that by 2-way SHO.

- SHO decreases the probability of over-power and QoS deterioration for the users at cell boundaries.

Based on the link level analysis in this chapter, the system level performance of soft handover will be investigated in the next chapter.

Chapter 5 System Level Performance Analysis

5.1 Introduction

In this chapter, the performance of soft handover is analysed at the system level, using the downlink capacity gain as the indicator. The whole chapter is organised as eight sections with the system performance of soft handover being studied from different angles.

Section 5.2 firstly gives the definition of the **soft handover gain** used in this thesis, then, the procedure for analysing the soft handover gain is presented and the impact of different factors is discussed. From section 5.3 to 5.6, the effects of cell selection, soft handover algorithm, power control and multi-rate service environment on the soft handover gain are analysed separately. Results are discussed and conclusions are drawn in section 5.7. Finally, section 5.8 summarises the content of this chapter.

5.2 Downlink Soft Handover Gain

5.2.1 Introduction

As mentioned in Chapter 3, the system level performance of soft handover can be evaluated by different indicators. One type is QoS-related, such as outage probability, call blocking probability and handover failure rate; the other kind is system optimisation related, such as capacity and coverage gain for a given QoS requirement. Driven by the fast growing demand for downlink capacity in future mobile networks because of the asymmetric nature of services, the soft handover effects on the *downlink* capacity of WCDMA systems are analysed in this thesis. Therefore, the downlink capacity gain caused by soft handover is defined as **soft handover gain**.

CDMA systems are interference-limited systems. One of the main differences between CDMA systems and FDMA/TDMA systems is that the capacity of a CDMA system is “soft”. How many users or how much throughout can be supported per cell relates closely to the system interference level. In this thesis, pole capacity that describes the system capacity limit is evaluated. Appendix D gives the derivation of the downlink pole capacity from the load equation.

By comparing the downlink pole capacity with soft handover to that without soft handover, it is possible to obtain the soft handover gain with a certain soft handover overhead. In next section, the method for analysing the soft handover gain is presented. Most of the analysis afterwards is based on this method.

5.2.2 Soft handover gain

Using the system model as described in section 4.2 of Chapter 4, Figure 5.1 shows part of a WCDMA system with ideal hexagonal topology.

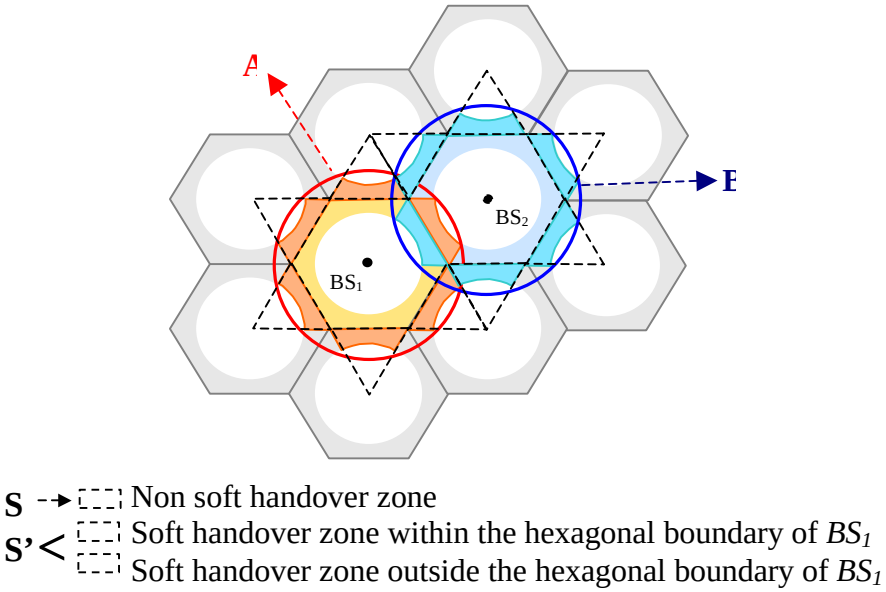

Figure 5.1 Soft handover zone and effective cell coverage

The blank area is the non-soft handover zone; the coloured area is the soft handover zone. All the mobiles in the soft handover zone are communicating with two (2-way SHO) or more BSs simultaneously. To support soft handover, the mobile has to be in the overlapping area of the BSs in the active set. Therefore, for cell 1 and cell 2 in Figure 5.1, the actual coverage should reach the red and blue circles (A and B). In later analysis, *S* is used to denote the non-soft handover zone and *S'* is used to denote the soft handover zone.

Assuming that active users are distributed evenly throughout the system, the pole capacity can be derived according to the following steps:

A. Outside soft handover zone

To a user outside the soft handover zone (as user 1 in Figure 5.2), which only has connection with BS_1, the transmit power of the downlink dedicated channel from BS_1 to user 1, P_{s1}, can be calculated from the following equation:

$$\frac{E_b}{I_0} = \text{processing gain of user 1} \cdot \frac{P_{s1} L_1}{I_{total}} \qquad \Rightarrow P_{s1} \tag{5.1}$$

Where E_b/I_0 is the user received bit energy-to-interference power spectral density ratio; L_1 is the propagation attenuation of the radio channel between BS_1 and the user; I_{total} is the total power (excl. own signal). L_1 and I_{total} are both related to the user's location. The process gain and the target value of E_b/I_0 depend on the type of service required by the user.

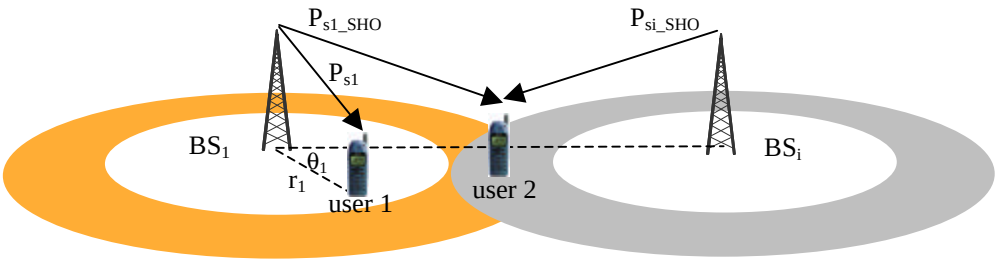

Figure 5.2 Cell layout

B. Inside soft handover zone

As in most of the previous literature, maximum ratio combining is assumed to be applied in the mobile terminal. Therefore, to a user inside the soft handover zone, the received E_b/I_0 is the sum of the E_b/I_0 from all the BSs in the active set. Assuming two-way soft handover is supported and BS_i is the other BS which is involved in the soft handover process, the received E_b/I_0 of user *2* in Figure 5.2 can be expressed as:

$$\frac{E_b}{I_0} = \left(\frac{E_b}{I_0}\right)_1 + \left(\frac{E_b}{I_0}\right)_i = \text{processing gain of user 2} \cdot \left[\frac{P_{s1\_SHO} L_1}{I_{total\,1}} + \frac{P_{si\_SHO} L_i}{I_{total\,i}}\right] \qquad \Rightarrow P_{s1\_SHO} \tag{5.2}$$

Where P_{s1_SHO} and P_{si_SHO} represent the transmit power for the dedicated channels from BS_1 and BS_i to user *2* separately. The relationship between P_{s1_SHO} and P_{si_SHO} is related to the power division scheme applied during the soft handover. Substituting

P_{si_SHO} as a function of P_{s1_SHO} to (5.2), P_{s1_SHO} can be obtained. Please note that I_{total1} and I_{totali} are not the same.

C. Derivation of downlink capacity

The total the total transmit power of BS_1 is thus

$$P_{T1} = P_{T1} \cdot (1-g) + \sum_{j=1}^{N} P_{s1,j} = P_{T1} \cdot (1-g) + \iint_{S} r \cdot P_{s1} \cdot ds + \iint_{S'} r \cdot P_{s1\_SHO} \cdot ds \quad (5.3)$$

Where g is the fraction of the total BS transmit power devote to the dedicated channels; *(1-g)* is devoted to the downlink common control channels; N is the average number of active users per cell; S represents the non-soft handover zone and S' represents the soft handover zone. Both S and S' rely on the soft handover algorithm and overhead; r is the density of users. Under the assumption of uniform distribution of mobile users, r can be expressed as

$$r = N/A = 2N/3\sqrt{3}R^2 \quad (5.4)$$

Where A is the area of each cell and R is the radius of the hexagonal cell.

Substituting r, P_{s1} and P_{s1_SHO} into (5.3), the average downlink capacity N with implementing soft handover throughout the system can be obtained as

$$N = \frac{\frac{3\sqrt{3}}{2} R^2 \cdot g \cdot P_{T1}}{\iint_{S} P_{s1} \cdot ds + \iint_{S'} P_{s1\_SHO} \cdot ds} \quad (5.5)$$

D. Derivation of soft handover gain

By comparing the capacity with soft handover to that without soft handover, the soft handover gain can be determined as

$$SHO\_gain = \left(\frac{capacity\_SHO}{capacity\_noSHO} - 1 \right) \times 100 \quad [\%] \quad or \quad 10 \cdot \log \frac{capacity\_SHO}{capacity\_noSHO} \quad [dB] \quad (5.6)$$

The downlink capacity without implementing soft handover can be expressed as

$$N_{\_noSHO} = \frac{\frac{3\sqrt{3}}{2} R^2 \cdot g \cdot P_{T1}}{\iint_A P_{s1} \cdot ds} \tag{5.7}$$

Where A is the area of the cell. Substituting (5.5) and (5.7) to (5.6), the soft handover gain can be calculated as

$$\text{SHO gain} = \left(\frac{\iint_A P_{s1} \cdot ds}{\iint_S P_{s1} \cdot ds + \iint_{S'} P_{s1\_SHO} \cdot ds} - 1 \right) \times 100 \quad [\%] \tag{5.8}$$

5.2.3 Impacts for soft handover gain

In the previous section, the derivation of the soft handover gain is described. There are several issues that have an impact on the downlink capacity shown as Table 5.1, in which a tick or cross indicates whether or not there is an association.

	Processing gain & target E_b/I_0	P_{s1}	P_{s1_SHO}	S & S'	Relationship between P_{s1_SHO} & P_{si_SHO}	N
Cell Selection Scheme	×	✓	✓	✓	×	✓
Soft handover algorithm	×	×	×	✓	×	✓
Soft handover overhead	×	×	×	✓	×	✓
Downlink power control	×	✓	✓	×	×	✓
Power division scheme	×	×	✓	×	✓	✓
Service type	✓	✓	✓	×	×	✓

Table 5.1 Association table

- The cell selection scheme decides which BS to camp on first. Different decision corresponds to different power level for the downlink channel. It also has an impact on S and S' because of the difference between the initiation and the termination conditions of the soft handover algorithm.
- Different soft handover algorithms and overhead lead to different S and S'.

- Different power control conditions bring out different P_{s1} and P_{s1_SHO}.
- Different power division schemes lead to different relationships between P_{s1_SHO} and P_{si_SHO}.
- Different service type corresponds to different processing gain and target E_b/I_0.

In the following sections, the impact of different issues on the downlink capacity and the soft handover gain is analysed respectively in more detail.

5.3 Cell Selection/Reselection Schemes

5.3.1 Introduction

Cell selection and reselection are two basic functionalities of mobile networks [ETSI TS 125 214]. Cell selection is responsible for finding a cell for the mobile to camp on: the selection decision is made based on the strength of the received E_c/I_0 of the downlink Common Pilot Channel (CPICH). Cell reselection is responsible for guaranteeing the required QoS by always keeping the mobile camped on a cell with good enough quality. By monitoring the nearby cells' information, the mobile can reselect a base station to camp on when the quality of the current serving base station deteriorates or when the network needs to balance the load between cells. The handover procedure is actually a kind of cell reselection process. The "Weak" mobiles near the cell boundaries can reselect a higher quality base station to communicate with (hard handover), or reselect two or more base stations to communicate with simultaneously (soft handover) in order to maintain the required QoS.

CDMA systems are interference-limited systems. In these systems, cell selection/reselection and handover control are not only responsible for guaranteeing the QoS of the individual mobile user: they can also bring benefits to the whole network by minimising the interference by choosing better quality base stations. In most of the previous literature, cell selection/reselection and handover control are investigated separately. Cell selection has been mainly analysed in systems with hierarchical cell structure [YN95] [AK99] and most analysis about soft handover simplified the initial cell selection scheme to a distance-based process [VVGZ94] [LS98]. In this thesis, the downlink soft handover gain is investigated under three different Cell Selection (CS) schemes: distance-based CS, perfect CS and normal CS.

5.3.2 Basic principles of different CS schemes

Consider a mobile located near the cell boundary as shown in Figure 5.3. E_{p1}, $E_{p2,}$ E_{p3} and E_{p4} represent the received pilot E_c/I_0 from the four surrounding BSs: BS_1, $BS_{2,}$ BS_3 and BS_4 respectively. Assuming that all the downlink pilot channels are allocated the same amount of power, E_{pi} can be expressed as

$$E_{pi} = \frac{P_{pilot} r_i^{-a} 10^{z_i/10}}{P_{Ti}(1-a) r_i^{-a} 10^{z_i/10} + \sum_j P_{Tj} r_j^{-a} 10^{z_j/10}} \tag{5.9}$$

Where P_{Ti} *i*s the total transmit power of BS_i; P_{pilot} is the transmit power of the downlink pilot channel; a is the downlink orthogonal factor; j is the index of the BSs around BS_i.

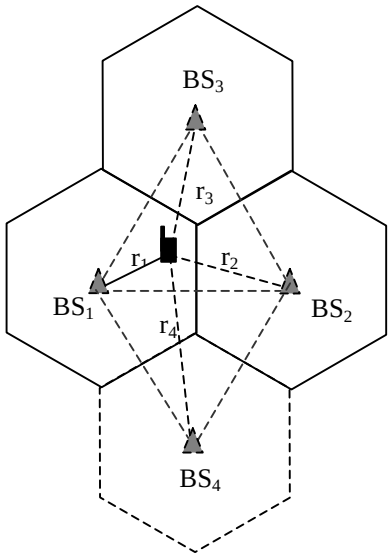

Figure 5.3 Cell layout for cell selection

A. Distance-based cell selection

In the distance-based CS scheme, the mobile always chooses the nearest BS to camp on. In the situation shown as Figure 5.3, a downlink dedicated channel would be set up between the mobile and BS_1.

B. Perfect cell selection

In the perfect CS scheme, the mobile always chooses the best BS to camp on: that from which the mobile receives the strongest pilot E_c/I_0. Because of shadowing, the nearest BS, BS_1, might not be the best BS. Figure 5.4 shows the flowchart of the perfect cell selection.

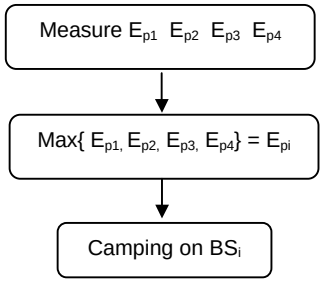

Figure 5.4 Flowchart of perfect cell selection

C. Normal cell selection

If the mobile can always chooses the best BS to camp on, the interference level of the system would be minimised. However, in a real situation, the mobile might not be always linked to the best BS because of the mobility of the user, the delay in reselection of a better cell, or the dynamic changes in the radio propagation channel. In this thesis, a threshold *CS_th* is used to include this kind of imperfect situations in the analysis. The basic principle is: the mobile always chooses the nearest BS to camp on except when the E_c/I_0 difference between the best BS and the nearest BS is higher than threshold *CS_th*. The pseudocode of the cell selection scheme can be expressed as

```
if  ( E_p_best − E_p_nearest > CS_th )
    camping on BS_best ;
else
   camping on BS_nearest ;
end
```

Figure 5.5 shows the flowchart of the normal cell selection. When the threshold *CS_th* equals to 0, normal cell selection corresponds to the perfect cell selection situation.

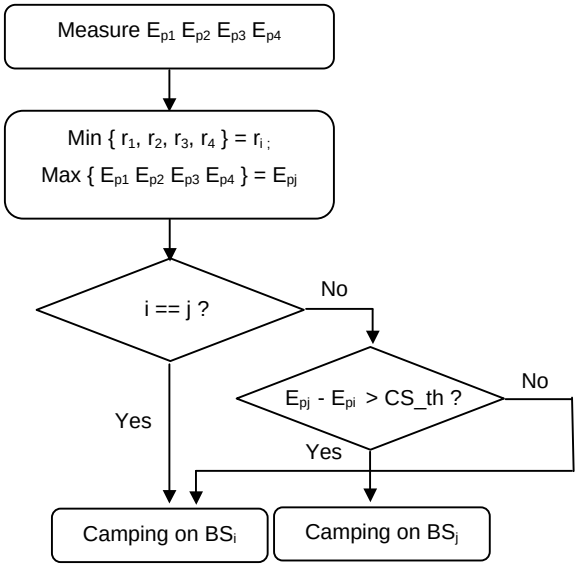

Figure 5.5 Flowchart of normal cell selection

5.3.3 Effects of different CS schemes on SHO gain

Choosing a different BS to camp on leads to different power allocation for a user at certain location who has a certain QoS target. This corresponds to different P_{s1} and P_{s1_SHO} in equation (5.5). Moreover, cell selection also has impact on the areas S and S' in (5.5) because the initiation and the termination conditions of the soft handover algorithm are normally different. Different choices of initial serving BS can lead to different soft handover decisions. The impact of different cell selection schemes on the soft handover gain is shown later in section 5.7.2.

5.4 Soft Handover Algorithms

5.4.1 Introduction

Soft handover gain depends closely on the soft handover algorithms. To date, quite a few algorithms have been proposed and evaluated [NH98] [ASAN-K01] and [HL01]. Among these algorithms, the IS-95A soft handover algorithm, UTRA soft handover algorithm and SSDT (Site Selection Diversity Transmit Power Control) are the most representative.

In the IS-95A algorithm (also called basic cdmaOne algorithm), the handover threshold is a fixed value of received pilot E_c/I_0. It is easy to implement, but has

difficulty in dealing with dynamic load changes. Based on the IS-95A algorithm, several modified cdmaOne algorithms were proposed for IS-95B and cdma2000 systems with dynamic rather than fixed thresholds [Chh99] [HKB00]. In WCDMA, more complicated schemes are used. In the UTRA soft handover scheme adopted by UMTS [ETSI TR 125 922], the handover decisions are made basing on relative thresholds. The greatest benefit of this algorithm is its easy parameterisation. Apart from UTRA soft handover algorithm, SSDT is an alternative scheme adopted by 3GPP [ETSI TR 125 922] [FHU00]. Compared to all the other algorithms, the most promising feature is that SSDT mitigates the interference caused by multiple site transmissions, but it doesn't have macrodiversity gain.

So far, some work has been done on comparing different soft handover schemes by numerical analysis or simulation. For example, [Chh99] and [HKB00] analysed and compared the performance of the IS-95A and IS-95B algorithms. In [YG-NT00], four soft handover algorithms with either fixed or dynamic thresholds are analysed in terms of mean active set number, active set update rate and outage probability. In [YG-NT01], the power-triggered and E_c/I_0–triggered UTRA soft handover algorithms are evaluated by simulation and results show that the latter achieves much less active-set update rate and outage probability but higher active-set number and call blocking probability than the former. However, all these comparisons are made based on either QoS-related or resource-allocation related indicators. In this thesis, the effects of different soft handover algorithms on the downlink capacity are compared.

5.4.2 Different SHO algorithms

In a similar way to the cell selection scheme, the soft handover decision is also made based on the received E_c/I_0 of the downlink Common Pilot Channel (CPICH). The mobile always monitors the E_c/I_0 of the Pilot channels from the nearby BSs and reports the result to the serving BS. Then the serving BS passes the information to the RNC. Inside the RNC, a judgement on whether the trigger and terminate conditions are fulfilled is made basing on the measured results. Because different algorithm have different trigger and terminate conditions, the same user in the same network could be in a different status when implementing different soft handover algorithms. This means the shape of the soft handover zone could be different with different soft handover

algorithms even though the network situation is the same. In this thesis, two typical soft handover algorithms are compared; they are the IS-95A and UTRA algorithms.

A. IS-95A soft handover algorithm

IS_95A algorithms have been described in Figure 3.5 in section 3.2.2. In this algorithm absolute handover thresholds are used. *T_ADD* and *T_DROP* are predetermined when dimensioning the network. More details about this algorithm can be found in [EIA/TIA/IS-95A]. Figure 5.6 shows the flow chat of the IS-95A soft handover algorithm. The trigger condition of IS-95A algorithm can be expressed as:

$$E_{pi} = \left(\frac{E_c}{I_0}\right)_{pilot\_BS_i} = \frac{P_{pilot} L_i}{P_T(1-a)L_i + \sum_j^M P_T L_j} \geq T\_ADD \qquad (5.10)$$

Where P_T is the total transmit power of BS; a is the downlink orthogonal factor; P_{pilot} is the transmit power of pilot channel; L_i is the transportation attenuation of the radio channel from BS_i to the mobile.

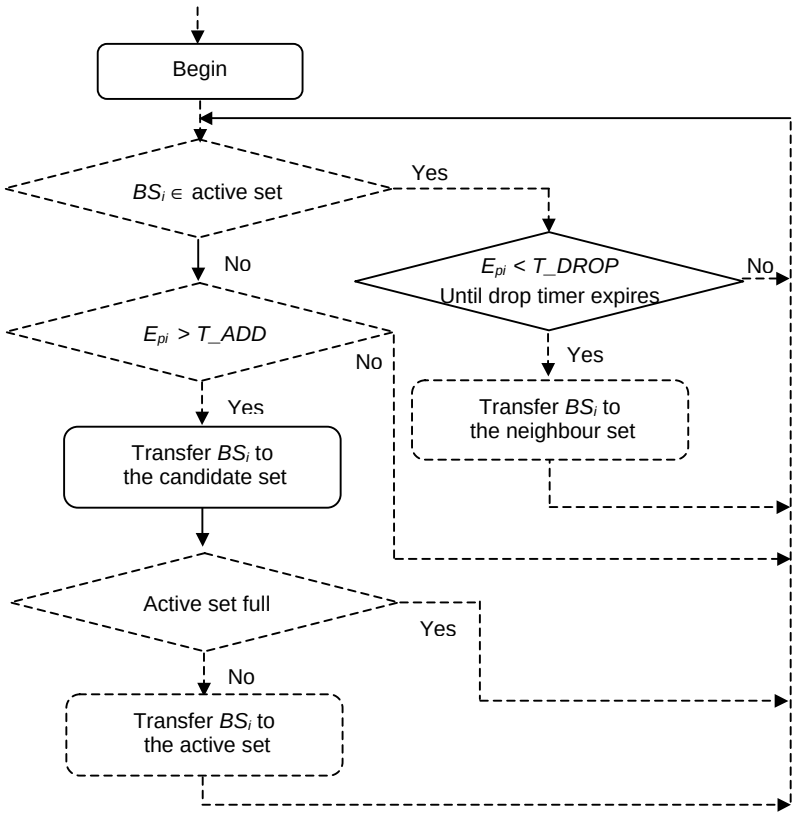

Figure 5.6 Flowchart of IS-95A soft handover algorithm

Unlike in the uplink, the interference in the downlink is related to the mobile's location. Therefore, the pilot E_c/I_0 of BS_i is not only related to r_i, but also related to the angle q_i. As a result, the border of the soft handover region is not a circle as assumed in some previous work, such as [SCH96] and [LS98]. Part (a) of Figure 5.8 shows the relationship between the soft handover zone and the soft handover overhead based with the IS-95A algorithm. The handover decision is made based on the average received pilot $E_c/I_{0.}$

B. UTRA Soft Handover Algorithm

The UTRA soft handover algorithm (also called the WCDMA soft handover algorithm) has also been presented in section 3.2.2, in Figure 3.6. Differing from IS-95A, *relative* rather than absolute thresholds are used in the UTRA algorithm. Figure 5.7 shows the flow chat of the UTRA soft handover algorithm

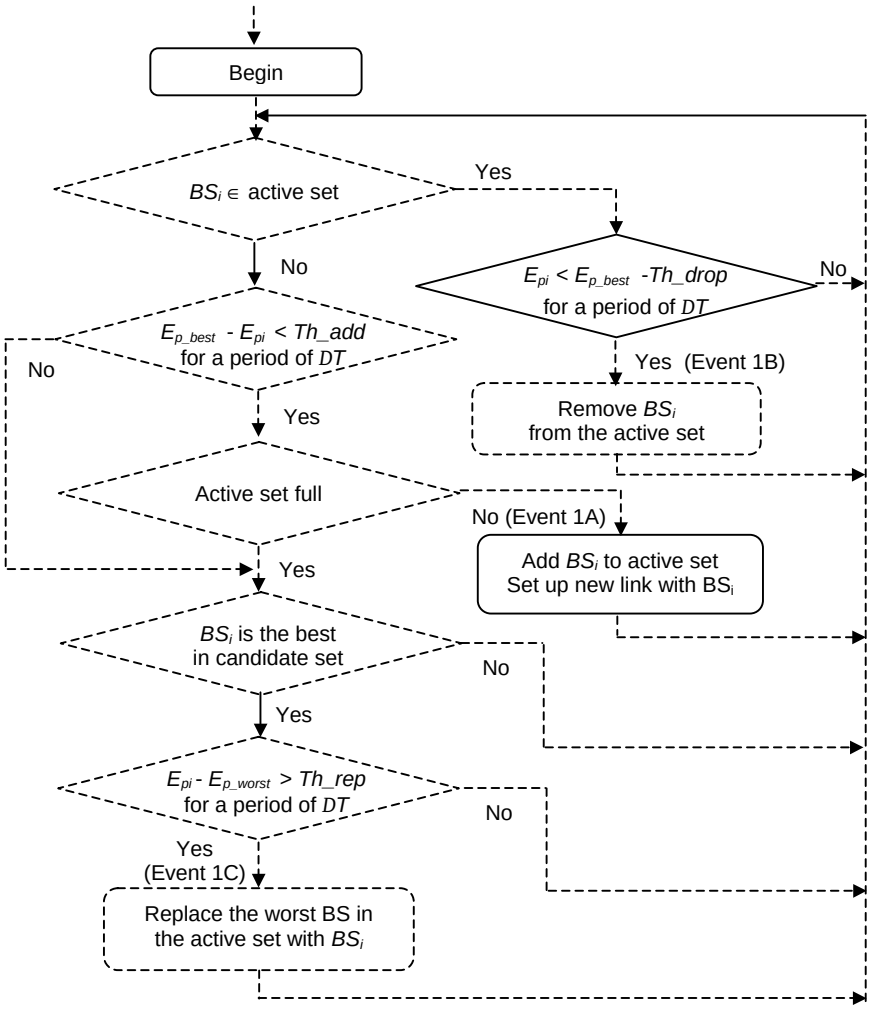

Figure 5.7 Flowchart of UTRA soft handover algorithm

Where E_{pi} represents the received E_c/I_0 of CPICH from BS_i; E_{p_best} is the E_c/I_0 of the strongest CPICH present in the active set; E_{p_worst} is the E_c/I_0 of the weakest CPICH present in the active set; $Th\_add = AS\_Th - AS\_Th\_Hyst$; $Th\_drop = AS\_Th + AS\_Th\_Hyst$; $Th\_rep = AS\_\mathrm{Re}p\_Hyst$. The definitions of *AS_Th*, *AS_Th_Hyst* and *AS_Rep_Hyst* have been given in Figure 3.6.

Assuming BS_i is the original serving BS of a user, the trigger condition of UTRA algorithm can be expressed as:

$$\left(\frac{E_c}{I_0}\right)_{pilot\_BS_i} - \left(\frac{E_c}{I_0}\right)_{pilot\_BS_j} \le AS\_Th - AS\_Th\_Hyst \qquad (5.11)$$

Part (b) in Figure 5.8 shows the soft handover zones of the UTRA algorithm with different soft handover overhead. The handover decision is also made based on the average received pilot E_c/I_0.

5.4.3 SHO zone of different SHO algorithms

Figure 5.8 shows the soft handover zone of IS-95A and UTRA algorithm with different soft handover overhead based on the average received pilot E_c/I_0. Here, two-way soft handover is considered and uniform load distribution is assumed. Therefore, the soft handover overhead equals the fraction of the area of the soft handover zone to the area of the cell.

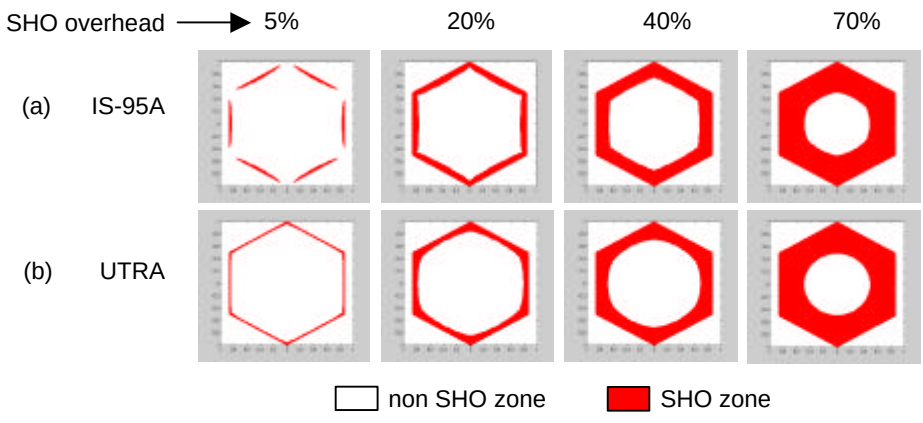

Figure 5.8 Comparison of soft handover zone of different algorithms

From Figure 5.8, it is clear that the shape of the soft handover zones of the two algorithms is extremely different when the soft handover overhead is small. When the overhead goes up, the differences tend to die out. Therefore, when estimate the soft handover gain from equation (5.8), different S and S' should be substituted according to the different soft handover algorithm.

5.5 Downlink Power Control

5.5.1 Introduction

As mentioned in Chapter 2, in CDMA systems, power control is one of the most crucial functionalities for radio resource management. In the uplink, power control is applied in order to overcome the near-far effect; in the downlink, the main reason for employing power control is to decrease the inter-cell interference. Because downlink power control is not as important as uplink power control, some previous work about soft handover ignored the downlink power control [LS98][MLG99].

According to the analysis in Chapter 4, to the mobiles in soft handover status near the edge of cells, the inter-cell interference is much higher than the intra-cell interference. This is especially true when the orthogonality between different downlink channels is well preserved. Therefore, it is not difficult to come to a conclusion that there is some kind of relationship between the power control and the soft handover gain. In this thesis, this intuitional conclusion is verified by analysing and comparing the soft handover gain under three different power control conditions separately.

5.5.2 Power allocation under three power control conditions

A. No power control

Because in the downlink, power control is not as crucial as in the uplink, some previous work on soft handover ignored it, such as [LS98] and [MLG99]. Without power control, each downlink traffic channel is allocated the same amount of power. Therefore,

$$P_{s1} = P_{s1\_SHO} = \frac{P_{T1} \cdot g}{N(1+x)} \tag{5.12}$$

Where x is the soft handover overhead; N is the number of active users per cell; $N(1+x)$ is the total number of downlink dedicated channels; g is the fraction of the total BS transmit power devoted to the traffic.

B. Perfect power control

The power allocation under perfect power control has been analysed in section 4.4 of Chapter 4. Perfect downlink power control equalises the received E_b/I_0 of all mobiles at the target value at all times. Therefore, the transmit power of the downlink dedicated channels can be derived from the link quality equations. To a user located at (r_1,q_1) outside the soft handover zone as user *1* in Figure 5.2, ignoring the thermal noise, the received bit energy-to-interference power spectral density ratio E_b/I_0 can be expressed as

$$\frac{E_b}{I_0} = \frac{W}{nR} \frac{P_{s1} r_1^{-a} 10^{z_1/10}}{P_{T1}(1-a) r_1^{-a} 10^{z_1/10} + \sum_{j=2}^{M} P_{Tj} r_j^{-a} 10^{z_j/10}} \tag{5.13}$$

Where W is the chip rate; R is the service bit rate; v is the activity factor; P_T is the total transmit power of all BSs; r_1 and r_j are distances from the mobile to BS_1 and BS_j; a is the path loss exponent; z is the dB attenuation due to shadowing, with a standard deviation of s; a is the orthogonal factor; M is the index of BSs that are taken into account for the inter-cell interference. Here the BSs in the first and second tiers around BS_1 are considered, so M=19.

Assume that users are distributed evenly throughout the network and the total transmit power of all BSs is the same, which is denoted by P_T. The required transmit power of the downlink dedicated channel from BS_1, P_{s1} can be solved from (5.13) as

$$P_{s1} = \frac{\frac{nR}{W}\left(\frac{E_b}{I_0}\right)_t P_T \left[(1-a) r_1^{-a} 10^{z_1/10} + \sum_{j=2}^{M} r_j^{-a} 10^{z_j/10}\right]}{r_1^{-a} 10^{z_1/10}} = \frac{nR}{W}\left(\frac{E_b}{I_0}\right)_t P_T \left[1 - a + \sum(1)\right] \tag{5.14}$$

Where $(E_b/I_0)_t$ is the target value of E_b/I_0; $\sum(1) = \sum_{j=2}^{M} \left(\frac{r_j}{r_1}\right)^{-a} 10^{(z_j - z_1)/10}$.

To a user inside the soft handover zone as user *2* in Figure 5.2, assuming that BS_1 and BS_i are in the active set (2-way SHO), maximal ratio combining and balanced power division strategy are used during soft handover, the received E_b/I_0 is

$$\frac{E_b}{I_0} = \left[\frac{E_b}{I_0}\right]_1 + \left[\frac{E_b}{I_0}\right]_i = \frac{W}{nR}\left[\frac{P_{s1\_SHO} r_1^{-a} 10^{V_1/10}}{P_T(1-a) r_1^{-a} 10^{V_1/10} + \sum_{j=2}^{19} P_T r_j^{-a} 10^{V_j/10}} + \frac{P_{si\_SHO} r_i^{-a} 10^{V_i/10}}{P_T(1-a) r_i^{-a} 10^{V_i/10} + \sum_{\substack{k=1 \\ (k\neq i)}}^{19} P_T r_k^{-a} 10^{V_k/10}}\right] \quad (5.15)$$

Thus, P_{s1_SHO} can be calculated as

$$P_{s1\_SHO} = \frac{\frac{nR}{W}\left(\frac{E_b}{I_0}\right)_t P_T}{\frac{1}{1-a+\sum(1)} + \frac{1}{1-a+\sum(2)}} \quad (5.16)$$

$$\text{Where } \sum(1) = \sum_{j=2}^{M}\left(\frac{r_j}{r_1}\right)^{-a} 10^{(z_j - z_1)/10} \text{ and } \sum(2) = \sum_{\substack{k=1 \\ (k\neq i)}}^{M}\left(\frac{r_k}{r_i}\right)^{-a} 10^{(z_k - z_i)/10} \quad (5.17)$$

The power allocation under 3-way soft handover can be derived in the similar way.

C. Imperfect power control

It has been experimentally verified that the power control error can be modelled as a random variable with log-normal distribution [KS00]. Letting P_e represent the error of power control in dB, P_{s1} and P_{s1_SHO} can be rewritten as

$$P_{s1} = P_{s1}' + P_e \quad [dB] \quad (5.18)$$

$$P_{s1\_SHO} = P_{s1\_SHO}' + P_{e1} \quad [dB] \quad \text{and} \quad P_{si\_SHO} = P_{si\_SHO}' + P_{ei} \quad [dB] \quad (5.19)$$

Where P_e is a Gaussian random variable with zero mean and variance, s_e^2. The standard deviation s_e reflects the degree of the imperfection. During the soft handover process, P_{e1} and P_{e2} are independent. Substituting (5.18) and (5.19) to (5.13) and (5.15), the actual transmit power under imperfect power control condition, P_{s1}' and P_{s1_SHO}' can be obtained.

5.5.3 Power control effects on SHO gain

The downlink capacity and soft handover gain with perfect or imperfect power control can be calculated by substituting P_{s1}, P_{s1_SHO}, P_{s1}' and P_{s1_SHO}' to (5.5) and (5.8).

Without power control, the downlink capacity can be calculated using a method similar to that proposed in [LS98]. To a user located at (r_1,q_1) outside the soft handover zone, substituting (5.12) to (5.13), E_b/I_0 can be expressed as

$$\frac{E_b}{I_0} = \frac{W}{vR}\frac{g \cdot r_1^{-a} 10^{z_1/10}}{N(1+x)(1-a)r_1^{-a}10^{z_1/10} + N(1+x)\sum_{j=2}^{M} r_j^{-a}10^{z_j/10}} = \frac{W}{vR}\frac{g}{N(1+x)\left[1-a+\sum_{j=2}^{M}\left(\frac{r_j}{r_1}\right)^{-a}10^{(z_j-z_1)/10}\right]} \tag{5.20}$$

It is clear that without power control, E_b/I_0 is a function of mobile location. Solving N from (5.20) gives

$$N = \frac{\frac{W}{vR}\frac{g}{(E_b/I_0)_t}}{(1+x)\left[1-a+\sum_{j=2}^{M}\left(\frac{r_j}{r_1}\right)^{-a}10^{(z_j-z_1)/10}\right]} \tag{5.21}$$

To a mobile inside the soft handover zone shown as user 2 in Figure 5.2, The E_b/I_0 can be expressed as

$$\frac{E_b}{I_0} = \frac{W}{vR}\left[\frac{g}{N(1+x)\left[1-a+\sum(1)\right]} + \frac{g}{N(1+x)\left[1-a+\sum(2)\right]}\right] \tag{5.22}$$

Where $\sum(1)$ and $\sum(2)$ are shown in (5.15).

From (5.22), N can be derived as

$$N = \frac{\frac{W}{\nu R}\frac{g}{(E_b/I_0)_t}}{(1+x)}\left[\frac{1}{1-a+\sum(1)}+\frac{1}{1-a+\sum(2)}\right] \tag{5.23}$$

Therefore, the average downlink capacity N without considering downlink power control can be expressed as:

$$N(r_1) = \min\left\{\begin{array}{ll} E\left[\dfrac{\frac{W}{\nu R}\frac{g}{E_b/I_0}}{(1+x)\left[1-a+\sum(1)\right]}\right] & \text{outside SHO zone} \\ E\left[\dfrac{\frac{W}{\nu R}\frac{g}{E_b/I_0}}{(1+x)}\left(\dfrac{1}{1-a+\sum(1)}+\dfrac{1}{1-a+\sum(2)}\right)\right] & \text{inside SHO zone} \end{array}\right\} \tag{5.24}$$

From (5.24), it can be seen that without power control, the downlink capacity is limited by the "weakest user"[5] in the cell.

5.6 Multi-rate Services Environment

5.6.1 Introduction

Aiming at "information at any time, at any place, in any form", 3G systems will operate in a more complicated environment with different types of service supported simultaneously, such as voice, data, Internet, and broadband multimedia services. Different type of services have different QoS requirement. The processing gain for each service is also different due to the differences in the bit rate. Thus, the resource that needs to be allocated is not the same for different type of services. In Most of the previous literature, the downlink capacity and soft handover gain are analysed on a single service basis [LS98][SHL-SW00]. In this thesis, the downlink capacity and soft handover gain with different multi-rate services structures are investigated.

[5] Weakest user refers to the user with lowest received E_b/I_0.

As mentioned in Chapter 2, CDMA systems are interference limited, each newly accepted connection causing additional interference to the existing connections. The non-real-time services, being bursty in nature, can be sporadic sources of interference during active periods. These bursts can cause interference fluctuation that is not easy to model. In this thesis, soft handover effects on the average downlink capacity are the issues that are being investigated, so the discontinuity of the non-real-time service is simply represented by the activity factor in the section. If the instantaneous bursty feature is to be taken into account in detail, more complicated models will be needed.

5.6.2 Multi-service structure

Three typical services supported by 3G systems have been chosen to build up the multi-service environment. They are AMR 12.2kbit/s voice service, 144kbit/s real-time data service and 384kbit/s non-real-time data service. Various multi-service environments can be structured by changing the proportion of different type of services. Table 5.2 shows the typical parameters of different services [HT00].

Service type	Bit rate R	Activity factor v	E_b/I_0 target $(E_b/I_0)_t$
Voice service	12.2 kbps	0.5	5 dB
Real time data service	144 kbps	1	1.5 dB
Non real time data	384 kbps	0.2	1 dB

Table 5.2 Parameters of different services

Considering different types of services, (5.14) and (5.16) can be rewritten as

$$P_{s1,k} = \frac{n_k R_k}{W}\left(\frac{E_b}{I_0}\right)_{t,k} P_T\left[1 - a + \sum(1)\right] \tag{5.25}$$

$$P_{s1\_SHO,k} = \frac{\frac{n_k R_k}{W}\left(\frac{E_b}{I_0}\right)_{t,k} P_T}{\frac{1}{1-a+\sum(1)} + \frac{1}{1-a+\sum(2)}} \tag{5.26}$$

Where k indicates the type of service required by the user. Using P_0 and P_{0_SHO} replacing the part that is independent of the service type, leads to:

$$P_{s1,k} = \frac{n_k R_k}{W}\left(\frac{E_b}{I_0}\right)_{t,k} P_T P_0 \quad \text{and} \quad P_{s1\_SHO,k} = \frac{n_k R_k}{W}\left(\frac{E_b}{I_0}\right)_{t,k} P_T P_{0\_SHO} \tag{5.27}$$

$$\text{Where } P_0 = \left[1 - a + \sum(1)\right] \text{ and } P_{0\_SHO} = \frac{1}{\frac{1}{1-a+\sum(1)} + \frac{1}{1-a+\sum(2)}} \tag{5.28}$$

When comparing the capacity of multi-service systems, throughput (also called information capacity[6]) is often used rather than the number of active users per cell. The throughput of a multi-service WCDMA system can be calculated as

$$Th = \sum_{n=1}^{N} R_n v_n \qquad [kbit/s/cell] \tag{5.29}$$

Where n is the index of users (n=1,2,….N); N is the number of active users per cell; R_n and v_n are the bit rate and the activity factor of the service required by the n^{th} user.

In a single service system, assuming that all the active users require the k type of service, the throughput Th_s can be derived from (5.5) as

$$Th_s = Nv_k R_k = \frac{g \cdot A}{\frac{1}{W}\left(\frac{E_b}{I_0}\right)_{t,k}\left[\iint_S P_0 \cdot ds + \iint_{S'} P_{0\_SHO} \cdot ds\right]} \qquad (kbit/s/cell) \tag{5.30}$$

Where A is the area of the hexagonal cell; S is the non-soft handover zone and S' is the soft handover zone.

In a multi-service system with three different types of service supported, equation (5.3) can be rewritten as

$$\begin{aligned} P_{T1} = P_{T1}(1-g) &+ \iint_S \left(r_1 \cdot P_{s1,1} + r_2 \cdot P_{s1,2} + r_3 \cdot P_{s1,3}\right) ds \\ &+ \iint_{S'} \left(r_1 \cdot P_{s1\_SHO,1} + r_2 \cdot P_{s1\_SHO,2} + r_3 \cdot P_{s1\_SHO,3}\right) ds \end{aligned} \tag{5.31}$$

[6] In specification [ETSI TS 125 214], information capacity is defined as the total number of user channel information bits that can be supported by a single cell.

Under the assumption of uniform distribution of active users, the densities of users requiring different type of service are

$$r_1 = {2N_m \cdot x}\Big/{3\sqrt{3}}, \quad r_2 = {2N_m \cdot y}\Big/{3\sqrt{3}}, \quad r_3 = {2N_m \cdot z}\Big/{3\sqrt{3}}, \quad x + y + z = 1 \tag{5.32}$$

Where N_m is the total number of active users in the multi-service system; x, y, z are proportions of 3 types of services respectively. N_m can be calculated from (5.31) as

$$N_m = \frac{g \cdot A}{\left(\frac{v_1 R_1}{W}\left(\frac{E_b}{I_0}\right)_{t,1} x + \frac{v_2 R_2}{W}\left(\frac{E_b}{I_0}\right)_{t,2} y + \frac{v_3 R_3}{W}\left(\frac{E_b}{I_0}\right)_{t,3} z\right)\left[\iint_S P_0 \cdot ds + \iint_{S'} P_{0\_SHO} \cdot ds\right]} \tag{5.33}$$

Thus, the throughput of the multi-service system, Th_m can be obtained as

$$\begin{aligned} Th_m &= N_m\left(v_1 R_1 x + v_2 R_2 y + v_3 R_3 z\right) \\ &= \frac{g \cdot A \cdot \left(v_1 R_1 x + v_2 R_2 y + v_3 R_3 z\right)}{\left(\frac{v_1 R_1}{W}\left(\frac{E_b}{I_0}\right)_{t,1} x + \frac{v_2 R_2}{W}\left(\frac{E_b}{I_0}\right)_{t,2} y + \frac{v_3 R_3}{W}\left(\frac{E_b}{I_0}\right)_{t,3} z\right)\left[\iint_S P_0 \cdot ds + \iint_{S'} P_{0\_SHO} \cdot ds\right]} \end{aligned} \tag{5.34}$$

The information capacity gain caused by soft handover with certain soft handover overhead can be expressed as

$$SHO_{gain} = \left(\frac{Th_{m\_SHO}}{Th_{m\_noSHO}} - 1\right) \times 100 = \left(\frac{\iint_A P_0 \cdot ds}{\iint_S P_0 \cdot ds + \iint_{S'} P_{0\_SHO} \cdot ds} - 1\right) \times 100 \quad [\%] \tag{5.35}$$

(5.35) shows that different multi-service structures do not have an impact on the soft handover gain when different types of users[7] are distributed evenly because P_0 and P_{0_SHO} are independent to the service type. Comparing (5.34) and (5.30) gives

$$\frac{Th_m}{Th_s} = \frac{\left(\frac{E_b}{I_0}\right)_{t,k} \frac{1}{W}\left(v_1 R_1 x + v_2 R_2 y + v_3 R_3 z\right)}{\frac{v_1 R_1}{W}\left(\frac{E_b}{I_0}\right)_{t,1} x + \frac{v_2 R_2}{W}\left(\frac{E_b}{I_0}\right)_{t,2} y + \frac{v_3 R_3}{W}\left(\frac{E_b}{I_0}\right)_{t,3} z} \tag{5.36}$$

[7] Different types of users refer to the users requiring different types of services.

From (5.36), it is clear that different multi-service structures do have an impact on the downlink throughput. The downlink throughput with different multi-service structures is shown later in section 5.7.5.

5.7 Results and Discussion

5.7.1 Introduction

In this section, the results obtained from the analysis in the previous sections of this chapter are presented and discussed. Table 5.3 shows the system parameters: all the values are taken from practical ranges. Results are obtained based on these values, although when analysing the sensitivities, the values of certain parameter might change, these changes being mentioned in the caption of the figures.

Symbol		Value
a	Path loss exponent	4
s	Standard deviation of shadowing	8 dB
g	traffic channel power ratio	0.8
a	Orthogonal factor	0.6
W	Chip rate	3.84 Mchip/s
R	Service bit rate	12.2 kbit/s
v	Activity factor	0.5

Table 5.3 System parameters

5.7.2 SHO gain with different CS schemes

Using the UTRA soft handover algorithm as an example, Figure 5.9 shows the downlink capacity and the capacity gain caused by soft handover with three different cell selection schemes. Two-way soft handover is considered here. Downlink power control, maximal ratio combining and balanced power division during soft handover are all assumed to be perfect.

It is clear that in the downlink the soft handover gain is related closely to the initial cell selection schemes. Using distance-based cell selection (blue curve), the soft

handover gain is overestimated and with perfect cell selection (green curve), the soft handover gain is under estimated. If all the active users can communicate with the best BS at all times, there is no need to implement soft handover for improving the downlink capacity. However, this perfect situation does not exist in practice. Because of the mobility of the user and the dynamic changes in the radio propagation channel, the best BS seen by a particular mobile terminal (especially to those users near the cell boundaries) changes frequently. It is undesirable to track the best BS under these circumstances because it leads to frequent switching between BSs and hence, "ping-pong" effects. Moreover, the time delay in making the decision and change may mean that the best BS at the start of the process in no longer the best on completion.

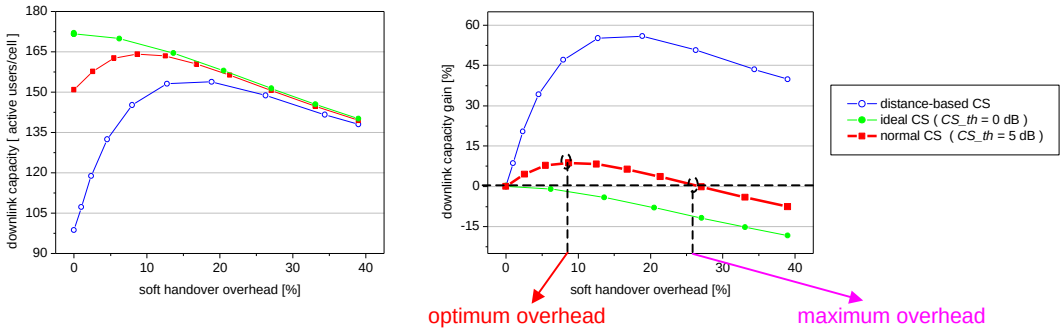

(a) DL capacity (b) SHO gain

Figure 5.9 Soft handover gain with different cell selection schemes

Under the normal cell selection scheme, shown as the red line in Figure 5.9, soft handover effects on the downlink capacity depend intimately on the soft handover overhead. This shows the trade-off between the macrodiversity gain and the extra resource consumption caused by the soft handover. On the red curve, there are two points (shown as black circles) that need further explanation. One is the peak that corresponds to the "optimum overhead" and the other is the intersection point with the *x* axis, which corresponds to the "maximum overhead". The "optimum overhead" shows the optimum proportion of the soft handover for maximising the downlink capacity and the "maximum overhead" shows the balance point of the macrodiversity gain and the extra resource consumption. When the overhead is kept under the "maximum overhead", macrodiversity gain overweighs the extra resource consumption and soft handover benefits the system by increasing the capacity. When the overhead goes beyond the "maximum overhead", the capacity is lower than that without

implementing soft handover. With the UTRA soft handover algorithm, when *CS_th*=5dB, the optimum overhead is about 9.35% with maximum 8.78% of soft handover gain and the maximum overhead is 26.7%.

In Figure 5.10, the soft handover gains under normal cell selection scheme with different threshold *CS_th* are compared. Results show that when the soft handover overhead is fixed, the soft handover gain is bigger with higher *CS_th*.

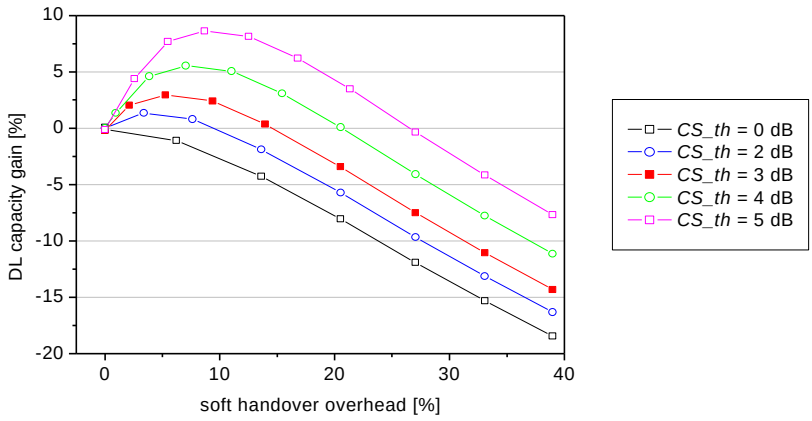

Figure 5.10 Soft handover gain under normal cell selection with different *CS_th*

In Figure 5.9 and 5.10, only two-way soft handover is considered and the maximum size of the active set is limited to two. Figure 5.11 compares the soft handover gain with different active set sizes. When the maximum size of the active set is three, three BSs can have connections with the user simultaneously as long as the soft handover criteria are fulfilled. In the two-way soft handover case, the soft handover overhead (defined in Chapter 4 on page 54) is equal to the proportion of users inside the soft handover zone. When the size of the active set is bigger than two, the soft handover overhead is bigger than the proportion of users inside the soft handover zone because some users need more than one extra downlink channels during the soft handover process. To make the two cases comparable, the proportion of users inside the soft handover zone rather than the soft handover overhead in shown along the *x* axis in Figure 5.11. The results are obtained based on the UTRA soft handover algorithm and normal cell selection with *CS_th* equals 5dB.

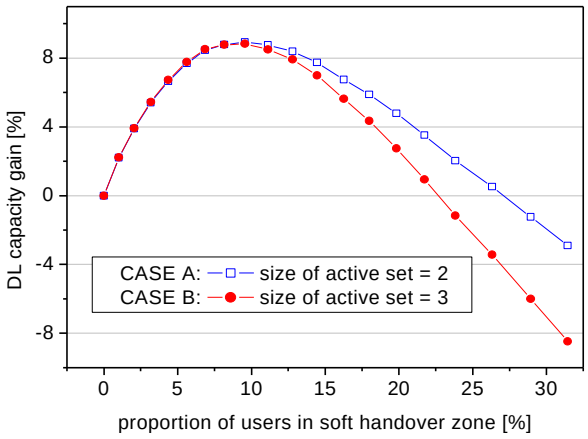

Figure 5.11 Soft handover gain with different size of active set

In Figure 5.11, when the proportion of users in soft handover status is small, there is not much difference between the two cases A (active set = 2) and B(active set = 3). However, when the proportion of users in soft handover status increases, the performance of case B is worse than the performance of case A because there is too much interference being added. This means that from the system level point of view, the size of the active set does not follow the rule “the bigger the better”, although the link level performance analysis of Chapter 4 shows that 3-way soft handover has a lower fade margin than 2-way soft handover. Therefore, considering the complexity and the increased signalling that comes with adding an extra BS in the active set when implementing soft handover, the size of the active set should be kept to two. This conclusion has not been drawn in any previous paper in the literature.

5.7.3 SHO gain with different algorithms

This section shows the results obtained from the analysis in section 5.4. The soft handover gains that come from the two typical algorithms are compared. Moreover, the sensitivity of the soft handover gain to different parameters is investigated. Figure 5.12 shows the downlink capacity gain caused by soft handover with IS-95A and UTRA algorithms respectively. Two-way soft handover and normal cell selection are considered here. Downlink power control, maximal ratio combining and balanced power division during soft handover are all assumed to be perfect.

From Figure 5.12, it is obvious that the performance of different soft handover algorithms is related closely to the soft handover overhead. When the overhead is lower than approximate 21%, UTRA has better performance than IS-95A. Beyond 21% overhead, IS-95A has slightly better performance. The difference between the two algorithms is caused by the different shape of the soft handover zones as shown in Figure 5.8. When the overhead is fixed, UTRA algorithm puts more corner users (see the definition in Chapter 4) inside the soft handover zone. According to the analysis in Chapter 4, the corner users suffer the biggest inter-cell interference. Soft handover can decrease the average total power needed for these users. This explains why the downlink capacity can be increased by soft handover when the overhead is kept under certain value.

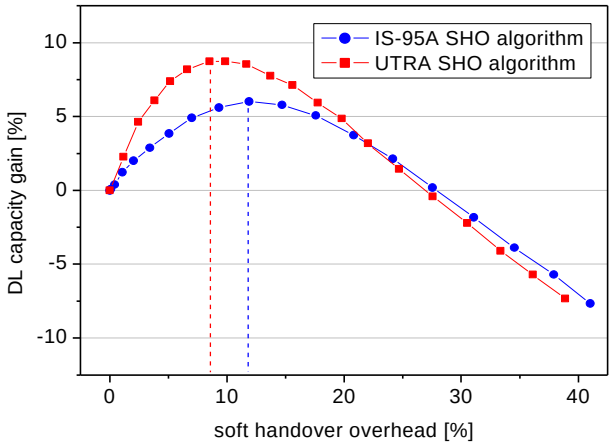

Figure 5.12 Comparison of IS-95A and UTRA soft handover algorithms

With the two different algorithms, the optimum overhead is different too. For the UTRA algorithm, the optimum overhead is 9.35% at 8.78% soft handover gain and with the IS-95A algorithm, the optimum overhead is 11.88% at 6.02% soft handover gain.

Figure 5.13 shows the sensitivities of the soft handover gain to different parameters: a is the path loss exponent; s is the standard deviation of shadowing and a is the downlink orthogonal factor. It is clear that the soft handover gain is sensitive to these three parameters. For example, with the UTRA soft handover algorithm ((a) in Figure 5.13), when the overhead is fixed, the soft handover gain is higher with higher s. This

means that the UTRA soft handover algorithm brings more benefits to systems with worse shadowing fading. Because different algorithms have different handover criteria, IS-95A and UTRA algorithm have different reactions to the parameter changes.

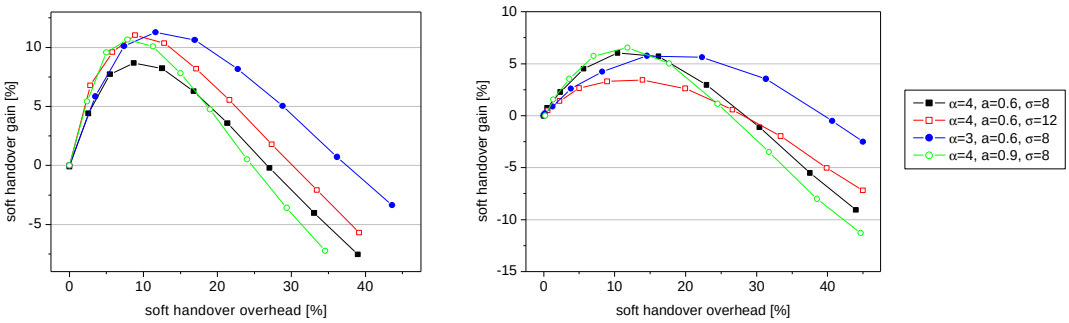

(a) UTRA algorithm (b) IS-95A algorithm

Figure 5.13 Sensitivities of soft handover gain

A conclusion, which can be obtained from Figure 5.13 is that the optimum and the maximum soft handover overhead (see definition in section 5.7.2) are not fixed values; they change along with the dynamic changes of the radio environment. In the IS-95A and UTRA algorithms, the different overheads correspond to different handover thresholds. Normally, these thresholds are preset in the RNC when dimensioning the network so that modifying these thresholds during the operation time is not an easy task because the dynamic changes are unpredictable. Later in Chapter 6, a new method for optimising soft handover will be proposed and the optimum soft handover overhead and threshold ranges will be obtained.

5.7.4 SHO gain under different power control conditions

In this section, the results obtained from the analysis in section 5.5 are presented. Figure 5.14 shows the mean E_b/I_0 (equation (5.18)) of users at different location when the downlink power control is not considered. System parameters are taken from Table 5.3. It is assumed that there are 50 active users each cell and the soft handover is simplified to a distance-based scenario (by doing this the edge of the soft handover zone is more clear in Figure 5.14 and it doesn't influence the E_b/I_0 of users at different locations): all the mobiles further than R_h from their serving BS are in soft handover status. The relative distance from the mobile to its serving BS is shown along the x

axis and the mean received E_b/I_0 in dB is shown along the *y* axis. Similar to previous analysis, maximal ratio combining and balanced power division during soft handover are assumed to be perfect. Inside the soft handover zone, two-way soft handover is considered.

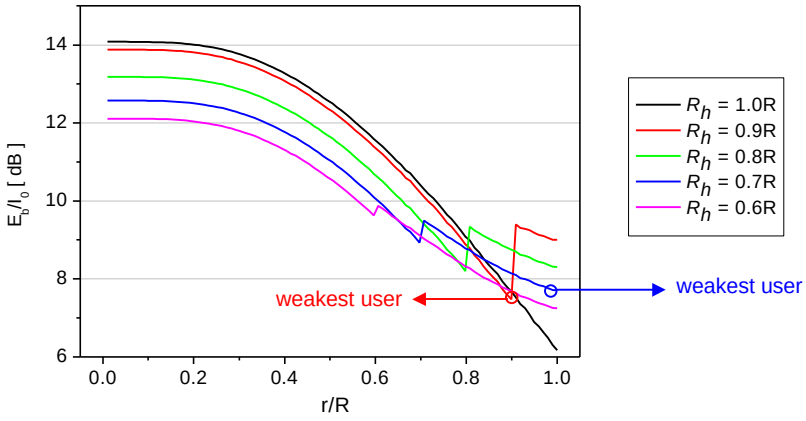

Figure 5.14 E_b/I_0 vs. mobile location

Form Figure 5.14, it is clear that without downlink power control, the received E_b/I_0 is related to the mobile's location: this is because the interference is location-related in the downlink (see Figure 4.5 and 4.6). Thus, the downlink capacity is limited by the weakest user who has the lowest E_b/I_0. Soft handover improves the QoS of the users near the cell boundaries and decreases the QoS of the users near the BS. The weakest user's location depends on the soft handover overhead.

Figure 5.15 shows the soft handover gain under three different power control conditions: no power control, perfect power control and imperfect power control. The UTRA soft handover algorithm is used and only two-way soft handover is considered. Other procedures such as cell selection, maximal ratio combining and balanced power division during soft handover are assumed to be perfect.

It is clear that although power control in the downlink direction is not as crucial as it in the uplink direction, it does have impact on the soft handover gain. The maximum downlink soft handover gain will be overestimated without considering the power control and underestimated without considering the imperfection of the power control process. When the power control is not perfect, the optimum overhead and the maximum soft handover gain are bigger with higher s_e. Choosing the proper soft

handover overhead according to different power control conditions can improve the downlink soft handover gain.

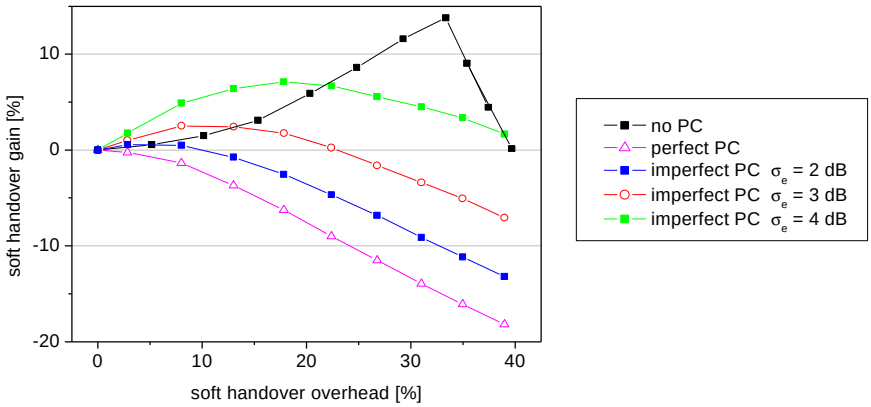

Figure 5.15 Soft handover gain under different power control conditions

5.7.5 SHO gain in multi-service environment

The analysis in section 5.6 has shown that different multi-service structures have no impact on the soft handover gain when all the active users are distributed evenly and the same handover criteria is employed to all these users. However, different multi-service structures do have an impact on the downlink throughput. Figure 5.16 shows the information capacity (throughput) gain of WCDMA systems with different multi-service structures.

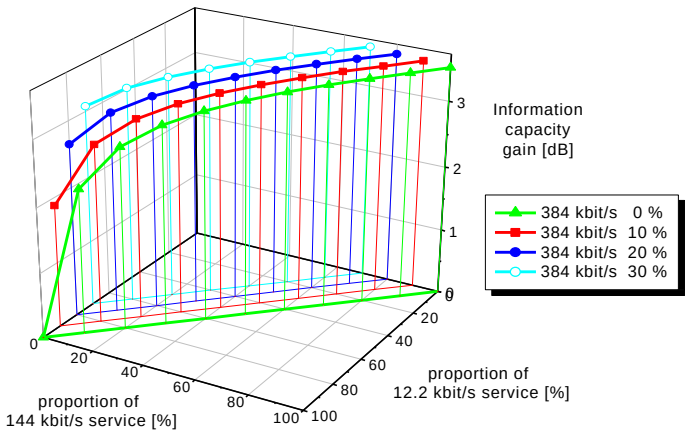

Figure 5.16 Capacity gain with different multi-service structures

The capacity gain is obtained by comparing the capacity with different multi-service structures to that with a single service (12.2 kbit/s speech service).

The results can be summarised as Table 5.4. "—" means the proportion of the service is fixed; "↑" means the proportion of the service goes up and "↓" means the proportion of the service goes down.

12.2 kbit/s —	144 kbit/s ↓	384 kbit/s ↑	Throughput ↑
	144 kbit/s ↑	384 kbit/s ↓	Throughput ↓
144 kbit/s —	12.2 kbit/s ↓	384 kbit/s ↑	Throughput ↑
	12.2 kbit/s ↑	384 kbit/s ↓	Throughput ↓
384 kbit/s —	12.2 kbit/s ↓	144 kbit/s ↑	Throughput ↑
	12.2 kbit/s ↑	144 kbit/s ↓	Throughput ↓

Table 5.4 Multi-service association table

The results can be explained by introducing two ratios. One is the "relative throughput contribution" (RTC) and the other is the "relative resource consumption" (RRC). As mentioned in section 5.6, the throughput of a multi-service WCDMA system can be calculated as

$$Th = \sum_{i=1}^{N} R_i v_i \qquad [kbit/s/cell] \tag{5.37}$$

Where i is the index of users (i=1,2,….N); N is the number of active users per cell; R_i and v_i are the bit rate and the activity factor of the service required by the i^{th} user. Thus, to a certain active user i, the contribution to the throughput is $R_i v_i$. When comparing two different services, the "relative throughput contribution" can be expressed as

$$RTC = \frac{R_1 \cdot v_1}{R_2 \cdot v_2} \tag{5.38}$$

Where R_1, v_1, and R_2, v_2 are the bit rate and the activity factor for service 1 and 2 respectively.

Based on the power allocation equation (5.27), the "relative resource consumption" of the two services can be written as

$$RRC = \frac{P_1}{P_2} = \frac{\frac{R_1 \cdot v_1}{W}\left(\frac{E_b}{I_0}\right)_{t,1} P_T P_0}{\frac{R_2 \cdot v_2}{W}\left(\frac{E_b}{I_0}\right)_{t,2} P_T P_0} = \frac{R_1 \cdot v_1}{R_2 \cdot v_2}\frac{\left(\frac{E_b}{I_0}\right)_{t,1}}{\left(\frac{E_b}{I_0}\right)_{t,2}} = RTC \quad \frac{\left(\frac{E_b}{I_0}\right)_{t,1}}{\left(\frac{E_b}{I_0}\right)_{t,2}} \quad (5.39)$$

Where $(E_b/I_0)_{t,1}$ and $(E_b/I_0)_{t,2}$ are the target E_b/I_0 of service 1 and 2 respectively.

If the ratio RTC is larger than the ratio RRC, the throughput changes with the same trend as that for the proportion of service 1. Equation (5.39) explains the results in Figure 5.16 and Table 5.4.

As mentioned in section 5.6, the non-real-time service model is simplified in this thesis, the throughput calculated being the average value. If the instantaneous bursty feature needs to be taken into account then more complicated models are needed.

5.8 Summary

In this chapter, the system level performance of soft handover in terms of downlink capacity gain has been investigated and the impact of different issues on the soft handover gain analysed. The basic method for analysing soft handover gain will be used later in Chapter 6 for soft handover optimisation and Chapter 7 performance evaluation of the new power control approach.

Chapter 6 Soft Handover Optimisation

6.1 Introduction

The results in the last two chapters show that the performance of the soft handover depends closely on the algorithm and the overhead. In order to benefit from the advantages of soft handover, it is important that the proper algorithm is applied and the handover parameters are well set. Some research has been conducted on the optimisation of different soft handover algorithms. For example, in [HL01], IS-95 soft handover algorithm is optimised for minimising the outage probability. The set of handover thresholds (T_ADD and T_DROP) that is robust to the propagation environment is obtained and results show that the mean number of active-set updates can be reduced by lowering T_DROP. In [HKOKS97], the IS-95 algorithm is modified with variable thresholds. Results show that the outage probability can be decreased by dynamically changing the handover thresholds according to the traffic density. In [CYJ99], a new algorithm also based on IS-95 is proposed for reducing the handover occurrence rate. The principle is to change the handover thresholds according to the speeds of mobiles.

In this chapter, a new method is proposed and the soft handover is optimised with the purpose of maximising the downlink capacity. As mentioned in Chapter 3, in future mobile networks the downlink is more likely to be the capacity bottleneck of the whole system. The analysis and results in this chapter are also valuable for radio network planning and dimensioning of WCDMA systems.

In most of the previous literature, the optimisation process is structured as follows:

1. Choose the aim of the optimisation (such as reducing outage probability, increasing the capacity, or extending the coverage etc.).
2. Vary the handover parameters (thresholds and timers) for different combinations.
3. Analyse and compare the performance of the soft handover with different combinations of parameters.
4. Obtain the optimum combination of the handover parameters.

The analysis of the IS-95 and UTRA soft handover algorithms in section 5.4 is based on the above steps. The downlink capacity gain is evaluated with different soft handover overheads and the optimum overhead is determined to correspond to the maximum capacity gain.

In this chapter, the optimisation of the soft handover is carried out using a different procedures: no handover parameters are preset; the optimum handover overhead and thresholds are derived from the analysis for maximising the downlink capacity so the optimisation is not limited to a particular algorithm.

The chapter is organised as five sections. Following the introduction in section 6.1, section 6.2 describes the principles of the optimisation for maximising the downlink capacity. Then, in section 6.3, the optimum overhead and the corresponding thresholds for maximum capacity gain are derived. Finally in section 6.4, results are presented and conclusions are drawn.

6.2 Principles of Optimisation

As explained in Chapter 3, the soft handover effects on the downlink are much more complicated than that on the uplink. In the uplink, soft handover does not lead to any extra consumption of resources because there is no extra channel needed. The macrodiversity gain offered by the selection combining in the RNC brings benefits to both capacity and coverage. However, in the downlink, soft handover has two opposing effects: macrodiversity gain offered by the maximal ratio combining in the mobile terminal benefits the system, but the extra resource consumed by the extra downlink channels increases the total downlink interference level. There is a trade-off between these two opposing effects and their combining effects decide the overall performance of the soft handover. In order to maximise the downlink capacity, the point where the macrodiversity gain overweighs the extra resource consumption needs to be found.

CDMA systems are interference limited, lower interference corresponding to higher capacity. Therefore, the basic principle for optimising the soft handover in order to increase the downlink capacity is trying to minimise the interference brought by each

user. Whether a particular user at a particular location should be in soft handover status or not depends on which case leads to lower interference to other users.

Using the user in Figure 6.1 as an example, where P_{s1_1BS} is the power needed for guaranteeing the QoS when the user only has connection with BS_1; P_{s1_2way} and P_{si_2way} are the power needed from BS_1 and BS_i respectively when the user is under 2-way soft handover; P_{s1_3way}, P_{si_3way} and P_{sj_3way} are the power needed from BS_1, BS_i and BS_j respectively when the user is under 3-way soft handover. The total interference brought by the user to the system is the sum of the power of all the active downlink channels linked to it.

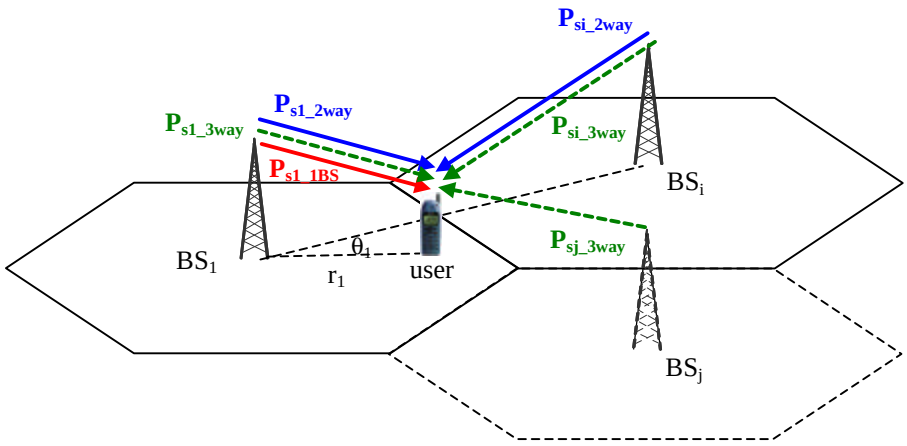

Figure 6.1 Principle of the soft handover optimisation

Assuming BS_1 is the original serving BS of the user, and BS_i and BS_j are the two strongest BSs in the candidate set, the pseudocode of the trigger process of the ideal optimised soft handover can be expressed as

```
if   min { Ps1_1BS , ( Ps1_2way + Psi_2way ), ( Ps1_3way + Psi_3way + Psj_3way) } = = (Ps1_2way + Psi_2way)
     add BSi to active set;
else if  min { Ps1_1BS, ( Ps1_2way + Psi_2way ), ( Ps1_3way + Psi_3way + Psj_3way) } = = (Ps1_3way + Psi_3way + Psj_3way)
     add BSi and BSj to active set;
end
```

Here the maximum size of the active set is assumed to be three. In order to minimise the interference and maximise the capacity, the decisions on whether to handover or not, and how many BSs should be in the active set are made based on the comparison of the total resource consumption.

6.3 Derivation of Optimum Overhead and Thresholds

When implementing any soft handover algorithm in a real system, it is impossible to calculate the power needed first, then make a decision on whether to handover or not. Therefore, an alternative way needs to be found out for making handover decisions. Fortunately, there is a link between the received pilot E_c/I_0 and the power needed for the downlink dedicated channel.

Still considering the user in Figure 6.1, assuming all the pilot channels are allocated the same power level, denoted by P_{pilot}, the received pilot E_c/I_0 from BS_1 can be expressed as

$$\left(\frac{E_c}{I_0}\right)_1 = \frac{P_{pilot} r_1^{-a} 10^{z_1/10}}{P_{T1}(1-a) r_1^{-a} 10^{z_1/10} + \sum_{k=2}^{M} P_{Tk} r_k^{-a} 10^{z_k/10}} \tag{6.1}$$

Where P_{Ti} *i*s the total transmit power of BS_i; a is the path loss exponent; s is the standard deviation of shadowing; a is the downlink orthogonal factor; k is the index of the BSs around BS_1; M is the number of the BSs that are taken into account for the inter-cell interference. As explained in Chapter 4, two tiers BSs around BS_1 are considered. So M=19.

Assume that active users are distributed evenly and the total transmit power of all BSs is the same and denoted by P_T. Also, assume that the pilot channel is the only common control channel in the downlink direction. Equation (6.1) can then be rewritten as

$$\left(\frac{E_C}{I_0}\right)_1 = \frac{1-g}{(1-a) + \sum_{k=2}^{M} \left(\frac{r_k}{r_1}\right)^{-a} 10^{(z_k - z_1)/10}} \tag{6.2}$$

Where g is the fraction of the total BS transmit power devote to the traffic. Similarly, the received pilot E_c/I_0 from BS_i and BS_j can be expressed as

$$\left(\frac{E_C}{I_0}\right)_i = \frac{1-g}{(1-a)+\sum_{\substack{l=1\\(l\neq i)}}^{M}\left(\frac{r_l}{r_i}\right)^{-a} 10^{(z_l - z_i)/10}}, \quad \left(\frac{E_C}{I_0}\right)_j = \frac{1-g}{(1-a)+\sum_{\substack{m=1\\(m\neq j)}}^{M}\left(\frac{r_m}{r_j}\right)^{-a} 10^{(z_m - z_j)/10}} \tag{6.3}$$

As derived in Chapter 5 (equation (5.12) on page 83), under perfect power control, P_{s1_1BS} can be calculated as

$$P_{s1\_1BS} = \frac{nR}{W}\left(\frac{E_b}{I_0}\right)_t P_T\left[1 - a + \sum_{k=2}^{M}\left(\frac{r_k}{r_1}\right)^{-a} 10^{(z_k - z_1)/10}\right] \tag{6.4}$$

Comparing (6.4) with (6.2) gives

$$P_{s1\_1BS} = \frac{\frac{nR}{W}\left(\frac{E_b}{I_0}\right)_t P_T(1-g)}{\left(\frac{E_c}{I_0}\right)_1} \tag{6.5}$$

Therefore, when the user only has a connection with BS_1, the transmit power required for the dedicated downlink channel is inversely proportional to the received pilot E_c/I_0 from BS_1.

Assuming perfect balanced power division strategy is employed during the soft handover, P_{s1_2way} can be calculated as (see equation (5.14))

$$P_{s1\_2way} = P_{si\_2way} = \frac{\frac{?R}{W}\left(\frac{E_b}{I_0}\right)_t P_T}{\frac{1}{1-a+\sum_{k=2}^{M}\left(\frac{r_k}{r_1}\right)^{-a} 10^{(?_k - ?_1)/10}} + \frac{1}{1-a+\sum_{\substack{l=1\\(l\neq i)}}^{M}\left(\frac{r_l}{r_i}\right)^{-a} 10^{(?_l - ?_i)/10}}} \tag{6.6}$$

Similarly, under 3-way soft handover situation, P_{s1_3way} can be calculated as

$$P_{s1\_3way} = P_{si\_3way} = P_{sj\_3way} = \frac{\frac{nR}{W}\left(\frac{E_b}{I_0}\right)_t P_T}{\frac{1}{1-a+\sum_{k=2}^{M}\left(\frac{r_k}{r_1}\right)^{-a} 10^{(?_k - ?_1)/10}} + \frac{1}{1-a+\sum_{\substack{l=1\\(l\neq i)}}^{M}\left(\frac{r_l}{r_i}\right)^{-a} 10^{(?_l - ?_i)/10}} + \frac{1}{1-a+\sum_{\substack{m=1\\(m\neq j)}}^{M}\left(\frac{r_m}{r_j}\right)^{-a} 10^{(z_m - z_j)/10}}} \tag{6.7}$$

Thus, the total power needed for 2-way and 3-way soft handover can be expressed as

$$P_{t2} = \frac{2\frac{nR}{W}\left(\frac{E_b}{I_0}\right)_t P_T(1-g)}{\left(\frac{E_c}{I_0}\right)_1 + \left(\frac{E_c}{I_0}\right)_i} \qquad (6.8)$$

$$P_{t3} = \frac{3\frac{nR}{W}\left(\frac{E_b}{I_0}\right)_t P_T(1-g)}{\left(\frac{E_c}{I_0}\right)_1 + \left(\frac{E_c}{I_0}\right)_i + \left(\frac{E_c}{I_0}\right)_j}$$

Equation (6.8) shows that for a user in soft handover status, the total power consumption is inversely proportional to the sum of the received pilot E_c/I_0 from all BSs in the active set. Therefore, in order to maximise the downlink capacity, the handover decision can be made based on the measurement of the downlink pilot channels. Figure 6.2 shows the flowchart of the trigger process of the optimised soft handover. Assume BS_1 is the original serving BS.

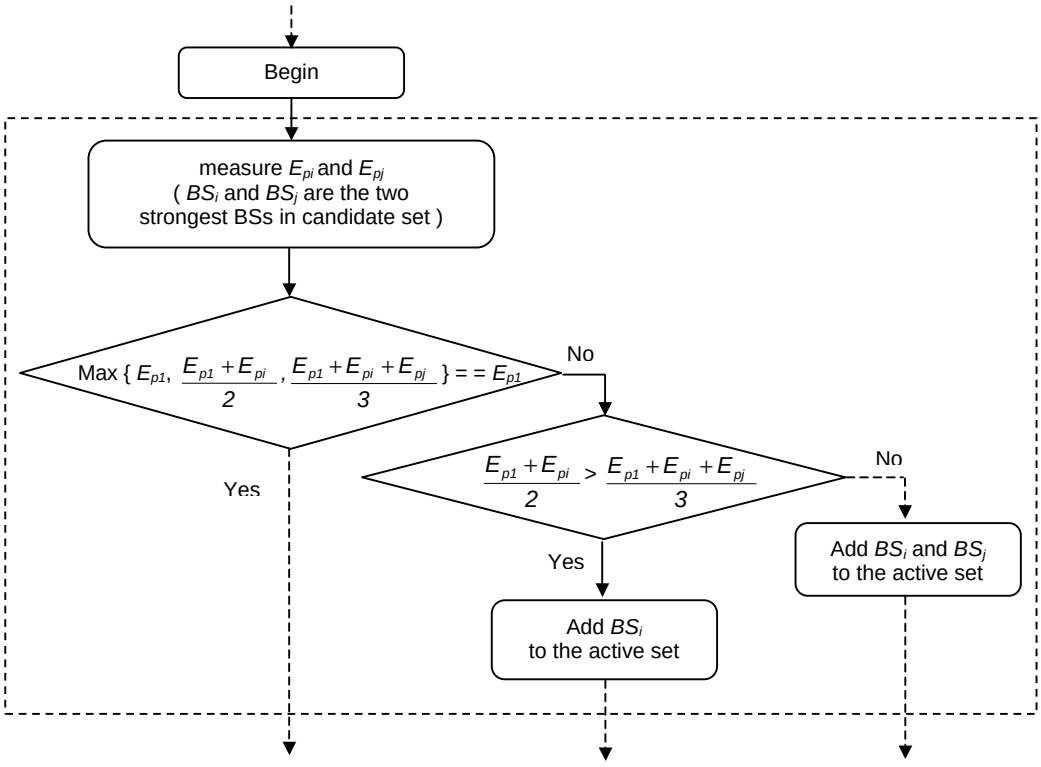

Figure 6.2 Flowchart of optimised soft handover

From Figure 6.2, it can be seen that if the mobile is always linked to the strongest BS (to achieve the maximum downlink capacity) soft handover should never be triggered. This agrees with the analysis in Chapter 5 about the perfect cell selection.

In the two-way soft handover case, assuming BS_1 is the original serving BS, the condition for adding BS_i into the active set is simply: $E_{pi} > E_{p1}$. This corresponds to the UTRA soft handover algorithm when the threshold *Th_add* (see Figure 5.7) equals 0 dB.

The optimum soft handover overhead can be derived from the capacity deduction. The total transmit power of BS_1 can be expressed as the sum of the power of common control channel and the power of dedicated channels.

$$P_{T1} = P_{T1} \cdot (1-g) + \iint_{S+S'} r \cdot P_{s1\_x} \cdot ds \tag{6.9}$$

Where g is the fraction of the total BS transmit power devote to the dedicated channels; S represents the non-soft handover zone and S' represents the soft handover zone; $S+S'$ represents the whole coverage of BS_1; r is the density of users. Under the assumption of having a uniform distribution of mobile users, r equals N/A; where A is the area of the hexagonal cell.

In (6.9), P_{s1_x} represents the transmit power of the dedicated channel from BS_1 to the user. P_{s1_x} could be P_{s1_1BS}, P_{s1_2way} or P_{s1_3way}, depending on the decision that is made based on the measurement of the pilot E_c/I_0.

The average downlink capacity with the optimised soft handover can be derived as

$$N = E\left[\frac{g \cdot A}{\iint_{S+S'} P_{s1\_x} \cdot ds}\right] \tag{6.10}$$

In two-way soft handover case, the optimum soft handover overhead is

$$overhead\_optimum = \frac{S'/2}{S'/2 + S} \tag{6.11}$$

Where *S* and *S'* represent the area of the non-soft handover zone and the soft handover zone respectively.

6.4 Results and Conclusions

Using the system model and assumptions described in Chapter 4, the maximum downlink capacity gain is 8.78% with the optimum soft handover overhead (obtained from equation (6.11)) being 9.35%. Here, normal cell selection with *CS_th* = 5dB (see section 5.3.3) is considered and the values of system parameters are taken from Table 5.3.

Retrieving the results obtained in section 5.7 on the UTRA soft handover algorithm (shown as the black line with the circle symbols in Figure 6.3) the optimum threshold ranges for maximising the downlink capacity can be obtained. The red star in the Figure 6.3 represents the maximum capacity gain, which is obtained from the analysis in this chapter. To keep the capacity gain within 90% and 80% of the maximum value, the handover threshold ranges are [-1.66, 1.66] dB and [-2.3, 2.3] dB respectively.

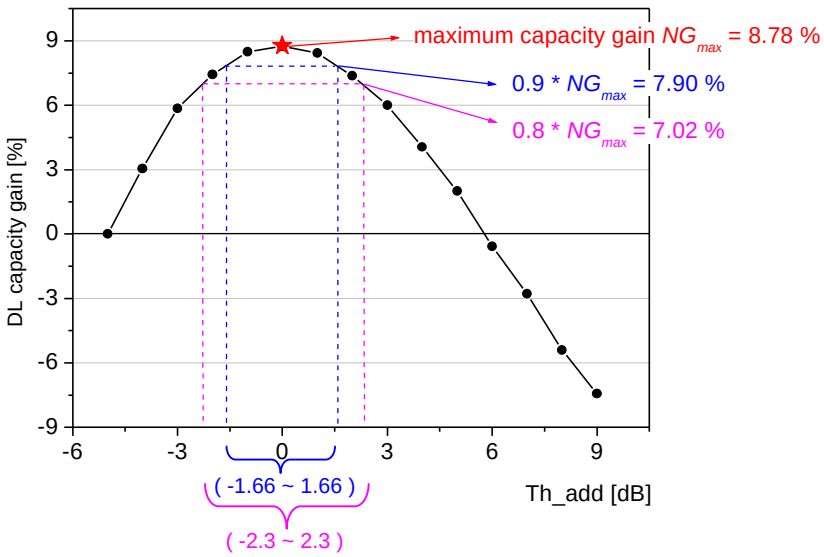

Figure 6.3 Soft handover optimisation for maximising downlink capacity

Note that there is a link between the value of the threshold and the handover update rate: the smaller the threshold, the larger the handover update rate. There is, therefore, a trade-off between the system capacity and the signalling load and to keep the

capacity gain within 90% and 80% of the maximum value; the handover threshold ranges are [0, 1.66] dB and [0, 2.3] dB respectively.

The novelty of the work in this chapter is that it does not follow the normal procedures for optimising soft handover as explained in section 6.1. The new method optimises the soft handover based on the principles of minimising the interference. The results are valuable for future mobile networks where the downlink is more likely to be the bottleneck of the whole systems.

Chapter 7 Optimised Power Control Strategy during Soft Handover

7.1 Introduction

In this chapter, a new power control schemes is proposed for optimising the power division between the BSs in the active set during soft handover. The chapter is composed of six sections. Section 7.2 gives an overview of power control during soft handover. Section 7.3 describes the principles of the proposed power control scheme. In section 7.4, the feasibility of the new scheme is evaluated. Afterwards, in section 7.5, the system level performance of the new scheme is investigated under UTRA soft handover algorithm by comparing to the balanced power control. Results are presented and conclusions are drawn in section 7.6.

7.2 Overview of Power Control during SHO

During soft handover, the power control procedure is more complicated because there are at least two BSs involved. In the uplink direction, the mobile terminal adjusts its transmit power based on the combination of the received transmit power control (TPC) commands from all the BSs in the active set. Therefore, the reliability of TPC bits and the proper combining strategy are fatal to the uplink power control during soft handover [SJLW99] [PKKS01] [GS01]. However the downlink direction is different, only one TPC command is sent by the mobile terminal and all the BSs in the active set adjust their transmit power based on this TPC command.

Several downlink power control schemes during soft handover have been proposed in the literature [HS00] [Ham00] [ETSI TS 125 214]. It is generally believed that the deviation in the transmit powers from different base stations in the active set can lead to the reduction of the macrodiversity gain. A couple of methods have been proposed to avoid the power drifting. For example, [HS00] showed that power drifting between base stations can be reduced by changing the way the mobile issues the TPC command; in [Ham00], the adjustment loop power control was proposed to maintain the balance of the transmit power from different base stations in the active set. As well as the inner closed loop power control, an adjustment loop is employed for balancing

the downlink power among active set cells during macrodiversity. Now the adjustment loop power control has been adopted by 3GPP as one of the standard downlink power control strategies during soft handover [ETSI TS 125 214] [ETSI TR 125 922]. However, in [DL98], an unbalanced power allocation scheme was investigated and results showed that it can reduce the overall transmit power. In this scheme, the BS that has a better link with the mobile transmits signals at a higher power. Site Selection Diversity Transmit power control (SSDT) [FHU00], which has been adopted by 3GPP as an alternative scheme for soft handover [ETSI TS 125 214] [ETSI TR 125 922], is the extreme version of this unbalanced scheme. The principle of SSDT is that the best BS of the active set is dynamically chosen as the only transmitting site, and other BSs involved turn down their DPDCHs (Dedicated Physical Data Channel), only transmitting DPCCH (Dedicated Physical Control Channel). In this way, the interference caused by the multiple site transmission is mitigated. However, SSDT loses the benefits of macrodiversity. In this thesis, an optimised downlink power control scheme is proposed. The new approach keeps the benefits of macrodiversity gain and also can reduce the interference caused by transmission from multiple sites.

7.3 Principles of New Approach

As mentioned and verified in previous chapters, CDMA systems are interference-limited. Minimising the total interference is one of the basic rules for optimising the radio resource in CDMA systems. The basic principle of the new power control approach is to minimise the total power consumption during the soft handover as lower power consumption means less interference to other active users.

Considering a mobile in a two-way soft handover status as shown in Figure 7.1, the total power consumed by this mobile is the sum of P_1 and P_2. P_1 and P_2 are the transmit power for the dedicated downlink channels from BS_1 and BS_2 respectively.

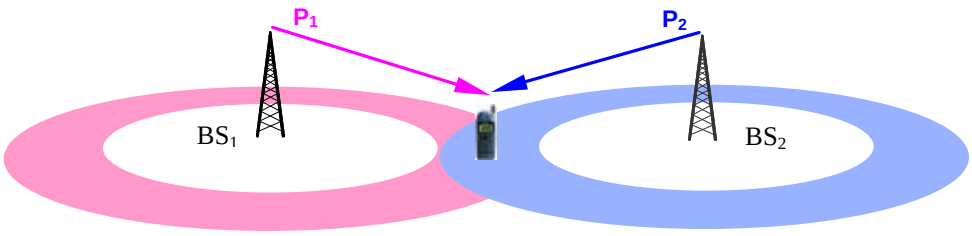

Figure 7.1 Downlink power control during soft handover

Assuming that load is distributed evenly within the system, the total transmit power of each BS is the same, denoted by P_T. After maximal ratio combining, the received bit energy-to-interference power spectral density radio E_b/I_0 of the mobile can be expressed as

$$\frac{E_b}{I_0} = \left[\frac{E_b}{I_0}\right]_1 + \left[\frac{E_b}{I_0}\right]_2 \tag{7.1}$$

with

$$\left[\frac{E_b}{I_0}\right]_1 = \frac{W}{?R}\frac{P_1 \cdot L_1}{P_T(1-a)L_1 + \sum_{i=2}^{M} P_T L_i} = \frac{W}{?R}\frac{P_1}{P_T\left(1-a+\sum_{i=2}^{M}\frac{L_i}{L_1}\right)} \tag{7.2}$$

and

$$\left[\frac{E_b}{I_0}\right]_2 = \frac{W}{?R}\frac{P_2 \cdot L_2}{P_T(1-a)L_2 + \sum_{\substack{j=1 \\ (j\neq 2)}}^{M} P_T L_j} = \frac{W}{?R}\frac{P_2}{P_T\left(1-a+\sum_{\substack{j=1 \\ (j\neq 2)}}^{M}\frac{L_j}{L_2}\right)} \tag{7.3}$$

Where W is the chip rate; R is the service bit rate; v is the activity factor of the service; a is the downlink orthogonality factor; L_i is the propagation attenuation from BS_i to the mobile; M is the index of BSs that are taken into account for the inter-cell interference. Substituting (7.2) and (7.3) to (7.1) gives

$$\frac{E_b}{I_0} = \frac{W}{vR}\frac{1}{P_T}\left[\frac{P_1}{1-a+\sum_{i=2}^{M}\frac{L_i}{L_1}} + \frac{P_2}{1-a+\sum_{\substack{j=1 \\ (j\neq 2)}}^{M}\frac{L_j}{L_2}}\right] \tag{7.4}$$

Define a parameter B that represents the relationship between P_1 and P_2, as

$$B = \frac{P_{s1}}{P_{s2}} \tag{7.5}$$

According to the “no more, no less” principle, the received QoS of the mobile is kept as the target value. Thus, from (7.4) and (7.5), the total power required by the mobile can be derived as

$$P_t = P_1 + P_2 = \left(1+\frac{1}{B}\right)\frac{\left(\frac{E_b}{I_0}\right)_t \frac{vR}{W} P_T}{\frac{1}{1-a+\sum_{i=2}^{M}\frac{L_i}{L_1}} + \frac{1/B}{1-a+\sum_{\substack{j=1 \\ (j\neq 2)}}^{M}\frac{L_j}{L_2}}} \tag{7.6}$$

Where $(E_b/I_0)_t$ is the target value for the service required by the user.

From (7.6), it is clear that the total power consumed by the user is related to the power ratio B. Different ratios of P_1 to P_2 lead to different total power consumption. The aim of the new optimised power control strategy is trying to find the proper ratio B for minimising the total power P_t.

7.4 Feasibility Evaluation

Using the standard balanced power division strategy [ETSI TS 125 214] as the reference, the derivation of B for mitigating the total power can be conducted as follows:

Let P_{t0} represents the total power consumed by the user when implementing the standard balanced power division strategy during soft handover. Substituting P_1=P_2 to (7.6), P_{t0} can be expressed as:

$$P_{t0} = \frac{2\cdot\left(\frac{E_b}{I_0}\right)_t \frac{vR}{W} P_T}{\frac{1}{1-a+\sum_{i=2}^{M}\frac{L_i}{L_1}} + \frac{1}{1-a+\sum_{\substack{j=1 \\ (j\neq 2)}}^{M}\frac{L_j}{L_2}}} \tag{7.7}$$

In order to mitigate the total power, the following inequality needs be fulfilled

$$P_t \leq P_{t0} \tag{7.8}$$

Letting $X = \dfrac{1}{1-a+\sum_{i=2}^{M}\dfrac{L_i}{L_1}}$ and $Y = \dfrac{1}{1-a+\sum_{\substack{j=1\\(j\neq 2)}}^{M}\dfrac{L_j}{L_2}}$, (7.8) can be rewritten as:

$$\frac{1+\frac{1}{B}}{X+\frac{1}{B}\cdot Y} \leq \frac{2}{X+Y}$$

$$\because \quad (X+Y)\left(X+\frac{1}{B}\cdot Y\right) > 0$$

$$\therefore \quad \frac{1+\frac{1}{B}}{X+\frac{1}{B}\cdot Y}\cdot(X+Y)\left(X+\frac{1}{B}\cdot Y\right) \leq \frac{2}{X+Y}\cdot(X+Y)\left(X+\frac{1}{B}\cdot Y\right)$$

$$X+Y+\frac{1}{B}\cdot X+\frac{1}{B}\cdot Y \leq 2X+\frac{2}{B}\cdot Y$$

$$\left(1-\frac{1}{B}\right)\cdot Y \leq \left(1-\frac{1}{B}\right)\cdot X \tag{7.9}$$

In order to satisfy (7.9), B depends on the relationship between X and Y.

$$\begin{aligned} &\text{if} \quad X \geq Y \quad , \quad 1-\frac{1}{B} > 0 \quad \Rightarrow \quad B > 1 \\ &\text{if} \quad X \leq Y \quad , \quad 1-\frac{1}{B} < 0 \quad \Rightarrow \quad B < 1 \end{aligned} \tag{7.10}$$

In Chapter 6, the received pilot E_c/I_0 from BS_i has been derived in equation (6.3) as:

$$\left(\frac{E_C}{I_0}\right)_i = \frac{1-g}{(1-a)+\sum_{j\neq i}^{M}\dfrac{L_j}{L_i}} \tag{7.11}$$

Therefore

$$X = \frac{1}{1-a+\sum_{i=2}^{M}\dfrac{L_i}{L_1}} = \frac{\left(\dfrac{E_c}{I_0}\right)_1}{1-g} \quad \text{and} \quad Y = \frac{1}{1-a+\sum_{\substack{j=1\\(j\neq 2)}}^{M}\dfrac{L_j}{L_2}} = \frac{\left(\dfrac{E_c}{I_0}\right)_2}{1-g} \tag{7.12}$$

(7.10) can be rewritten as:

$$\begin{aligned} &\text{if } \left(\frac{E_c}{I_0}\right)_1 \geq \left(\frac{E_c}{I_0}\right)_2 \quad , \quad 1-\frac{1}{B} > 0 \quad \Rightarrow \quad B>1 \\ &\text{if } \left(\frac{E_c}{I_0}\right)_1 \leq \left(\frac{E_c}{I_0}\right)_2 \quad , \quad 1-\frac{1}{B} < 0 \quad \Rightarrow \quad B<1 \end{aligned} \tag{7.13}$$

When the load is distributed evenly within the system, all the downlink pilot channels are allocated with the same amount of power. Higher received pilot E_c/I_0 from BS_i corresponds to lower propagation attenuation from BS_i to the user. Therefore, choosing $B = L_1/L_2$, (7.13) is satisfied. Tracing back the proofs, (7.8) is satisfied as well. This means, when the power ratio between the BSs in the active set equals the propagation attenuation ratio between the BSs, the total power consumption during the soft handover can be reduced compare to the balanced power division scheme.

Therefore, in the optimised power control scheme proposed in this thesis, the BSs in the active set change their transmit power dependently and the power ratio is kept as the propagation attenuation ratio.

Note that choosing $B=L_1/L_2$ for the optimised power control scheme is because the propagation attenuation from a particular BS can be obtained by measuring the downlink pilot channel of that BS. This guarantees the feasibility of the new power control approach because measuring pilot channels is the basic procedure of soft handover.

Under 3-way soft handover, the analysis is quite similar. Assuming BS_1, BS_2 and BS_3 are the three BSs in the active set, the relationship between P_1, P_2 and P_3 is:

$$\frac{P_1}{P_2} = \frac{L_1}{L_2} \quad , \quad \frac{P_1}{P_3} = \frac{L_1}{L_3} \quad , \quad \frac{P_2}{P_3} = \frac{L_2}{L_3} \tag{7.14}$$

Figure 7.2 shows the average relative total power needed by the user in soft handover status. *X* axis shows the normalised distance from the user to the nearest BS in the active set. Radio channel model and system assumptions are the same as mentioned in Chapter 4 and system parameters are taken from Table 5.3. P_{t0}/P_T and P_t/P_T are calculated from (7.6) and (7.7) respectively. Results show that compared with

the balanced power division scheme, the unbalanced power division in the optimised power control scheme does reduce the total power consumed by the user in soft handover. In the next section, the performance of the new power control approach will be verified by analysing the downlink capacity and the soft handover gain.

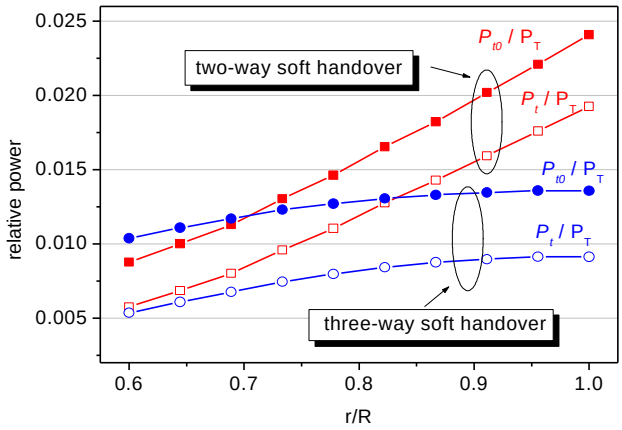

Figure 7.2 Relative total transmit power for mobiles in soft handover

7.5 Performance Analysis

Using the method described in section 5.2, the performance of the optimised power control scheme can be compared with the balanced power control scheme in terms of the downlink capacity gain.

Still using the system model described in Chapter 4, 19 co-channel cells have the same ideal hexagonal shape, users are distributed evenly within the system and a single type of service is supported.

To a mobile outside the soft handover zone, the required transmit power for the downlink dedicated channel P_{1_out} can be expressed as:

$$P_{1\_out} = \left(\frac{E_b}{I_0}\right)_t \frac{nR}{W} P_T \left[1 - a + \sum_{i=2}^{M} \frac{L_i}{L_1}\right] \tag{7.15}$$

Where W is the chip rate; R is the service bit rate; v is the activity factor; $(E_b/I_0)_t$ is the target value for the service required by the user; P_T is the total transmit power of all BSs; a is the orthogonal factor; L_i is the propagation attenuation from BS_i to the

mobile; *M* is the index of BSs that are taken into account for the inter-cell interference.

To a mobile inside the soft handover zone, the power level of P_{1_in} is related to the power control schemes used during the soft handover

$$P_{1\_in} = \begin{cases} \dfrac{\left(\dfrac{E_b}{I_0}\right)_t \dfrac{nR}{W} P_T}{\dfrac{1}{1-a+\sum_{i=2}^{M}\dfrac{L_i}{L_1}} + \dfrac{1}{1-a+\sum_{\substack{j=1 \\ (j\neq k)}}^{M}\dfrac{L_j}{L_k}}} & \text{balanced power control} \\ \dfrac{\left(\dfrac{E_b}{I_0}\right)_t \dfrac{nR}{W} P_T}{\dfrac{1}{1-a+\sum_{i=2}^{M}\dfrac{L_i}{L_1}} + \dfrac{1}{\dfrac{L_1}{L_k}\left(1-a+\sum_{\substack{j=1 \\ (j\neq k)}}^{M}\dfrac{L_j}{L_k}\right)}} & \text{optimised power control} \end{cases} \tag{7.16}$$

The total transmit power of BS_1 can be expressed as:

$$P_T = (1-g)P_T + \iint_S r \cdot P_{1\_out} \cdot ds + \iint_{S'} r \cdot P_{1\_in} \cdot ds, \qquad r = {2N}\big/{3\sqrt{3}R^2} \tag{7.17}$$

Where *g* is the fraction of the total BS transmit power devote to the dedicated channels; *r* is the density of users; *N* is the number of active users per cell; *R* is the radius of the cell; *S* and *S'* correspond to the non-soft handover zone and the soft handover zone respectively.

Substitute (7.15) and (7.16) to (7.17), the downlink capacity can be obtained. Different *S* and *S'* correspond to different soft handover overhead and different P_{1_in} represents different power control schemes during soft handover.

7.6 Results and Discussions

Figure 7.3 shows the average downlink capacity gain as a function of soft handover overhead with different power control schemes. The capacity gain is obtained by comparing the downlink capacity with soft handover to that without soft handover. Two-way UTRA soft handover and normal cell selection with *CS_th* equals 5dB (see

section 5.3.3) are considered and the values of system parameters are taken from Table 5.3.

It is clear that when the soft handover overhead is fixed, the downlink capacity gain is higher with the optimised power control scheme. The difference between the two power control schemes is more obvious with higher soft handover overhead. Compared to the balanced power control, the optimised power control does not change the optimum overhead, but it does change the maximum overhead[8]. With the optimum overhead of 9.2%, the maximum downlink capacity gains are 8.7% and 10.4% for the balanced and optimised power control schemes respectively. with the balanced power control, the maximum overhead is 26.7%. In order to prevent capacity loss due to the soft handover, the overhead has to be kept under this maximum value. However, with the optimised power control, more users are allowed to be in soft handover status without capacity loss.

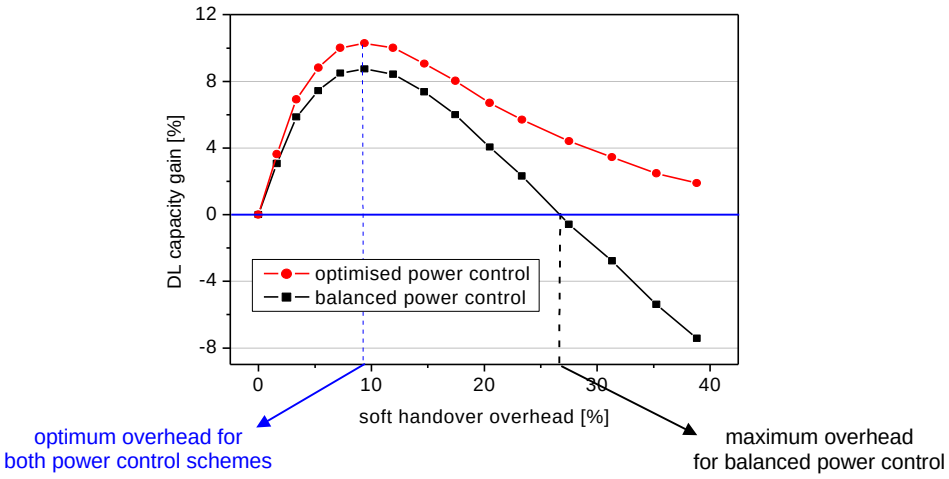

Figure 7.3 DL capacity gain with different power control schemes

Figure 7.4 shows the capacity gain in dB with different size of the active set. Here, the capacity gain is defined as *N_o/N_b*: where *N_o* represents the average downlink capacity with implementing the optimised power control during the soft handover and *N_b* represents the average downlink capacity with implementing the balanced power control during the soft handover. It is obvious that the capacity gain is quite similar

[8] As defined in Chapter 5, the "optimum overhead" corresponds to the maximum downlink capacity gain and the "maximum overhead" represents the balance point of the macrodiversity gain and the extra resource consumption.

when the proportion of users in soft handover status is kept under about 15%. When the proportion goes beyond 15%, the capacity gain is higher with the larger size of the active set. For example, when the approximately 30% of the users are in soft handover status, the average downlink capacity gain is 0.25 dB when the size of the active set is 2 and 0.37 dB when the size of the active set is 3. This means the more BSs that are involved in the soft handover, the better the performance of the optimised power control compared with the balanced power control.

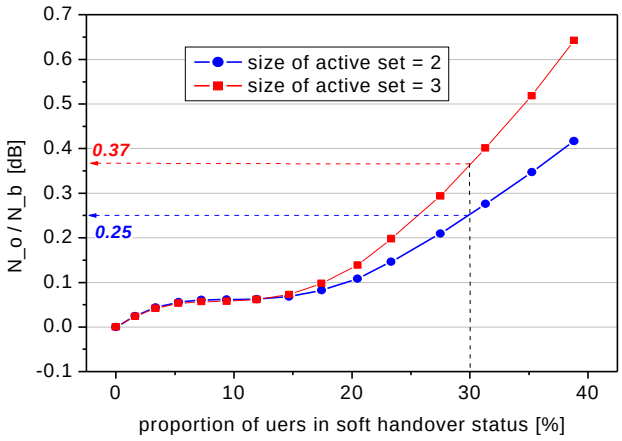

Figure 7.4 Capacity gain with different active set size

Figure 7.5 shows the sensitivities of *N_o/N_b* to different system parameters: a is the path loss exponent; s is the standard deviation of shadowing and a is the downlink orthogonal factor. Two-way soft handover is considered here. It can be seen that when the soft handover overhead is kept under approximate 20%, *N_o/N_b* is not very sensitive to all the parameters. However, when the overhead is larger than 20%, the capacity gain is higher with higher s and higher a. This means that compared with the balanced power control, the optimised power control scheme brings more benefits to the systems with a worse radio environment. Another conclusion that can be drawn from Figure 7.5 is that the capacity gain is higher with higher orthogonal factor a. This means that the optimised power control works better in a system where the orthogonality is well preserved between downlink channels.

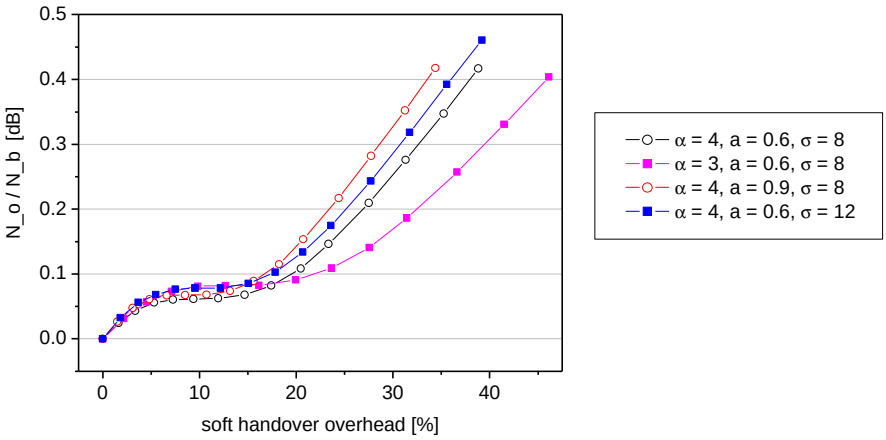

Figure 7.5 Sensitivities of the capacity gain due to the optimised power control

Considering the optimisation in Chapter 6, Figure 7.6 shows the optimum soft handover overhead ranges of the optimised power control and the balanced power control when keeping the capacity gain within 80% of the maximum value. It is clear that the optimised power control increases the range of the optimum overhead from (4.78~15.25) to (4.62~16.91). This brings more flexibility to the soft handover planning. When the capacity gain is fixed, more users can get benefits from the link quality improvement.

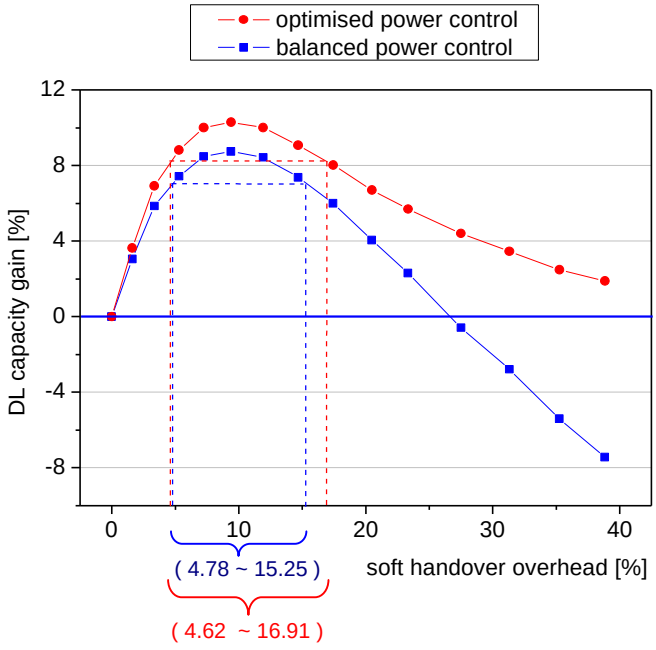

Figure 7.6 Optimum overhead with different power control schemes

7.7 Conclusions

In this chapter, a new power control scheme is proposed for optimising the power division between the BSs in the active set during soft handover. In stead of splitting the power equally between the BSs in the active set, it controls the power division according to the propagation attenuation of each radio channel.

The optimised power control minimizes the interference and maintains getting benefits from the macrodiversity at the same time. Compared with the balanced power control scheme adopted by 3GPP, the overall interference for a user in soft handover status is reduced by applying the optimised power control. Compared with the SSDT, the optimised power control is more robust to the fluctuating attenuation of the radio environment because it keeps macrodiversity. The signals from all the BSs in the active set are combined in the mobile terminal. If one of the channels suddenly experiences bad attenuation, the overall quality of service will not drop as badly as could happen with SSDT.

Compared with the balanced power control scheme adopted by 3GPP, the optimised power control increases the soft handover gain. The new approach is especially suitable for the WCDMA systems with higher soft handover overhead and operating in a radio environment with worse propagation attenuation.

Chapter 8 Conclusions

8.1 Conclusions

In a WCDMA system, soft handover has two opposing effects on the downlink: macrodiversity and extra resource consumption. Macrodiversity improves the link level performance (verified by the analysis in Chapter 4), but for system level performance there is a trade-off between these two effects (verified by the analysis in Chapter 5). To maximise the downlink capacity, there is an optimum soft handover overhead. This optimum overhead is sensitive to the cell selection scheme, power control conditions and variety of the radio parameters.

The size of the active set is not governed by “the bigger the better”. Considering the complexity and the increased signalling that comes with adding an extra BS when implementing soft handover, the size of the active set should be kept as two.

The optimisation of soft handover shows that the capacity gain is related closely to the handover threshold. However, there is a trade-off between the system capacity and the signalling load.

The new power control scheme proposed for controlling the power division between the BSs in the active set shows better performance than the conventional balanced power control scheme adopted by 3GPP. It minimizes the interference and maintains the benefits obtained from the macrodiversity at the same time. This optimized power division scheme improves the downlink capacity and makes the mobile system more robust to the fluctuating attenuation of the radio environment. It is especially suitable for WCDMA systems with high soft handover overhead and operating in the radio environment with higher shadow fading.

The results obtained from the analysis in this thesis are valuable for radio network planning and dimensioning. By optimising the soft handover and implementing the new power control scheme, possible downlink bottleneck situation would be mitigated in future mobile networks.

8.2 Future Work

Future work on soft handover could be carried out from the following different aspects. As mentioned in Chapter 5, if the instantaneous bursty feature of the non-real time service is to be taken into account in detail, more complicated models will be needed for analysing soft handover effects on these packet-switched services. Therefore, the first possibility for future work is to investigate the soft handover effects on bursty traffic. Different handover criteria might need to be applied and it is may not be necessary to support soft handover to these services because of their non continuous nature.

Another possibility for future work is to optimise the soft handover algorithm and thresholds under more complicated situations. Uniform load distribution and different mobility class of the mobile users need to be considered. The soft handover performance on hot spot is also worth investigating. Moreover, the trade-off between the benefits coming from soft handover and the increasing signalling load needs future evaluation as well.

Appendix A Author's Publications

[CC01a] L.G. Cuthbert, Y. Chen, L. Tokarchuk, and J. Bigham, "Selection Mechanisms for Resource Provision in an Agent-based System for 3G Networks", *Proceeding of the Ninth International Conference on Telecommunication Networks,* pp: 448-454, March 2001.

[CC01b] Y. Chen and L.G. Cuthbert, "Soft Handover Effects on UMTS Downlink", *Proceeding of EPSRC PREP2001,* Keele, UK, April 2001.

[CC01c] Y. Chen and L.G. Cuthbert, "Radio Resource Re-configuration in Agent-based 3G systems", *Proceeding of IST Mobile Communications Summit 2001*, pp: 413-421, September 2001.

[CC02a] Y. Chen and L. G. Cuthbert, "Optimum size of soft handover zone in power-controlled UMTS downlink systems," *Electronic Letters*, Vol. 38, No. 2, pp. 89-90, Jan 2002.

[CC02b] Y. Chen and L. G. Cuthbert, "Downlink Soft Handover Gain in UMTS Networks Under Different Power Control Conditions", *Proceeding of the third international conference on Mobile Communication Technologies, 3G2002*, pp. 47-51, London, UK, March 2002.

[CC02c] Y. Chen and L. G. Cuthbert, "Downlink Performance of Different Soft Handover Schemes for UMTS Systems" *Proceedings of the international conference on Telecommunications, ICT'2002*, June 2002.

[CC02d] Y. Chen and L.G. Cuthbert, " Downlink Performance of Different Soft Handover Algorithms in 3G Multi-Service Environments ", *the fourth IEEE conference on Mobile and wireless communications networks, MWCN 2002,* pp, 406-410, September 2002.

[CC02e] Y. Chen and L.G. Cuthbert, " Soft Handover Effects on Downlink Capacity-Coverage Trade-off in 3G WCDMA Networks "; *Wireless and Mobile Communications (APOC08), Asia-Pacific Optical and Wireless Communications Networks*, Vol: 4911, pp: 187-193, October 2002.

[CC03a] Y. Chen and L.G. Cuthbert, “Optimised Downlink Transmit Power Control during Soft Handover in WCDMA Systems”, *IEEE Wireless Communications and Networking Conference. WCNC2003,* March 2003

[CC03b] Y. Chen and L.G. Cuthbert, “Joint Performance of Cell Selection/Reselection and Soft Handover in the Downlink Direction of 3G WCDMA Systems”, *the Fourth International Conference on 3G Mobile Communication Technologies, 3G2003*; pp: 227-231, June 2003

[CC03c] Y. Chen and L.G. Cuthbert, “Downlink Radio Resource Optimisation in Wide-band CDMA Systems”, [Accepted] *Special Issue on "Ultra-Broadband Wireless Communications For the Future" in Journal on Wireless Communications and Mobile Computing (WCMC).* Autumn 2003

Appendix B Verification and Validation

The work in this thesis is a theoretical analysis. The foundation of the research is based on pre-verified equations and theories proposed in the 3GPP standard. All the work is derived from this standard and it is these derivations that must be validated.

All derivations are made using assumptions and typical values that are clearly stated and adopted by most of the previous literature. The correctness of the derivations can be checked by tracing back all substitutions and manipulations though mathematical calculations.

To obtain the numerical results, translation of the equations to computer code must be undertaken. By breaking down the equations into manageable parts it is possible to easily and quickly produce an accurate program. When the work first started, the fast development package **Matlab** is used. Matlab is a straightforward tool for calculation of mathematical formulas. All the codes are checked by the debugger and the mathematical correctness of the implemented algorithm is checked line by line by hand. Later, these Matlab codes are converted to C code to speed up the calculation.

To validate the results, comparison against similar past work is carried out. For example, in Chapter 4, the new analysis about the Cumulative Distribution Function (CDF) of the total transmit power for the corner user agrees with the well accepted fade margin reduction conclusion being verified by previous work [VVGZ94]. In Chapter 7, the proposed optimised power control scheme shows that unbalanced power division decreases the total power needed for the user in soft handover status. This agrees with the previous work in [DL98].

Moreover, the agreement of the link level performance in Chapter 4 and the system level performance in Chapter 5 also validates the results. For example, the mean total power distribution in Figure 4.11 and the soft handover zone shapes of different soft handover algorithms in Figure 5.8 give the explanation of the different performance of the IS-95A and the UTRA algorithms in Figure 5.12.

To validate the new approach proposed in this thesis, comparisons are made with other known algorithms to ensure that any changes are in-line with current standards. For example, in Chapter 7, the new optimised power control scheme is compared with the balanced power control scheme adopted by 3GPP. The new approach is tested by comparing against the existing standard for improvement. Once again, all references are stated to show how the research is derived and what assumptions are made for certain situations.

By analysing results at each stage validation of work can be done step by step. This reduces the chance of error at a later stage of development and provides a return path if mistakes are found.

Appendix C Interference Calculation of 37 cells

Consider the downlink inter-cell interference coming from the 3 tiers around BS_1 as shown in Figure 1.

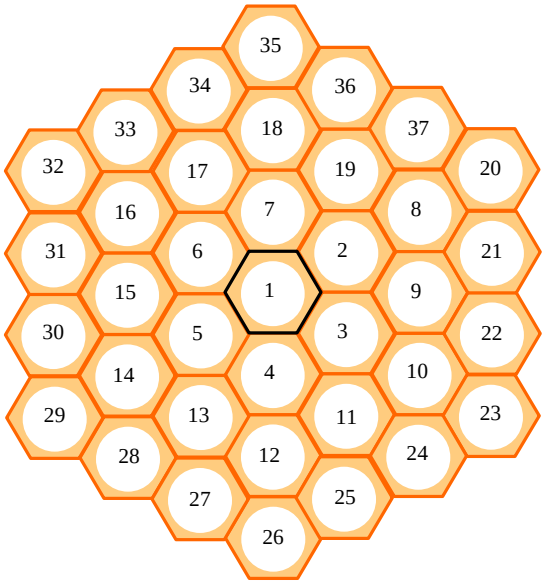

Figure 1. 37 co-channel cell layout

The relationship between r_i and r_1, q_1 can be expressed as

$$r_i = \begin{cases} \sqrt{r_1^2 + \left(\sqrt{3}R\right)^2 - 2 \cdot r_1 \cdot \sqrt{3}R\cos\left[q_1 + (i-2)p/3\right]} & 2 \le i \le 7 \\ \sqrt{r_1^2 + \left(2\sqrt{3}R\right)^2 - 2 \cdot r_1 \cdot 2\sqrt{3}R\cos\left[q_1 + (i-8)p/6\right]} & i = 8, 10, 12, \ldots, 18 \\ \sqrt{r_1^2 + (3R)^2 - 2 \cdot r_1 \cdot 3R\cos\left[q_1 + (i-8)p/6\right]} & i = 9, 11, 13, \ldots, 19 \\ \sqrt{r_1^2 + (3D)^2 - 2 \cdot r_1 \cdot 3D\cos\left[q_1 + (i-20)p/9\right]} & i = 20, 23, 26, 29, 32, 35 \\ \sqrt{r_1^2 + (D_S)^2 - 2 \cdot r_1 \cdot D_S\cos\left[q_1 + (i-21)p/9 + p/6 - q_S\right]} & i = 21, 24, 27, 30, 33, 36 \\ \sqrt{r_1^2 + (D_S)^2 - 2 \cdot r_1 \cdot D_S\cos\left[q_1 + (i-22)p/9 + p/6 + q_S\right]} & i = 22, 25, 28, 31, 34, 37 \end{cases}$$

Where

$$D = \sqrt{3}R \qquad D_s = \sqrt{(4.5R)^2 + (0.5D)^2} \qquad q_s = tg^{-1}\left(\frac{0.5D}{4.5R}\right)$$

Considering 36 cells around the middle cell, the inter-cell interference can be expressed as

$$I_{\text{int } er-cell} = \sum_{i=2}^{39} P_{Ti} \cdot r_i^{-a} \cdot 10^{z_i/10}$$

Comparing the results obtained from the above equation and (4.3), on the average, the difference is less than 1%. Therefore, considering 19 cells for inter-cell interference is a reasonable approximation.

Appendix D Load Factor & Downlink Pole Equation

The theoretical pole capacity of a WCDMA cell can be calculated from the load equation [HT00] [SHL-SW00] whose derivation is shown in this appendix. Here, only the downlink direction is considered.

To certain user j, the E_b/N_0, bit energy-to-interference power spectral density ratio can be expressed as

$$\left(\frac{E_b}{N_0}\right)_j = \text{Processing gain of user } j \cdot \frac{\text{Signal of user } j}{\text{Total received power (excl.own signal)}} \tag{1}$$

The link quality equation for the downlink connections can be rewritten as

$$\left(\frac{E_b}{N_0}\right)_j = \frac{W}{v_j R_j} \cdot \frac{P_{i,j} L_{i,j}}{P_T (1-a_j) L_{i,j} + P_T \sum_{k=1,k\neq i}^{M} L_{k,j} + P_N} \tag{2}$$

Where W is the chip rate; $P_{i,j}$ is the required transmit power at BS_i for user j; $L_{i,j}$ is the propagation attenuation from BS_i to user j; v_j is the activity factor of user j; R_j is the bit rate of user j and P_T is the total BS transmit power. Here, the total transmit power of different BS is equal; P_N is the thermal noise power; a_j is the downlink orthogonal factor, which depends on multipath propagation condition; M is the number of relevant neighbouring BSs. Solving equation (2) for P_j gives

$$P_{i,j} = \frac{(E_b/I_0)_j v_j R_j}{W} \left[P_T (1-a_j) + P_T \sum_{k=1,k\neq i}^{M} \frac{L_{k,j}}{L_{i,j}} + \frac{P_N}{L_{i,j}} \right] \tag{3}$$

By summing up the power of all the downlink channels, the total transmit power of BS can be expressed as

$$P_T = P_T \sum_{j=1}^{N} \left[\frac{(E_b/I_0)_j v_j R_j}{W} \left(1 - a_j + \sum_{k=1,k\neq i}^{M} \frac{L_{k,j}}{L_{i,j}} \right) \right] + P_N \sum_{i=1}^{N} \frac{(E_b/I_0)_j v_j R_j}{W} \frac{1}{L_{i,j}} \tag{4}$$

Where N is the number of radio link connections per cell. Solving (4) for P_T gives

$$P_T = \frac{P_N \sum_{i=1}^{N} \frac{(E_b/I_0)_j \nu_j R_j}{W} \frac{1}{L_{i,j}}}{1 - \sum_{j=1}^{N} \left[\frac{(E_b/I_0)_j \nu_j R_j}{W} \left(1 - a_j + \sum_{k=1,k\neq i}^{M} \frac{L_{k,j}}{L_{i,j}} \right) \right]} \quad (5)$$

The downlink load factor h_{DL} is define as

$$h_{DL} = \sum_{j=1}^{N} \left[\frac{(E_b/I_0)_j \nu_j R_j}{W} (1 - a_j + f_{DL,j}) \right] \quad (6)$$

Where

$$f_{DL,j} = \sum_{k=1,k\neq i}^{M} \frac{L_{k,j}}{L_{i,j}} \quad (7)$$

Factor $f_{DL,i}$ is the other-to-own-cell received power ratio for user j.

When h_{DL} approaches 1 the downlink capacity approaches to its maximum, pole capacity.

References

[AH97] S. Agarwal, J. M. Holtzman, "Modelling and analysis of handoff algorithms in multi-cellular systems**",** *Vehicular Technology Conference, 1997 IEEE 47th,* Vol. 1, pp. 300-304, May 1997

[AK99] A. S. Anpalagan and I. Katzela, "Overlaid cellular system design with cell selection criteria for mobile wireless users", *Electrical and Computer Engineering, 1999 IEEE Canadian Conference on* , Vol. 1 , pp: 24 -28, May 1999

[ARY95] J. B. Anderson, T. S. Rappaport and S. Yoshida, "Propagation measurements for wireless communication channels," *IEEE Communication Magazine*, Vol. 33, pp. 42-44, Jan. 1995

[ASAN-K01] F. Ashtiani, J. A. Salehi, M. R. Aref, M. Nasiri-Kenari, "A new soft-handoff management algorithm with two decision boundaries," *Personal, Indoor and Mobile Radio Communications, 2001 12th IEEE International Symposium on,* Vol. 1, pp. 54-58, Sept. 2001

[Cas01] J. P. Castro. *The UMTS Network and Radio Access Technology: Air Interface Techniques for Future Mobile Systems*. Wiley, John & Sons, Incorporated: UK, May 2001

[CH02] J. Cho and D. Hong, "Statistical model of downlink interference for the performance evaluation of CDMA systems" *Communications Letters, IEEE,* Vol. 6, Issue: 11, pp: 494 -496 , Nov. 2002

[Che95] X. H. Chen, "Adaptive traffic-load shedding and its capacity gain in CDMA cellular systems," *Communications, IEE Proceedings-*, Vol. 142, Issue. 3, pp. 186-192, June 1995

[Chh99] A. Chheda, "A performance comparison of the CDMA IS-95B and IS-95A soft handoff algorithms," *Vehicular Technology Conference, 1999 IEEE 49th,* Vol. 2, pp. 1407-1412, 1999

[CK01] W. Choi and J. Y. Kim, "Forward-link capacity of a DS/CDMA system with mixed multirate sources", *Vehicular Technology, IEEE Transactions on*, Vol. 50, pp. 737-749, May 2001

[CS01] J. W. Chang and D. K. Sung, “Adaptive channel reservation scheme for soft handoff in DS-CDMA cellular systems,” *Vehicular Technology, IEEE Transactions on*, Vol. 50, Issue. 2, pp. 341-353, March 2001

[CYJ99] W-Y. Choi, K. Yeo and C-H Jun, “Soft handoff algorithm with pilot signal thresholds adjustment in CDMA cellular systems,” *TENCON 99. Proceedings of the IEEE Region 10 Conference* , Vol. 1, pp. 498-501, 1999

[DGNS98] E. Dahlman, B. Gudmundson, M. Nilsson, and J. Skold, “UMTS/IMT2000 Based on Wideband CDMA, ” *IEEE Communications Magazine*, pp. 70-80, Sep. 1998

[DKOPR94] E. Dahlman, J. Knutsson, F. Ovesjo, M. Persson and C. Roobol, “WCDMA- The Radio Interface for Future Mobile Multimedia Communications,” *Vehicular Technology, IEEE Transactions on*., Vol.47, No.4, pp. 1105-1118, Nov. 1994

[DL98] A. A. Daraiseh and M. Landolsi, “Optimised CDMA Forward Link Power Allocation During Soft Handoff,” *Proceedings of VTC’98, IEEE VTS 48th*, vol. 2, pp. 1548-1552, 1998

[EIA/TIA/IS-95A] EIA/TIA/IS-95A, ‘Mobile Station-Base Station Compatibility Standard for Dual-Mode Wideband Spread Spectrum Cellular System’, Telecommunication Industry Association, Washington CD, May 1995

[ETSI TR 101 112] Universal Mobile Telecommunications System (UMTS); Selection procedures for the choice of radio transmission technologies of the UMTS, (UMTS 30.03 version 3.2.0)

[ETSI TR 125 922] Universal Mobile Telecommunications System (UMTS); Radio Resource Management Strategies, (3GPP TR 25.922 version 5.0.0 Release 5)

[ETSI TS 125 211] Universal Mobile Telecommunications System (UMTS); Physical channels and mapping of transport channels onto physical channels (FDD). 3GPP TS 25.211 version 5.1.0 Release 5

[ETSI TS 125 214] Universal Mobile Telecommunications System (UMTS); Physical layer procedures (FDD), 3G TS 25.214 version 5.5.0 Release 5

[FHU00] H. Furukawa, K. Harnage, A. Ushirokawa, “SSDT-site selection diversity transmission power control for CDMA forward link,” *IEEE J. Select. Areas Commun.*, Vol. 18, No. 8, pp. 1546-1554, Aug. 2000

[FL96] B. H. Fleury and P.E. Leuthold, “Radiowave propagation in mobile communications: an overview of European research,” *IEEE Communication Magazine*, Vol. 34, pp. 70-81, Feb. 1996

[FT02] H. Fu, J. S. Thompson, “Downlink capacity analysis in 3GPP WCDMA networks system”, *3G Mobile Communication Technologies, 2002. Third International Conference on*, pp. 534 - 538, May 2002

[GS01] J. Grandell and O. Salonaho, “Closed-Loop Power Control Algorithms in Soft Hnadover for WCDMA Systems,” *Proceedings of ICC’2001*, vol. 3, pp. 791-795, 2001

[GSMweb] http://www.gsmworld.com/news/presse_2003/press_02.shtml “GSM to Hit One Billion Subscribers by Year End 2003”, London, UK, 14th January 2003

[Ham00] K. Hamabe, “Ajustment Loop Transmit Power Control during Soft Handover in CDMA Cellular Systems,” *Proceedings of VTC’2000, IEEE VTS 52nd*, vol. 4, pp. 1519-1523, Fall 2000

[Has93] H. Hashemi, “The indoor propagation channel,” *Proc. IEEE*, Vol. 81, pp. 943-968, July 1993

[Hes93] G. C. Hess, *Land-Mobile Radio System Engineering*, Boston: Artech House, 199

[HKB00] B. Homnan, V. Kunsriruksakul, W. Benjapolakul, “A comparative performance evaluation of soft handoff between IS-95A and IS-95B/cdma2000,” *IEEE APCCAS’2000*, pp. 34 –37, 2000

[HKOKS97] S-H. Hong, S-L. Kim, H-S. Oh, C-E. Kang and J-Y Son, “Soft handoff algorithm with variable thresholds in CDMA cellular systems” *Electronics Letters*, Vol. 33, Issue. 19, pp. 1602-1603, 1997

[HL01] S. J. Hong and I. T. Lu, “Soft Handoff Algorithm Parameter Optimisation in Various Propagation Environments”, *IEEE VTC’01*, pp. 2549-2553, 2001

[HS00] B. Hashem and E. L. Strat, “On the Balancing of the Base Station Transmitted Powers during Soft Handoff in Cellular CDMA Systems,” *Proceedings of ICC’2000*, vol. 3, pp. 1497-1501, 2000

[HT00] H. Holma and A. Toskala, *WCDMA for UMTS, Radio Access For Third Generation Mobile Communications*, Johe Wiley & Sons, LTD. 2000

[HY96] C. Huang and R. Yates, “Call Admission in Power Controlled CDMA Systems,” *Proceedings of VTC’96*, pp. 1665-1669, Atlanta, GA, May 1996.

[ITU-R] Recommendation ITU-R M.[FPLMTS.REVAL], “Guidelines for Evaluation of Radio Transmission Technologies for IMT-2000/FPLMTS.”

[JL00] M. Juntti and M. Latva-aho, “Multiuser receivers for CDMA systems in Rayleigh fading channels,” *IEEE Trans. Vehic. Tech.*, 2000

[JP95] M. G. Jansen and R. Prasad, “Capacity, Throughput, and Delay Analysis of a Cellular DS CDMA System with Imperfect Power Control and Imperfect Sectorization” *IEEE Trans. Veh. Technol.*, vol. VT-44, no. 1, pp: 67-75, Feb. 1995

[KBPY97] J. Knutsson, T. Butovitsch, M. Persson and R. Yates, “Evaluation of Admssion Control Algorithms for CDMA System in a Manhattan Environment,” *Proceedings of 2nd CDMA International Conference, CIC’97*, pp. 414-418, Seoul, South Korea, October 1997

[KBPY98] J. Knutsson, P. Butovitsch, M. Persson and R. Yates, “Downlink Admssion Control Strategies for CDMA System in a Manhattan Environment,” *Proceedings of VTC’98*, pp. 1453-1457, Ottawa, Canada, May, 1998

[KMJA99] S. Kari, J. Mika, L. S. Jaana, W. Achim, “Soft Handover Gains in A Fast Power Controlled WCDMA Uplink”, *IEEE VTC’99*, pp. 1594-1598, 1999

[KS00] J. Y. Kim and G. L. Stuber, “CDMA soft handoff analysis in the presence of power control error and shadowing correlation”, *Spread Spectrum Techniques and Applications, 2000 IEEE Sixth International Symposium on*, Vol. 2, pp. 761-765, Sept. 2000

[LA01] J. Lee and R. Arnott, “System performance of multi-sector smart antenna base stations for WCDMA”, *3G Mobile Communication Technologies, 2001. Second International Conference on*, No. 477, pp: 1-6, 2001

[LDS00] J. Luo, M. Dilliger, and E. Schulz, “Research on Timer Settings for the Soft Handover Algorithm with Different System Loads in WCDMA”, *Communication Technology Proceedings, 2000. WCC - ICCT 2000. International Conference on* , Vol. 1, pp. 741 -747, 2000

[LKCKW96] D. D. Lee, D. H. Kim, Y. J. Chung, H. G. Kim, K. C. Whang, “Other-cell interference with power control in macro/microcell CDMA networks” *Vehicular Technology Conference, VTC’96. 'Mobile Technology for the Human Race'., IEEE 46th* , Vol. 2 , pp: 1120-1124, 1996

[LLW00] F. Ling, B. Love and M. M. Wang, “Behavior and performance of power controlled IS-95 reverse-link under soft handoff,” *Vehicular Technology, IEEE Transactions on*, 49, pp. 1697-1704, 2000

[LLWBFX00] F. Ling, R. Love, M. M. Wang, T. Brown, P. Fleming, and H. Xu, “Behavior and Performance of Power Controlled IS-95 Reverse-Link Under Soft Handoff” *IEEE Trans. Veh. Technol.*, vol. 49, no. 5, pp: 1697-1704, Sept. 2000

[LS98] C. C. Lee and R. Steele, “Effects of soft and softer handoffs on CDMA system capacity”, *Vehicular Technology, IEEE Transactions on*, Vol. 47, No. 3, pp. 830-841, Aug. 1998

[L-SJSWK99] J. Laiho-Steffens, M. Jasberg, K. Sipila, A. Wacker and A. Kangas, “Comparison of three diversity handover algorithms by using measured propagation data”, *proceedings of VTC’99 Spring*, Houston, TX, pp. 1370-1374, May 1999

[LUK96] D. J. Lee, C. K. Un and B. C. Kim, “An improved soft handover initiation algorithm in microcellular environment,” *Universal Personal Communication, 5th IEEE International Conference on*, vol. 1, pp. 310-314, 1996

[LWY03] Z. P. Liu; Y. F. Wang and D. Ch. Yang, “ Effect of soft handoff parameters and traffic loads on soft handoff ratio in CDMA systems,” *Communication Technology Proceedings, 2003. ICCT 2003. International Conference on* , Vol. 2, pp. 782-785, 2003

[MLG99] C. Mihailescu, X. Lagrange and Ph. Godlewski, “Soft handover analysis in downlink UMTS WCDMA system”, *Mobile Multimedia Communications, (MoMuC '99) IEEE International Workshop on*, pp. 279 –285, 1999

[Mol91] D. Molkdar, “Raview on radio propagation into and within buildings,” *Proc. IEEE*, Vol. 138, pp. 61-73, Feb. 1991

[NH98] N. Zhang and J. M. Holtzman, “Analysis of a CDMA Soft-handoff Algorithm,” *IEEE Trans. on Vehicular Technology*, Vol. 47, No. 2, pp. 710-714, May 1998

[NT01] R. P. Narrainen and F. Takawira, “Performance analysis of soft handoff in CDMA cellular networks,” *Vehicular Technology, IEEE Transactions on*, Vol. 50, Issue. 6, pp. 1507-1517, Nov. 2001

[OP98] T. Ojanpera and R. Prasad, *Wideband CDMA for Third Generation Mobile Communications*, Artech House, 1998

[OPH98] T. Ojanpera, R. Prasad, and H. Harada, “Qualitative comparison of some multiuser detector algorithms for wideband CDMA,” *Proc. IEEE Vehic, Tech. Conf.*, 1, pp. 46-50, 1998

[PKKS01] S. Park, D. K. Keun, C. S. Kang and S. M. Shin, “Uplink transmit power control during soft handoff in DS-CDMA systems,” *Proceedings of VTC’2001, IEEE VTS 53rd*, vol. 4, pp. 2913-2917, Spring 2001

[Pra98] R. Prasad, *Universal Wireless Personal Communications*, Boston: Artech House, 1998

[PRP99] R. Pirhonen, T. Rautava and J. Penttinen, “TDMA convergence for packet data services”, *IEEE Personal Communications Magazine*, Vol. 6, No. 3, June 1999

[Qualcomm97] Qualcomm Corporation, “Diversity-Handover method and performance”, *ETSI SMG2 Wideband CDMA Concept Group Alpha Meeting*, Stockholm, Sweden, Sept. 1997

[Sau02] G. Saussy, “Key business challenges in the 3G network evolution”, *International Forum on 4th Generation Mobile Communications*, May 2002.

[Scr02] A. Scrase, “An introduction to 3rd generation mobile systems”, *Tutorial, the third international conference on Mobile Communication Technologies, 3G2002*, London, UK, March 2002.

[SCH96] S-L. Su; J-Y. Chen and J-H. Huang, “Performance analysis of soft handoff in CDMA cellular networks”, *Selected Areas in Communications, IEEE Journal on*, Vol. 14, Issue. 9, pp. 1762-1769, Dec. 1996

[SH93] F. Simpson and J. M. Holtzman, “Direct sequence CDMA power control, interleaving, and coding” *IEEE J. Select. Areas Commun.*, vol. 11, no. 7, pp. 1085-1095, 1993

[SHL-SW00] K. Sipila, Z-C. Honkasalo, J. Laiho-Steffens and A. Wacker, “ Estimation of capacity and required transmission power of CDMA downlink based on a downlink pole equation”, *Vehicular Technology Conference Proceedings, 2000. VTC 2000-Spring Tokyo. 2000 IEEE 51st* , Vol. 2 , pp. 1002 -1005, May 2000

[SJLW99] K. S. Sipila, M. Jasberg, J. Laiho-Steffens and A. Wacker, “Soft Hnadover Gains in A Fast Power Controlled WCDMA Uplink,” *Proceedings of VTC’1999, IEEE VTS 49th*, vol. 2, pp. 1594-1598, 1999

[SL-SWJ99] K. Sipila, J. Laiho-Steffens, A. Wacker and M. Jasberg, “Modelling the Impact of the Fast Power Control on the WCDMA uplink,” *Proc. of VTC’99 Spring*, Houston, TX, pp. 1266-1270, May 1999

[Stu96] G. L. Stuber, *Principles of Mobile Communications*, Boston: Kluwer Academic Publishers, 1996

[TR00] O. Tero and P. Ramjee, *WCDMA: Towards IP Mobility and Mobile Internet*, Artech House, 2000

[VBM00] A. M. Vernon, M. A. Beach and J. P. McGeehan, "Planning and optimisation of smart antenna base stations in 3G networks", *Capacity and Range Enhancement Techniques for the Third Generation Mobile Communications and Beyond, IEE Colloquium on*, pp: 1-7, 2000

[Ver86] S. Verdu, "Minimum probability of error for asynchronous Gaussian multiple-access channels," *IEEE Trans. Inform. Theory*, 32(1), pp. 85-96, 1986

[Vit95] A. J. Viterbi, *CDMA: Principles of Spread Spectrum Communication.* Reading, MA: Addison-Wesley, pp. 218-227, 1995

[VVGZ94] A. Viterbi, A. M. Viterbi, K. S. Gilhousen, and E. Zehavi, "Soft handoffs extends CDMA coverage and increase reverse link capacity," *IEEE J. Select. Areas Commun*., Vol. 4, No. 8, pp. 1281-1288, 1994

[Wis02] D. Wisely, "An IP solution for system beyond 3G", *International Forum on 4th Generation Mobile Communications*, May 2002.

[WL97] D. Wong and T. J. Lim, "Soft handoffs in CDMA mobile systems," *Personal Communications, IEEE [see also IEEE Wireless Communications]*, Vol. 4, Issue. 6, pp. 6-17, Dec. 1997

[WSG02] S. S. Wang, S. Sridsha and M. Green, "Adaptive soft handoff method using mobile location information," *Vehicular Technology Conference, 2002, VTC Spring 2002. IEEE 55th*, vol. 4, pp. 1936-1940, 2002

[WW93] S-W. Wang and I. Wang, "Effects of soft handoff, frequency reuse and non-ideal antenna sectorization on CDMA system capacity," *Vehicular Technology Conference, 1993, VTC Spring 1993. IEEE 43rd*, pp. 850-854, 1993

[YG-NT00] X. Yang, S. Ghaheri-Niri and R. Tafazolli, “Evaluation of soft handover algorithms for UMTS,” *Personal, Indoor and Mobile Radio Communications, 2000 11th IEEE International Symposium on*, Vol. 2, pp. 772-776, 2000

[YG-NT01] X. Yang, S. Ghaheri-Niri and R. Tafazolli, “Performance of power-triggered and E_c/N_0-triggered soft handover algorithms for UTRA,” *3G Mobile Communication Technologies, Conference Publication*, No. 477, pp. 7-10, 2001

[YN95] K. L. Yeung and S. Nanda, “Optimal mobile-determined micro-macro cell selection”, *Personal, Indoor and Mobile Radio Communications, 1995. PIMRC'95. Sixth IEEE International Symposium on*, vol. 1, pp: 294-299, 1995

[ZBW95] J. Zou, V. K. Bhargava and Q. Wang, “Reverse link modeling and outage analysis for DS/CDMA cellular systems”, *Wireless Pers. Commun.* , pp. 189-215, Kluwer, 1995

[ZH98] N. Zhang and J. M. Holtzman, “Analysis of a CDMA Soft-handoff Algorithm,” *IEEE Trans. on Vehicular Technology*, Vol. 47, No. 2, pp. 710-714, May 1998

[ZJK98] Z. Zvonar, P. Jung, and K. Kammerlander (eds.), *GSM: Evolution Towards 3rd Generation System*, Boston: Kluwer Academic Publishers, 1998